Effects of uncertainty on conservation decisions and ecological inference

by

Kylee Denise Dunham

A dissertation submitted to the Graduate Faculty of
Auburn University
in partial fulfillment of the
requirements for the Degree of
Doctor of Philosophy

Auburn, Alabama
August 3, 2019

Doctoral Committee Members

James B. Grand, Chair, Cooperative Research Unit Supervisor, U.S. Geological Survey
Christopher A. Lepczyk, Professor of Wildlife Sciences
Conor P. McGowan, Associate Research Professor of Wildlife Sciences
David N. Koons, Associate Professor, Colorado State University

Abstract

Uncertainty is pervasive in ecology and conservation. Ecological systems are dynamic, and therefore inference from observations and subsequent decision-making can be hampered due to observation and process error. Assessing and characterizing the relative impacts of observation and process errors is important for sound ecological inference and conservation or management decisions. My research evaluates the effects of uncertainty on a threatened species listing decision and explores the reduction of uncertainty on predictive measures of species viability, understanding demographic and ecological mechanisms influencing population variation, and the impacts of accounting for these uncertainties on making conservation decisions. I apply this research to spectacled eiders (*Somateria fischeri*), a federally threatened species listed under the Endangered Species Act. My research aims to further our understanding of the effects of uncertainty by addressing the following questions; (1) How does uncertainty affect conservation decisions? and (2) What is the relative value of accounting for, and ultimately reducing those uncertainties for ecological inference and decision-making? I specifically address the impacts of imperfect detection, sampling variation, ecological uncertainty, and structural uncertainty on gaining ecological knowledge and making conservation decisions. Understanding the role of uncertainty in studying species ecology and informing conservation decisions is imperative for effective biodiversity conservation strategies.

Acknowledgements

I would like to express my deepest thanks to all those who made this dissertation possible. To my major advisor, Barry Grand, for taking a chance on me back in 2013 for my M.S. and again for my Ph.D. I have learned, grown, and experienced so much over the past six years and two graduate degrees. I am so grateful for the many hours long coding sessions and insightful conversations. The multiple trips to Alaska for work on the project certainly didn't hurt either! To my committee, Conor McGowan, Chris Lepczyk, and Dave Koons, I could not have done this without you. Over the years you have provided a great deal of wisdom, opportunity, and helped me become the scientist I am today. Conor, you graciously adopted me into your lab and I could not be more grateful for the weekly meetings with you and the members of lab McGowan. Further, you offered multiple teaching and networking opportunities that have been and will continue to be beneficial for my career. Chris, you fostered philosophical discussions with graduate and undergraduate students in your reading classes that pushed me to think critically and to develop skills to communicate science effectively. Dave, I am forever grateful for your help with my project and for providing me with such a great opportunity to continue pursuing my passions in a postdoctoral position.

I am deeply indebted to two key mentors from high school and college for their immense help that made all of this possible. Mr. Donald Quindley, without you, I do not believe I would have pursued college at all. I certainly would not have developed a love for writing that has become the cornerstone of my career. I cannot thank you enough for your guidance through those tumultuous years at Holliston High. To my undergraduate mentor, Dr. Steven Dinkelacker, you provided me with the opportunities that made all of this possible. You took a chance on a girl that thought pinto beans in lab were “gross” and tossed me into the field to wade through muck to capture turtles and alligators. I can never thank you enough for giving me the opportunities to work with you in the field and to manage your lab. I did not know then just how important that experience would be for sparking my love of research and for getting me into graduate school. I cannot express my gratitude for your advice and support over the years.

I wish to thank my friends and family whose support and encouragement has been invaluable. I am specifically grateful that my husband, Nick, has been willing to take this journey with me. Last but not least, I need to thank my dogs, Oscar, Ellie, and Mia, whose unwavering enthusiasm for life has been an inspiration. There has been no greater feeling than coming home after a long day of work to find three dogs waiting by the door to greet you. I will be forever grateful to you for reminding me to smile and laugh each and every day.

Table of Contents

List of Tables

List of Figures

Chapter 1: General Introduction

Understanding population and ecological processes using observations of a system is the primary goal of ecology, conservation, and management. Ecological systems are dynamic, and therefore inference from observations can be hampered due to partial observability, stochasticity in environmental processes, and uncertainty in model and parameter specification. Determining the mechanisms driving population dynamics has always been a central focus in ecology and uncertainty has always been a pervasive factor hindering our ability to fully understand and predict ecological systems. Assessing the relative impact of these sources of uncertainty and characterizing them is important for sound ecological inference and natural resource management decisions (Regan et al. 2005). However, in many cases these uncertainties affecting estimation of population state are epistemic and therefore can be reduced through further scientific investigation (Regan et al 2002). It logically follows that as our understanding of a system increases through data collection and modeling efforts, uncertainty would decrease providing stronger ecological understanding and predictive abilities. Using all available population data and statistical modeling tools we can decompose uncertainty to improve inference and predictions about future states in a probabilistic manner. Furthermore, inference from such statistical analyses can be combined with statistical decision theory (SDT) to directly inform decisions while accounting for uncertainties (Berger 1985, Williams and Hooten 2016). Despite the potential for such approaches to improve decision-making under uncertainty, these methods are relatively new and have yet to be implemented in a decision-theoretic framework.

Many types of uncertainty exist in ecology and conservation and there are numerous ways to classify the forms of uncertainty (Regan et al. 2002, Nichols et al. 2011). Here, I focus on two broad classifications of error sources highly relevant to ecological inference and conservation decisions; 1) observation error, and 2) process error. Observation error arises as a function of our inability to completely observe natural processes. Three major components of observation error include imperfect detection, availability bias, and sampling error (Williams et al. 2001, Regan et al. 2002, Nichols and Williams 2006, Ahrestani et al. 2013). Process error characterizes the variation in population state (size, trend) over time in response to biotic and abiotic processes (Ahrestani et al. 2013). The processes that drive population fluctuations are typically the subject of interest for ecologists and this information can be used to inform conservation strategies. However, observation errors can directly affect our ability to identify, understand, and model the processes that govern changes in population state (Nichols and Williams 2006). Ecological uncertainty can stem from our lack of knowledge about the effects of biotic and abiotic processes on population demography and dynamics (Williams et al. 2001, Nichols et al. 2011). Information may be lacking for several reasons, but often, it is difficult to obtain the data required to quantify ecological relationships with population demography due to imperfect detection or availability issues. For instance, certain age or sex classes may be unavailable to monitor or difficult to detect thereby limiting the scope of inference (Nichols and Williams 2006). Further, a lack of information may also produce structural uncertainty regarding the correct model structure (i.e. functional form of demographic relationships, or model parameterization) for making inference or decisions (Williams et al. 2001, Regan et al. 2002, Nichols et al. 2011). In this dissertation, I examine the role of imperfect detection, availability bias, sampling error, and structural and ecological uncertainty in the context of observation and process errors and ultimately their impacts on inferring population dynamics and making conservation decisions using statistical modeling.

When surveying populations, it is difficult (or impossible) to detect every individual, sample the entire population (conduct a census), and it is highly likely that some portion of the population will be unavailable for detection. First, in order to detect an individual, it must be within the sampling area or otherwise available to be detected. For many species, surveys may be conducted during the breeding season, when non-breeding individuals are not available to be detected (Nichols and Williams 2006). Alternatively, it may be difficult to detect individuals when present because they may be cryptic, demonstrate behavioral aversion, or environmental factors may influence sightability (Kellner and Swihart 2014). Further error arises through sampling processes due to the constraint of observing a sample of the population and not the entire population itself (Nichols and Williams 2006). When using population metrics (abundance, trends, demographic rates, etc.) for species classifications, harvest regulations, or other management actions, it is important to consider the accuracy and precision of those estimates and their influence on the decision (Kéry and Schmidt 2008). Abundance estimates are often used as thresholds for use in management decisions.

However, estimates of true abundance are difficult or impossible to obtain without accounting for observation error. Surveys are often implemented to collect counts over time to detect trends and estimate population size. But, these surveys are prone to multiple sources of uncertainty related to observation processes, such as imperfect detection, sampling error, and availability bias (Kéry and Schmidt 2008, Kellner and Swihart 2014). Without accounting for observation errors, abundance estimates will only account for a portion of the true population size and changes in abundance may be caused by changes in detectability, availability or sampling error and will not accurately reflect population dynamics.

Whenever possible, observation error should be partitioned from process error, the variation in population state (size, trend) over time in response to biotic and abiotic processes (Ahrestani et al. 2013, Linden and Knape 2009). State-space models (SSM, or; hierarchical models) simultaneously account for both process error and observation error and can partition these errors for stronger inference (Clark et al. 2004, Linden and Knape 2009). When both process and observation errors are high, models overestimate population declines which may result in poorly informed conservation decisions (Rueda-Cedial et al. 2015). Errors in estimates of population size are likely to produce estimates of population persistence that are of little value for making conservation decisions (McLoughlin and Messier 2004). Further, process variation is often of interest whereas observation error is typically considered a nuisance for making ecological inference and conservation decisions (Clark et al. 2004). The intrinsic and extrinsic factors that drive population dynamics are generally the true subject of interest in ecology and are useful for informing conservation decisions (Kéry and Schaub 2012).

Quantifying drivers of population dynamics is difficult due to complex and often unobservable processes acting upon individuals throughout the annual cycle. To account for environmental variation, we need to consider which environmental factor(s) are important, how they affect population dynamics, and what the magnitude of the environmental factor(s) will be in the future. Further uncertainty arises in our models or parameter estimates that reflect the biological system. By extending the SSM described above to integrate additional data sets (e.g., counts, mark-recapture) in a single modeling framework, we can make joint inference on processes driving population state and compare competing models of those processes (Schaub and Abadi 2011). Using an integrated framework we can address both structural and ecological uncertainty to develop the appropriate biological structure of the model. Integration and analysis of multiple data sets results in increased precision of parameter estimates, allows for estimation of processes not directly measured, and can relate these parameters to changes in environmental factors (Schaub and Abadi 2011, Zipkin and Saunders 2018). When analyzing only subsets of data (e.g. count data), we cannot identify the demographic mechanisms that cause changes in population dynamics. Further, using multiple sources of data we can estimate demographic rates for which we have no data and model these rates with environmental covariates (Schaub and Abadi 2011). Therefore, we can reduce uncertainty in parameter estimates, quantify effects of ecological processes on demography (and population dynamics), and identify the influence of each demographic rate on population growth.

Further integration with full annual cycle (FAC) models includes effects of events in breeding and non-breeding seasons on population dynamics of migratory species

(Hostetler et al. 2015, Rushing et al. 2017). Combined IPM's and FAC models can be used to identify and quantify vulnerability to specific threats throughout the annual cycle, estimate population viability, test alternative process models, and reduce uncertainty in the true population state. Increased precision of parameter estimates, population size, and trend is particularly useful when the objective is to evaluate temporal patterns in parameters or to detect population trends (Rhodes et al. 2011). IPM's separate the underlying ecological mechanisms from observation error, thus unravelling process variation from sampling variation. Integrated population models outperform their non-integrated counterparts because the parameter estimates are more precise (Abadi et al 2010), can be formulated to reduce structural uncertainty, estimate latent parameters, and directly estimate demographic responses to stressors. Gains in accuracy and precision in parameters are helpful for identifying multiple interacting threatening processes and make IPMs useful tools for species conservation (Rhodes et al. 2011, Saunders et al. 2018).

Measures of extinction probability are commonly used to assess risk and inform conservation actions, such as species classifications status for legal protection. However, for listing under the Endangered Species Act, researchers need to assess risk and assign species to either endangered, threatened, or not warranted categories. There are no explicit guidelines for categorizing a species by risk, therefore, the decision is based on both scientific and value judgements for what level of risk warrants protection (Cummings et al. 2018). Statistical decision theory uses the results of a statistical analysis to reduce uncertainty in a decision problem and help the decision maker choose the optimal decision based on the objectives (Williams and Hooten 2016). Integrating decision theoretic methods with SSM's and IPM's allows decision makers to consider the various sources of uncertainty affecting the decision.

Spectacled eiders (*Somateria fischeri*) are used as the primary focus for this research because (1) they are a federally threatened species with quantitative listing criteria, (2) recent surveys indicate that spectacled eiders have likely met recovery criteria but there is considerable uncertainty in population state, and (3) they are Arctic sea ducks with a unique combination of life-history traits linked to Arctic marine habitats, making them difficult to study but also exposing them to significant threats under global change.

Spectacled eiders were listed as threatened under the Endangered Species Act (ESA, as amended) in 1993 following extreme population declines throughout their breeding and nesting range in Alaska (Ely et al. 1994, Flint et al. 2016, Taylor et al. 1996, USFWS 2002). Recent surveys indicate that the population of spectacled eiders breeding on the Yukon-Kuskokwim Delta of Alaska have likely met recovery criteria (Fischer et al. 2017). However, there is considerable uncertainty in population size, trend, and environmental factors affecting population dynamics. Spectacled eiders are monitored primarily during the breeding season when birds nest in coastal tundra habitats. Individuals do not breed until their second or third year and all non-breeding individuals are unobservable. Population indices from aerial surveys of spectacled eiders include a great deal of observation error due to imperfect detection, availability bias, and sampling error making it difficult to estimate population size and detect trends.

Spectacled eiders are an Arctic sea duck species that inhabit remote and extreme environments throughout the annual cycle. Given their listing status, it is imperative to understand the underlying mechanisms that influence population dynamics in a rapidly changing climate. Spectacled eiders remain unobservable until reaching breeding age (2-3+ years old) (Flint et al. 2016). Individuals are widely dispersed in open ocean areas along Russian and Alaska during the spring and fall migration periods and the global population winters together south of St. Lawrence Island in the northern Bering Sea (Sexson et al. 2014). Monitoring during the non-breeding period is logistically challenging and thus the species remains unobservable for a majority of the annual cycle. The unobservable portion of the population has contributed to uncertainty in population state (size, trend), along with uncertainty in demographic rates. Given the paucity of data, first and second year survival and effects of environmental factors are inestimable when analyzing only survival data. Further, the relative influence of each demographic rate on the change in population growth could not be quantified because they have not been estimated. The lack of information on this portion of the population introduced uncertainty in the optimal model structure, relationships between demographic parameters, and effects of environmental factors and further complicates our ability to understand population state. I will evaluate the effects of these uncertainties on making decisions regarding species listing status and on gaining ecological information about a threatened species facing global environmental change.

Here, I explore the use of breeding population monitoring data for assessing the role of uncertainty in making ecological inference and conservation decisions, with a focus on spectacled eiders in Alaska. The next four chapters were prepared for submission to peer-reviewed journals and written in collaboration with co-authors; therefore, I use the third person plural throughout the remainder of this document. In Chapter 2, I investigate the effects of imperfect detection on the probability of meeting population thresholds for conservation decisions. I model uncertainty in detection, assess the probability of meeting a threshold, and discuss the implications of this uncertainty on setting and evaluating population thresholds for management and conservation. In Chapter 3, I assess the probability that spectacled eiders have met the quantitative recovery criteria for reclassification to delist from threatened under the Endangered Species Act (ESA, as amended 1973). I use Bayesian state-space models to partition observation and process error, estimate population size and trend for two breeding populations of spectacled eiders. Using the estimates of population size, trend, and process error, I calculate the probability of extinction and the expected loss associated with making the decision to maintain threatened status or to delist. In Chapter 4, I develop an integrated population model using abundance data, mark-recapture data, and productivity data for spectacled eiders. Using this modeling framework, I quantify the demographic responses to environmental factors during the breeding and wintering period, and estimated latent demographic rates, population size, and trend. I resolve structural uncertainty in the mechanisms governing population dynamics and ecological uncertainty in the role of environmental effects on demographic rates. In Chapter 5, I compare the estimates of population size, trend, and process error produced by the integrated population model and the state-space model to demonstrate the benefits of using an integrated model and statistical decision theory for species classification decisions. I address the effects of structural uncertainty (model parameterization) and ecological uncertainty in assessing threats and making species classification decisions.

Literature Cited

Abadi, F., O. Giminez, R. Arlettaz, and M. Schaub. 2010. An assessment of integrated population models: bias, accuracy, and violation of the assumption of independence. Ecology 91(1).

Ahrestani, F.S., M. Hebblewhite and E. Post. 2013. The importance of observation versus process error in analyses of global ungulate populations, Scientific Reports, 10.1038/srep03125.

Berger, J. O. 1985. Statistical decision theory and Bayesian analysis. Springer, New York, New York, USA.

Clark, J.S. and O.N. Bjornstad. 2004. Population time series: process variability, observation errors, missing values, lags, and hidden states. Ecology 85(11).

Cummings, J.W., S.J. Converse, D.R. Smith, S. Morey, and M.C. Runge. 2018. Implicit decision framing as an unrecognized source of confusion in endangered species classification. Conservation Biology 32(6): 10.1111/cobi.13185

De Valpine, P. and A. Hastings. 2002. Fitting population models incorporating process noise and observation error. Ecological Monographs 72, 57–76, 10.2307/3100085

Ely, C.R., C.P. Dau, and C.A. Babcock. 1994. Decline in a population of spectacled eiders nesting on the Yukon-Kuskokwim Delta, Alaska. Northwestern Naturalist 75:81–87.

Fischer, J.B., A.R. Williams, and R.A. Stehn. 2017. Nest population size and potential production of geese and spectacled eiders on the Yukon-Kuskokwim Delta, Alaska, 1985-2016. Unpubl. Rep., U.S. Fish and Wildlife Service, Anchorage, AK.

Flint, P.L., J.B. Grand, M.R. Petersen, and R.F. Rockwell. 2016. Effects of lead exposure, environmental conditions, and metapopulation processes on population dynamics of spectacled eiders. North American Fauna 81:1-41

Hostetler, J.A., T.S. Sillett, and P.P. Marra. 2015. Full-annual-cycle population models for migratory birds. The Auk: Ornithological Advances 132:433–449.

Kellner, K.F., and R.K. Swihart. 2014. Accounting for imperfect detection in ecology: A quantitative review. PLoS ONE 9.

Kéry, M., and M. Schaub. 2012. Bayesian population analysis using WinBUGS: A hierarchical perspective. Academic Press, Boston, Massachusetts, USA.

Kéry M., and B. Schmidt. 2008. Imperfect detection and its consequences for monitoring for conservation. Community Ecology 9: 207–216.

Linden, A. and J. Knape. 2009. Estimating environmental effects on population dynamics: consequences of observation error. Oikos 118: 675–680, 10.1111/j.1600-0706.2008.17250.x

McLoughlin, P.D., and F. Messier. 2004. Relative contributions of sampling error in initial population size and vital rates to outcomes of population viability analysis. Conservation Biology 18(6): 1665-1669.

Nichols, J.D. and B.K.Williams.2006. Monitoring for conservation. Trends in Ecology and Evolution. 21: 668–673.

Nichols, J.D., M.D. Koneff, P.J. Heglund, M.G. Knutson, M.E. Seamans, , J.E. Lyons, J.M. Morton, M.T. Jones, G.S. Boomer, and B.K. Williams. 2011. Climate change, uncertainty, and natural resource management. Journal of Wildlife Management **75**: 6– 18.

Regan, H.M., M. Colyvan, and M.A. Burgman. 2002. A taxonomy and treatment of uncertainty for ecology and conservation biology. Ecological Applications 12(2): 618-628.

Regan, H.M., Y. Ben-Haim, B. Langford, W.G. Wilson, P. Lundberg, S.J. Andelman, and M.A. Burgman. 2005. Robust decision-making under severe uncertainty for conservation management. Ecological Applications, 15(4), 1471-1477. https://doi.org/10.1890/03-5419

Rhodes, J.R., C.F. Ng, D.L. deVilliers, H.J. Preece, C.A. McAlpine, and H.P. Possingham. 2011. Using integrated population modelling to quantify the implications of multiple threatening processes for a rapidly declining population. Biological Conservation 144(3): 1081-1088.

Rueda-Cediel, P., K.E. Anderson, T.J. Regan, J. Franklin, H.M. Regan and A.J. Lustig. 2015. Combined Influences of Model Choice, Data Quality, and Data Quantity When Estimating Population Trends, PLOS ONE, **10**, 7, (e0132255).

Rushing, C.S., J.A. Hostetler, T.S. Sillett, P.P. Marra, J.A. Rotenberg, and T.B. Ryder. 2017. Spatial and temporal drivers of avian population dynamics across the annual cycle. Ecology 98(11): 2837-2850. doi: 10.1002/ecy.1967.

Saunders, S.P., F.J. Cuthbert, and E.F. Zipkin. 2018. Evaluating population viability and efficacy of conservation management using integrated population models. Journal of Applied Ecology 55(3): 1380-1392.

Schaub, M., and F. Abadi. 2011. Integrated population models: a novel analysis framework for deeper insights into population dynamics. Journal of Ornithology 152: S227– S237.

Schaub, M., O. Gimenez, A. Sierro, and R. Arlettaz. 2007. Use of integrated modeling to enhance estimates of population dynamics obtained from limited data. Conservation Biology 21:945–955.

Sexson, M.G., J.M. Pearce, and M.R. Petersen. 2014. Spatiotemporal distribution and migratory patterns of Spectacled Eiders. BOEM 2014-665. U.S. Department of the Interior, Bureau of Ocean Energy Management, Alaska Outer Continental Shelf Region, Anchorage, AK.

Taylor, B.L., P.R. Wade, R.A. Stehn, and J.F. Cochrane. 1996. A Bayesian approach to classification criteria for spectacled eiders. Ecological Applications 6(4):1077-1089.

U.S. Fish and Wildlife Service. 1993. Final rule to list the Spectacled Eider as threatened. Federal Register 58:27374– 27480.

U.S. Fish and Wildlife Service. 2002. Spectacled eider recovery plan. Anchorage, Alaska: U.S. Fish and Wildlife Service.

Williams, B.K., J.D. Nichols, and M.J. Conroy. 2001. Analysis and management of wildlife populations. San Diego: Academic.

Williams, P.J. and M.B. Hooten. 2016. Combining statistical inference and decisions in ecology. Ecological Applications 26(6): 1930-1942.

Zipkin, E.F. and S.P. Saunders. 2018. Synthesizing multiple data types for biological conservation using integrated population models. Biological Conservation 217: 240-250.

Chapter 2: Evaluating the probability of meeting population management thresholds

Abstract

The recovery of many threatened and endangered species and management of harvested species are assessed using population size thresholds. When defined, managers work under the assumption that they will be able to determine if the population has met the threshold, given available data. Our approach takes a simple problem, where a population threshold has been set for a threatened species, to demonstrate how we can break the population size threshold into its component parts to determine the values of detection probability and level of certainty in those values necessary to determine if the threshold was met. We demonstrate this approach using spectacled eiders, a federally listed species, as a case study. Mean detection probability and precision had important consequences on the ability to determine if a population had met a designated threshold. Certainty in the distribution of detection probability had a significant influence on the probability that the population met the threshold. There was an increase in the probability that the threshold had been met when uncertainty in detection was greater, demonstrating that uncertainty in the measurement of detection could lead to improper conclusions about population status. In real-world applications, the sensitivity of a threshold to uncertainty should be evaluated to make conservation and management decisions using the best available data.

Introduction

Effective conservation and management rely upon monitoring programs to detect changes in a system and employ appropriate actions. Classification of conservation status is often based on a threshold in metrics (e.g. population size or trend) that serve to trigger or inform a change in conservation status (Martin et al. 2009, Connors and Cooper 2014, Cook et al. 2016, de Bie et al. 2018). Determining conservation status is an influential process that may affect regulatory procedures with potentially significant consequences for managing agencies and species. Threatened and endangered species may be classified according to thresholds which once met may indicate recovery and trigger delisting actions or indicate a decline thus warranting further protection (i.e. reclassification from threatened to endangered) (U.S. Endangered Species Act (ESA 1973, as amended)) (Lindenmayer et al. 2013). Evaluating whether such thresholds are met is a critical component to management and conservation of these species.

Establishing thresholds to trigger management actions or changes in conservation status implicitly links population monitoring data to management decisions. Many monitoring programs are implemented to collect counts or indices of abundance over time in an effort to detect change and are often extrapolated to estimate population size (Nichols and Williams 2006). Valid inference from counts or abundance indices depends on invariable or homogenous detection probability or the assumption of a constant linear relationship between counts and abundance throughout a time series (Williams et al. 2001). However, changes in the number of animals counted over time could be caused by observation errors such as detectability rather than actual abundance. Hence, indices of abundance or raw counts may not be sufficient to determine if a population has reached the management threshold.

One of the simplest approaches to estimate abundance from counts or indices and correct for detection probability is the use of the canonical population estimator (Williams et al. 2001). Population size is estimated as a function of the number of individuals counted on a survey of the population, and the probability of detecting an individual given that it is present in the population (Williams et al. 2001). The population estimator is typically described as $\widehat{N} = C/p$, where $\widehat{N}$ is the estimated population size, C is the number of individuals counted, and p is the probability of detecting an individual (Williams et al. 2001). Accuracy and precision of abundance estimates and subsequent decisions are largely dependent on assumptions regarding detection probability and inclusive observation processes. Without accounting for detection processes, and uncertainty in them, using counts or abundance indices to make decisions regarding population size or trend may lead managers to make erroneous conclusions regarding population recovery or effects of management actions (White 2005).

Globally, many endangered and harvested species are monitored using aerial surveys due to wide-ranging distributions across large and remote geographic areas (Lubow and Ransom 2016, USFWS 2016). Surveys flown in fixed wing planes are prone to low detection rates and typically only provide rough indices or raw counts over the sampled region (Buckland et al. 2008, Lubow and Ransom 2016, USFWS 2016). When lacking information on detectability, managers are required to make decisions regarding the population under the assumption that counts are directly related to abundance (White 2005, Williams et al. 2001). If this assumption is not met, managers risk misclassifying population status and implementing poor management actions (Williams et al. 2002, Buckland et al. 2008, Kellner and Swihart 2014). For species such as spectacled eiders (*Somateria fischeri*), evaluating the probability of meeting the population threshold has been problematic due to the difficulty in quantifying the probability of detection on surveys and subsequent ability to accurately estimate population size (Flint et al. 2016). Challenges associated with estimating detection include, but are not limited to; availability bias, observer error, and the logistical and financial constraints of methods required to explicitly estimate detection. Managers currently believe that the breeding population of spectacled eiders on the Yukon-Kuskokwim Delta (YKD), Alaska has increased and has met or is close to meeting the population recovery threshold. Here, we estimate the probability that the YKD breeding population of spectacled eiders met the population threshold for delisting detailed in the species recovery plan (USFWS 1996) using the canonical population estimator.

When using population metrics to inform conservation or management actions, it is important to consider the accuracy and precision of those estimates and their influence on the decision (Kéry and Schmidt 2008). Our objective was to assess the probability of meeting a population threshold objective given the relationship between abundance, counts, and detection. Further, we sought to examine the effect of uncertainty in detection probability on the probability of meeting a population threshold. Here, we identify the range of values for detection that indicate the population has met the threshold, and explore the effect of the expected value(s) of detection on estimates of abundance and thus the probability of meeting a threshold.

Methods

Study species

Spectacled eiders were listed as threatened under the Endangered Species Act in 1993 following extreme population declines throughout their breeding and nesting range in Alaska (Ely et al. 1994, Taylor et al. 1996, Ryding et al. 2007) . There are two subpopulations of Alaskan breeding spectacled eiders, one population on the Yukon-Kuskokwim Delta (YKD) and the other on the Arctic Coastal Plain (ACP), and a large breeding population in Arctic Russia (USFWS 1996, Flint et al. 2016). Both subpopulations of Alaskan breeding spectacled eiders have been monitored annually since the early 1990’s by aerial surveys (Flint et al. 2016, Platte and Stehn 2015). Recovery criteria for the two populations state that the lower 95% confidence interval on the population estimate is greater than or equal to 6,000 breeding pairs (12,000 breeding birds) and they must have an increasing trend over the last 10 years (USFWS, 1996). For simplicity, we focus on estimating abundance using the breeding bird index (number of breeding birds) generated from the 2016 aerial survey ($C \sim Normal(6336, 511)$, pers. comm. J. Fischer). Indices (C) are the number of indicated breeding birds observed on line transects adjusted for unequal transect lengths and sampling area (Platte and Stehn, 2015). Aerial survey methods follow standard protocol for Waterfowl Breeding and Population Habitat Survey (WBPHS) and count data is analyzed using a ratio estimator (Cochran 1977) to calculate mean density of observations for each species (Platte and Stehn 2015). Mean density is calculated by dividing the sum of the indicated total or observed total birds by the sum of the sampled transect area and the variance of the density estimate was calculated based on the variability among sampling units within each stratum. Density was multiplied by stratum area to calculate the population index, and the indicated breeding bird number is the sum of the population indices and the sum of the variances over the strata (Platte and Stehn 2015).

Model formulation

The canonical population estimator relates the estimated abundance to a count and detection probability of individuals from the sampled population. The general approach began with estimating population size ($\widehat{N}$) using the canonical estimator, with the 2016 index (C) from aerial surveys on the YKD breeding grounds, and a series of different probability distributions on detection (p) (Table 2-1)

$$\widehat{N} = \frac{C}{p}.$$

We then use the principle of conditional probability which measures the probability of event A occurring given that event B has occurred $P(A|B) = P(A,B)/P(B)$ where $P(B) \neq 0$. We apply the concept of conditional probability to meeting a population threshold by examining the probability of abundance being greater than or equal to the threshold given the known number of observed breeding birds (C) over a range of possible detection probabilities written as:

$$P\left(\widehat{N} \geq 12{,}000 \middle| C, p\right).$$

Next, we identified the values of detection probability that resulted in estimated population sizes greater than or equal to the population recovery threshold:

$$P(p|C, \widehat{N} \geq 12{,}000).$$

To evaluate the probability of meeting the population threshold we used the following procedure:

(1) Generate initial values (here, n = 10,000) for parameter distributions (C, p) and set the threshold population size ($N^* = 12{,}000$).

(2) Generate a distribution for detection probability and the count (or abundance index) using n values. We used a uniform or beta distribution for detection probability and a Normal distribution for the abundance index (see Table 2-1).

(3) Estimate population size using the canonical population estimator, $\widehat{N} = \frac{C}{p}$ where C is the abundance index distribution and p is the distribution on detection probability.

(4) Save the values of $\widehat{N} \geq 12{,}000$ using logical indexing to preserve the position of each value from the distribution on abundance to locate the combined values of detection and count that resulted in abundance estimates above the threshold.

(5) Estimate the probability of meeting the threshold by dividing the number of values of $\widehat{N} \geq 12{,}000$ by the number of initial values n. In this example, when the probability of meeting the threshold is > 95% the population has met the abundance criteria due to the equivalency between the 95% LCL and the 95% probability of exceeding the threshold (see Study Species).

(6) Repeat steps 1-5 for additional scenarios. This framework was repeated for a total of 6 alternative data scenarios (Table 2-1). The analysis was coded using MATLAB version 8.4.0.15 (The Mathworks, Inc., Natick, Massachusetts, United States, code available from authors).

We initialized scenario YKD 1 using the 2016 index with a uniform distribution on detection probability to evaluate the relationship between the recent count, detection probability, uncertainty, and the probability of meeting the population threshold (Table 2-1). We initialized six additional scenarios each with a different distribution on detection probability (Table 2-1). We generated beta distributions for scenarios YKD 2 through YKD 5 to reflect relatively low ($\mu = 0.3$) and high ($\mu = 0.7$) mean detection rates, with low ($\sigma = 0.05$) and high ($\sigma = 0.2$) error rates, to reflect the level of uncertainty in the possible distribution of values for detection probability. Scenarios YKD 6 and YKD 7 utilize detection probabilities estimated as the inverse of the visibility correction factor (VCF) where $P(p) = 1/VCF$ estimated for the aerial surveys on the YKD. For YKD 6, the traditional visibility correction factor is a general VCF developed in 1968 for all eider species on the YKD, calculated as the ratio of ground-observed nest counts to aerially-observed pair counts (VCF = 3.58; Lensink 1968). Scenario YKD 7 used the VCF developed specifically for spectacled eiders, following the addition of extensive ground-based surveys in 1985 (VCF = 2.35; Stehn and Platte 2015). These VCF's do not account for uncertainty but are considered a useful metric for correcting counts from aerial surveys.

Results

We found that conditional probability distributions on detection indicated that mean detection probability must be below 0.6 for the recent count to result in a population estimate that had met the specified threshold (Figure 2-1, Table 2-1). Under data scenarios YKD 4, YKD 5, YKD 6, and YKD 7, the results indicated that the population was likely to have met the population threshold (Table 2-1). Mean detection probability and certainty in the distribution of values had important consequences on the probability that the population met the designated threshold. As expected, as mean detection probability increased the probability that the threshold was met increased (Figure 2-1). Further, the certainty in the distribution of detection probabilities had a significant influence on the confidence that the population reached the threshold (Table 2-1). For instance, under scenario YKD 5, there was a 0.85 probability that the population met the threshold given the count and the scenario with low detection probability and high uncertainty, whereas YKD 4 with the same count results in a 0.99 probability of having met the criteria when error was low (Table 2-1). Additionally, when detection probability was increased, certainty that the population did not meet the threshold increased when certainty was high and error rates were low ($P(\widehat{N} \geq\ 12{,}000)$ = 0.0056). Alternatively, there was an increase in the probability that the threshold had been met when there was more uncertainty in the distribution of detection probability ($P(\widehat{N} \geq\ 12{,}000)$ = 0.21) (Table 2-1). In this case, the increase in the probability of meeting the threshold under the high detection - high uncertainty scenario demonstrated that the uncertainty in the measurement in detection could have led to false conclusions about population state (Table 2-1).

Discussion

Our results establish that when there is a population target, and we have an observed count, we can use the canonical population estimator and conditional probability to determine the detection probabilities necessary to meet the threshold. Furthermore, we can reduce uncertainty in meeting the threshold when the distribution on detection is more certain. Our approach demonstrates that we can break a population threshold into its component parts to determine the values of detection probability and level of certainty necessary to accurately evaluate the probability of meeting the threshold.

The certainty in the distribution of detection probabilities had important consequences on the ability to determine if a population had met a designated population threshold. When mean detection probability was low, abundance estimates were inflated indicating a higher probability that the threshold was met. Additionally, certainty in the distribution of detection probabilities influenced the probability that the population had met the threshold. Increasing uncertainty in detection increased the probability of meeting the threshold when compared to estimates from high certainty (low error) scenarios (Table 2-1). The increase in the probability of meeting the threshold under high uncertainty scenarios demonstrates that uncertainty in the measurement of detection could lead to false inference about the population. The sensitivity of a decision threshold to uncertainty in observation processes should be considered in real-world applications.

The certainty or confidence in the estimates of all variables, including the probability of meeting the criteria should be a priority when setting population management thresholds. For instance, how certain do we need to be that a population met the designated threshold? Consider the results from YKD4 and YKD5, the probability that the population threshold was met for YKD4 was 0.9999 and 0.8521 for YKD5 (Table 2-1). Under scenario YKD4, Spectacled eiders would meet the abundance threshold; however, they would not meet the threshold under scenario YKD5. When expected value of outcomes is poorly defined, managers may be willing to establish an arbitrary level of confidence in meeting an established threshold. Some may be willing to accept the 85.21% certainty in meeting the threshold; while others might believe that even 99.99% certainty in meeting the threshold is inadequate, (i.e. managers may be risk-averse and choose not to accept this probability). In either case, we argue that the certainty or risk preference in estimating the probability of meeting a population threshold is just as important as setting the population threshold criteria for designating population recovery. Both clarity in the certainty of the estimate of abundance and the certainty of a population meeting a threshold is critical to management and conservation decisions.

Currently, projects are underway to provide robust estimates of detection probability for spectacled eiders from aerial surveys on both the Yukon-Kuskokwim Delta and Arctic Coastal Plain breeding grounds. Both breeding populations may be near the designated recovery criteria. However, without estimates of detection probability it is not possible to evaluate the probability that either population has met the recovery threshold. Our results indicate that when mean detection is low and certainty is high we have greater certainty that the population has met the threshold. Given models YKD 6 and YKD 7, which use the inverse of visibility correction factors previously used to estimate abundance in the area, the results indicate the population has met, or is very close to meeting the population threshold (Table 2-1). However, the estimated VCF's do not account for spatial or temporal variation, and spectacled eiders nest in varying densities throughout the surveyed area and observations may be affected by observer effects and environmental conditions (Ely et al. 1994, Flint et al. 2016). Spatial or temporal variation in detection probability can result in detecting spurious trends in abundance (Kéry and Schmidt 2008). Without accounting for such variability in detection managers risk misclassification of population state and thus conservation status.

Effective conservation of threatened and endangered species and management of harvested species is ultimately rooted in decision theory, which depends heavily on statistical inference from estimated abundance, trend, and/or viability. Our approach can quickly illustrate when current monitoring efforts may be insufficient for a species, and when alterations to surveys may be required to gain important information. More formal and specialized methods exist to the same end, such as expected value of perfect information (EVPI) (Runge et al. 2011, Williams et al. 2011), but the expertise is not always easily accessible. Developing studies to estimate detection rates and the heterogeneity therein are costly and difficult to implement but using conditional probabilities is intuitive and easy to apply. Many threatened and endangered species are characteristically difficult to detect making the estimation of abundance difficult (Thompson 2004). Proper planning should include acceptable levels of precision in surveys and subsequent estimates for conservation needs (Lubow and Ransom 2016). Exploring the effects of uncertainties and evaluating decision thresholds should be conducted prior to analyzing available data or implementing new monitoring protocols. Furthermore, promoting more certain estimates of detection probability through informed sampling design will increase precision of abundance and trend estimates, supporting decision-making. We believe our approach serves to assess and inform survey design to meet measurable targets for certainty in the probability of detection. Finally, we stress the importance of accounting for the uncertainty in observation processes for population management decisions.

Literature Cited

Buckland, S.T, S.J. Marsden, and R.E. Green. 2008. Estimating bird abundance: making methods work. Bird Conservation International 18.

Cochran, W.G. 1977. Sampling techniques. 3rd ed. John Wiley and Sons, New York.

Connors, B.M. and A.B. Cooper. 2014. Determining Decision Thresholds and Evaluating Indicators when Conservation Status is Measured as a Continuum. Conservation Biology 28: 1626–1635.

Cook, C.N., K. de Bie, D.A. Keith, and P.F.E Addison. 2016. Decision triggers are a critical part of evidence-based conservation. Biological Conservation 195: 46–51.

de Bie, K., P.F.E. Addison, and C.N. Cook. 2018. Integrating decision triggers into conservation management practice. Journal of Applied Ecology 55: 494–502.

Ely, C.R., C.P. Dau, and C.A. Babcock. 1994. Decline in a Population of Spectacled Eiders Nesting on the Yukon-Kuskokwim Delta , Alaska. Northwestern Naturalist 75: 81–87.

Flint, P.L., J.B. Grand, M.R. Petersen, and R.F. Rockwell. 2016. Effects of lead exposure, environmental conditions, and metapopulation processes on population dynamics of Spectacled Eiders. North American Fauna.

Kellner, K.F., and R.K. Swihart. 2014. Accounting for imperfect detection in ecology: A quantitative review. PLoS One 9.

Kéry, M., and B. Schmidt. 2008. Imperfect detection and its consequences for monitoring for conservation. Community Ecology 9: 207–216.

Lensink, C.J. 1968. Clarence Rhode National Wildlife Refuge Annual Narrative Report. Available at Alaska Resources Library and Information Service, Anchorage, AK. http://www.arlis.org/.

Lindenmayer, D.B., M.P. Piggott, and B.A. Wintle. 2013. Counting the books while the library burns: Why conservation monitoring programs need a plan for action. Frontiers in Ecology and the Environment. 11: 549–555.

Lubow, B.C., and J.I. Ransom. 2016. Practical bias correction in aerial surveys of large mammals: Validation of hybrid double-observer with sightability method against known abundance of feral horse (Equus caballus) populations. PLoS One 11: 1–15.

Martin, J., M.C. Runge, J.D. Nichols, B.C. Lubow, L. William, and W.L. Kendall. 2009. Structured decision makingas a conceptual framework to identify making thresholds for conservation and management. Ecological Applications. 19: 1079–1090.

Nichols, J.D. and B.K. Williams. 2006. Monitoring for conservation. Trends Ecology and Evolution. 21: 668–673.

Platte, R.M. and R.A. Stehn. 2015. Abundance and trend of waterbirds on Alaska’s Yukon-Kuskokwim Delta Coast based on 1988 to 2015 aerial surveys. Unpublished report, U.S. Fish and Wildlife Service, Anchorage, AK.

Runge, M.C., S.J. Converse, and J.E. Lyons. 2011. Which uncertainty? Using expert elicitation and expected value of information to design an adaptive program. Biological Conservation 144: 1214-1223

Ryding, K.E., J.J. Millspaugh,and J.R. Skalski. 2007. Using Time Series to Estimate Rates of Population Change from Abundance Data. Journal of Wildlife Management. 71: 202–207.

Taylor, B.L., P.R. Wade, R.A. Stehn, and J.F. Cochrane. 1996. A Bayesian Approach to Classification Criteria for Spectacled Eiders. Ecological Applications. 6: 1077–1089.

Thompson, W.L. 2004. Sampling Rare and Elusive Species. Island Press, Washington.

USFWS. U. S. Fish and Wildlife Service. 1996. Spectacled eider recovery plan. Anchorage, Alaska: U.S. Fish and Wildlife Service: 157 pages.

USFWS. U. S. Fish and Wildlife Service. 2016. Waterfowl population status, 2016. U.S. Department of the Interior, Washington, D.C. USA.

White, G.C. 2005. Correcting wildlife counts using detection probabilities. Wildlife Research. 32: 211–216.

Williams, B.K., J.D. Nichols, and M.J. Conroy. 2002. Analysis and Management of Animal Populations. Academic Press, San Diego.

Williams, B.K., M.J. Eaton, and D.R. Breininger. 2011. Adaptive resource management and the value of information. Ecological Modelling 222: 3429-3436.

Tables

Table 2-1. Probability distributions used to initiate models to estimate detection probabilities necessary to meet population threshold (12,000 birds) and estimate the probability that the count (C ~ N (6336, 511), index of breeding birds) could indicate that the population threshold has been met, designated in the recovery plan for spectacled eiders (*Somateria fischeri*).

Model	Detection probability			Probability of meeting threshold
	μ	σ	Distribution	
YKD 1	0.5	0.289	Uniform (0-1)	0.5247
YKD 2	0.70	0.05	Beta (58.1, 24.9)	0.0056
YKD 3	0.70	0.20	Beta (2.975, 1.275)	0.2100
YKD 4	0.30	0.05	Beta (24.9, 58.1)	0.9999*
YKD 5	0.30	0.20	Beta (1.275, 2.975)	0.8521
YKD 6	0.2793[a]	--	--	1.0*
YKD 7	0.4255[b]	--	--	0.9921*

[a] Inverse of the traditional visibility correction factor (1/VCF) developed in 1968 for all eider species on the YKD (Lensink, 1968).

[b] Inverse of the Spectacled eider specific visibility correction factor estimated following extensive ground based surveys in addition to aerial surveys on the YKD (Stehn Platte, 2015).

* Scenario met the population threshold.

Figures

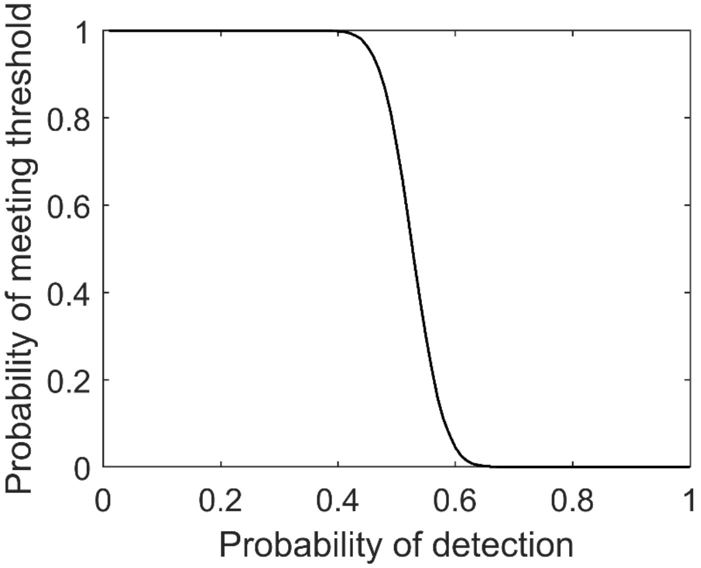

Figure 2-1. The relationship between the probability of detection and the probability of meeting the 12,000-bird threshold necessary to meet the population recovery criteria for spectacled eiders (*Somateria fischeri*), conditional on the most recent aerial survey count from the Yukon Kuskokwim Delta. The probability of meeting the population threshold decreases rapidly after a 40% detection rate and the probability of meeting the threshold is zero at roughly 70% detection, given the most recent count.

Chapter 3: Assessing recovery of spectacled eiders using a Bayesian decision analysis

Abstract

Recent surveys indicate threatened spectacled eider populations are increasing in Alaska, prompting the USFWS to reconsider federal listing status. There are two breeding populations, one in western Alaska on the Yukon-Kuskokwim Delta (YKD) and one in northern Alaska on the Arctic Coastal Plain (ACP). Criteria for delisting include the minimum estimated breeding population size is ≥ 6,000 breeding pairs (or 12,000 breeding birds) designated by the 95% lower credible interval, and based on a Bayesian decision analysis, the overprotection loss exceeds the underprotection loss based on at least 10 years of data. For spectacled eiders, loss is the cost of making classification errors measured as the probability of the population declining to the designated quasi-extinction level of 250 breeding birds (125 breeding pairs) for a range of values of population growth and estimated population size. Here, we estimate abundance and population growth rate using a Bayesian state-space model for the two Alaskan breeding populations of spectacled eiders. Further, we quantify the expected loss and risk of committing a classification error using a Bayesian decision analysis**.** Loss functions for the decision analysis are calculated given the posterior estimates of population growth r and abundance in the final year N_{2016} converting these metrics into a measure of risk according to probability of extinction. We generated the loss function by projecting the population over 50 years for a range of population growth rates. Our results indicate that the YKD breeding population has met recovery criteria but the ACP population has not. We are 1.16 times more likely to be committing an overprotective error for the YKD population. Higher underprotection loss than overprotection loss indicates the ACP population is at risk of falling below the quasi-extinction value of 125 breeding pairs in the next 50 years. Decision-makers are tasked with trying to choose the best action to take for conservation or management despite these uncertainties. The methods employed here provide an example of accounting for these uncertainties in such a way that the decision-makers may understand the probability of committing a classification error. Incorporating the abundance threshold and decision analysis in the reclassification criteria greatly increases the transparency and defensibility of the classification decision.

Introduction

The goal of the Endangered Species Act (ESA 1973, as amended) is to protect and recover imperiled species and the ecosystems upon which they depend so federal protection is not necessary for survival. Recovery plans for species listed under the ESA are developed to provide guidance regarding management actions and must include objective, measurable criteria to indicate species reclassification is warranted. For many species, the measurable criteria for reclassification is based on abundance, trend, and extinction risk deemed appropriate by the species recovery team. Distinguishing when these criteria are met is inherent in the concept of setting measurable criteria and has significant implications for listed species and agencies tasked with their protection (U.S. Fish and Wildlife Services [USFWS] and/or National Marine Fisheries Service [NMFS]).

Recent surveys indicate spectacled eiders (*Somateria fischeri*) listed as threatened under the ESA (USFWS 1993) have been increasing on one of their primary breeding grounds in Alaska, prompting the USFWS to consider population status relative to recovery criteria. Following the drastic decline and subsequent listing of spectacled eiders in 1993 (USFWS 1993), programs monitoring abundance (Stehn et al. 1993, Ely et al. 1994, Fischer et al. 2018, Wilson et al. in prep) and demography (Flint et al. 1999, Flint et al. 2006, Flint et al. 2016, Grand and Flint 1999) were employed on Alaskan breeding grounds. The global population of spectacled eiders includes three distinct breeding populations in Arctic Russia, northern Alaska along the Arctic Coastal Plain (ACP), and western Alaska on the Yukon-Kuskokwim Delta (YKD) (Dau and Kistchinski 1977). The species will be considered for delisting when each of the three breeding populations meets one of the following criteria: 1) the minimum estimated breeding population size is ≥ 6,000 breeding pairs (or 12,000 breeding birds) designated by the 95% lower credible interval, and based on a Bayesian decision analysis, the overprotection loss exceeds the underprotection loss based on at least 10 years of data; 2) the minimum population size is ≥ 10,000 breeding pairs over ≥ 3 surveys; or, 3) the minimum estimate of abundance exceeds 25,000 breeding pairs in any survey (see Criteria for delisting from threatened status pp. 36-38 in USFWS 1996). The Russia breeding population has likely exceeded the third abundance criterion based on limited aerial surveys of the breeding and the wintering areas (Hodges and Eldridge 2001, Larned et al. 2012). Recent nest surveys indicate that the YKD breeding population has significantly increased since listing and may be close to meeting the first set of delisting criteria (USFWS 1996, Fischer et al. 2018, Lewis et al. 2019). Furthermore, studies to estimate detection were employed on both the YKD and ACP breeding grounds. Prior to these detection studies, researchers were unable to estimate breeding population size, which is a critical component to both the abundance threshold criterion and the decision analysis. Here, we assess the probability of both Alaskan breeding populations (YKD and ACP) meeting the first reclassification criterion.

Species classification decisions are liable to two possible errors: 1) failing to classify a species as threatened or endangered that should be classified (underprotection), or 2) classifying a species as threatened or endangered when it is not warranted (overprotection) (Taylor et al. 1996). Statistical decision theory provides a framework for linking statistical inference on population metrics to the risk of making a classification error (Taylor et al. 1996, Regan et al. 2013, Williams and Hooten 2016). The link between statistical inference and decision making occurs through the specification of a loss function that expresses the cost associated with the decision and the true state of nature (Berger 1985, Williams and Hooten 2016). For spectacled eiders loss is the cost of making classification errors measured in terms of the probability of the population declining to the designated quasi-extinction level of 250 breeding birds (125 breeding pairs) for a range of values of population growth (r) and estimated population size ($\widehat{N}$) (USFWS 1996). In the scope of this analysis, the spectacled eider classification problem consists of three action alternatives; 1) to delist the species, 2) maintain current (threatened) status, or 3) reclassify as endangered. However, we only consider alternatives one and two because recent surveys indicated the population size was close to the population threshold and the population size had increased over time.

Here, our specific objectives were to estimate the probability that Alaskan breeding populations met recovery classification thresholds by estimating abundance and population growth rate and quantify the risk of committing a classification error using a Bayesian decision analysis. First, we use Bayesian state-space models to estimate abundance and population growth rate for both populations. We estimate the probability of meeting the abundance threshold as the proportion of the posterior where $N_{2016} \geq$ 6,000 breeding pairs (or 12,000 breeding birds). Finally, we integrate abundance and growth rate with the loss functions to estimate over/underprotection loss (classification error). The results serve to inform classification decisions regarding spectacled eider populations with significant implications for the species and the Bureau of Land Management (BLM) and USFWS that expend considerable resources on their stewardship.

Methods

Survey Methods

Aerial surveys have been flown annually since the early 1990's to monitor both subpopulations of Alaskan spectacled eiders (Wilson et al. in prep, Amundson et al. in prep, Fischer et al. 2018). Here, we describe the specific details of the respective surveys and subsequent data collection.

Arctic Coastal Plain

U.S. Fish and Wildlife Service Division of Migratory Bird Management conduct annual aerial surveys sampling nearly 60,000 km^2 in the ACP to monitor the distribution, abundance, and trend of bird species. Original ACP surveys were flown 1986 – 2006, monitoring many avian species in the area. Following the listing of spectacled eiders in

1992, the North Slope Eider (NSE) survey was established and flown through 2006. In 2007, the ACP and NSE surveys were merged to form a redesigned ACP survey which has been flown from 2007 to the present (Wilson et al. *in prep,* Amundson et al. *in prep*). Here, we will focus on aerial survey data collected using the redesigned ACP survey (2007 to 2016). In 2015 and 2016, USFWS implemented double-observer techniques to estimate aerial detection probabilities of spectacled eiders breeding on the ACP (for details, see Wilson et al. *in prep*). Applying the estimated detection probabilities, Wilson et al. calculated detection-adjusted estimates of population size of indicated breeding pairs and variance. These estimates were used as data in our model and represent the best available data to date (Table 1).

Yukon-Kuskokwim Delta

Aerial surveys of spectacled eiders have been conducted over 12, 832 km of YKD tundra wetland habitat annually since 1988 (Fischer et al. 2018). Eider density varies widely across the YKD with low densities throughout a majority of the region. Lewis et al. (2019) identified three density-specific strata; low-density (0-1.60 nest/km), medium-density (1.60-3.50 nests/km), and high-density (>3.50 nests/km). Ground based surveys have been conducted annually on the YKD since 1985 to estimate the numbers of nests for geese and eiders. This survey samples randomly selected plots within the core nesting area of spectacled eiders in the central coast zone encompassing 716 km^2 (Fischer et al. 2018). Estimates of nests and aerial observations among low, medium, and high-density stratum on the YKD were used to calculate density-specific aerial visibility correction factors (VCF) to account for incomplete detection on aerial surveys. Lewis et al. (2019) converted the aerial indices of spectacled eider abundance to annual estimates of breeding numbers using the average density-specific visibility correction factors. The estimates generated from 2002-2016 were provided as observation data and error in our analysis and are the best available estimates to date.

State-space models

Our goal was to estimate mean population growth rate, $\bar{r}$, and process error or temporal variation in population growth rate σ_r from detection adjusted abundance estimates from aerial surveys of spectacled eiders on the YKD and ACP. We utilized a Bayesian state-space model to partition population dynamics into two components, the hidden state process and the observation model, and fit the process model to the time series of observations. State-space models simultaneously account for both process error and observation error caused by partial observability. Our state-space model describes population growth mathematically as

$$\log(N_{t+1}) = \log(N_t) + r_t \qquad (1)$$

where N_t is the number of breeding birds (YKD) or breeding pairs (ACP) in year t, r_t is population growth rate and

$$r_t \sim Normal(\bar{r}, \sigma_r). \qquad (2)$$

Prior distributions for initial abundance were the mean detection adjusted estimates for 2007 (Table 1) where for the ACP $\log(N_{2007}) \sim N(\log(3{,}698)\,, 0.1)$ and for the YKD $\log(N_{2007}) \sim N(\log(12{,}457)\,, 0.1)$ (Lewis et al. 2019, Wilson et al. *in prep*). Based on expert opinion, it is unlikely that spectacled eiders could exhibit more than 10% process related variation within a given year. Thus, for both models mean population growth was normally distribution around 0 with 10% variation, $\bar{r} \sim N(0, 0.1)$, and the variance of mean growth $\sigma_r \sim Gamma(a, s)$ was kept low, with shape parameter, $a = 3$, and the scale parameter $s = 0.2$.

The observation model relates the true population size N_t to the observations corresponding to the detection adjusted abundance indices for each breeding ground. Thus, our observation process was

$$\widehat{y_t} \sim Normal\left(N_t, \hat{\sigma}_{\widehat{y_t}}\right) \tag{3}$$

where the observations, $\widehat{y_t}$, were the detection adjusted abundance indices of spectacled eiders from the aerial surveys on the respective breeding grounds (i.e., ACP and YKD) (Lewis et al. 2019, Wilson et al. *in prep*) (Figure 1, Table 1). Annual observation error from aerial survey sampling ($\hat{\sigma}_{\widehat{y_t}}$) were provided as data (see similar approach in Rotella et al. 2009 and Koons et al. 2017) (Table 1).

In 2011, aerial surveys were not flown on the YKD and therefore there is no observation for that year. We estimated observation error for 2011 using a zero-intercept linear regression model where $\hat{\sigma}_{x_t}$ is the predicted observation error as a function of estimated population size N_t and $\beta \sim Normal(0{,}30)$

$$\hat{\sigma}_{x_t} = \beta * N_t \tag{4}$$

$$\hat{\sigma}_{z_t} \sim N(\hat{\sigma}_{x_t}, \sigma) \tag{5}$$

and where $\hat{\sigma}_{z_t}$ is the estimated observation error in year t and is normally distributed about $\hat{\sigma}_{x_t}$ with a standard deviation $\sigma \sim Gamma(a, s)$ where the shape parameter, $a = 2$, and the scale parameter $s = 100$. The recovery team expressed interest in understanding the effects of differing model structures (i.e. prior distributions, use of linear regression) on the decision analysis. To address these concerns we formulated three alternative state-space models and using the outputs from each we calculated the misclassification errors. Details are outlined in the Supporting Information.

We fit the state-space models in a Bayesian framework implementing Markov chain Monte Carlo methods (MCMC, Gelfand and Smith 1990) to sample the posterior distributions in JAGS 3.3.0 (Plummer 2012), using the jagsUI package in R (Kellner 2015). We ran three MCMC chains for 100,000 iterations, set thin to 2, discarded 70,000 as burn-in, and ran 5,000 iterations in the JAGs adaptive phase. We checked convergence using the Gelman-Rubin statistic (Gelman and Rubin 1992) and all results were satisfactory (all $\hat{R} <$1.01).

Decision Analysis

Loss functions are calculated given the posterior estimates of population growth $r \sim N(\bar{r}, \hat{\sigma}_r)$ and abundance in the final year N_{2016} converting these metrics into a measure of risk according to probability of extinction (Table 2). The cost of making decision errors is measured in terms of the probability of decreasing to under 250 adults (125 breeding pairs) in 50 years (USFWS 1996). The recovery team specified that this abundance would leave only one management option; to capture the birds and breed them in captivity. It was therefore set as the quasi-extinction threshold for measuring risk as a function of extinction probability and management options. The recovery team chose a symmetrical loss function, which penalizes overprotection and underprotection equally (Figure 2) (Taylor et al. 1996, USFWS 1996). The loss functions follow a sigmoid curve. There is an increasing penalty for progressively larger differences between the decision and true state of nature until the probability of quasi-extinction reaches 0 or 1 indicating equivalent loss for more extreme values (Figure 2).

The basic elements in statistical decision analyses include, θ the state of nature which affects the decision process and Θ is all possible states of nature (Berger 1985, Williams and Hooten 2016). The decisions or actions are denoted by a, and all possible actions considered may be denoted $\mathcal{A}$. The loss function, $L(\theta, a)$ describes the loss associated with taking action (a) and θ is the state of nature and the function is defined for $(\theta, a) \in \Theta * \mathcal{A}$. Following Berger (1985) and Williams and Hooten (2016), the general notation for Bayesian expected loss is:

$$P(a) = E_{\theta|y} L(\theta, a) = \int_{\Theta} L(\theta, a)[\theta|y]\, d\theta\ . \qquad (6)$$

In this analysis, the unknown state of nature, θ, is the unknown probability of quasi-extinction within 50 years and is a function of abundance (N_{2016}), population growth rate (r), and process error (σ_r). The action or decision (a) refers to species classification errors. If the population is stable or increasing ($r \geq 0$), classifying the species as threatened would not be warranted and thus results in overprotection. If the population is decreasing($r < 0$), not classifying the species as threatened when it is warranted results in underprotection.

We generated the loss function by projecting the population over 50 years for a range of population growth rates denoted rs. The range of rs was set from -0.4 to 0.4 because the posterior distributions on r produced from the state-space model fell within these limits. First, initial abundance is chosen from the distribution of N_{2016} (see Table 2 for values); (2) process variance s_r is selected from the posterior distribution generated in the state-space model; (3) r' is pulled from $N(rs, s_r)$ for each year; (4) project population until N < 250 breeding birds (125 breeding pairs); and (5) steps 1-4 are repeated 10,000 times for each value of r, and the year abundance falls below the quasi-extinction threshold is saved. The first loss function assesses the probability of falling below the quasi-extinction level (underprotection) for values when $-0.4 \leq rs < 0$. The secondary loss function for values of $0 \leq rs \leq 0.4$ is simply the mirror image of the first loss function because they are symmetrical. The interpretation of the secondary loss function is the probability of not falling below the quasi-extinction level and corresponds to overprotection. Finally, to calculate loss for each error type, we multiply the posterior distribution of mean population growth rate generated from the state-space model by each loss function. The expected loss for each error type is a single value generated after integrating out all possible values of r.

Results

We found differing results in the ACP and YKD populations based on posterior estimates of abundance, population growth rates, and over/underprotection losses (Table 2). Estimated mean abundance for the ACP population in 2016 was 3,557 breeding pairs (95% CRI 2,630 to 4,476 (Figure 1). Based on estimated abundance in year 2016, the ACP population has nearly zero probability (P = 0.000007) of meeting the abundance threshold (95% LCRI $= \widehat{N} \geq$ 6,000 breeding pairs). The 10-year mean growth rate for the ACP population was negative $\bar{r}$ = -0.005 but variable, evident by the wide credible intervals (95% CRI -0.125 to 0.115) (Figure 2). Furthermore, underprotection loss for the ACP population was greater than overprotection loss (Table 2). Alternatively, estimated mean abundance for the YKD population in 2016 was 14,541 breeding birds (95% CRI 12,840 to 16,114). The 95% LCRI of abundance in 2016 was above 12,000 breeding birds indicating the YKD breeding population had met the abundance threshold criterion. Additionally, the overprotection loss exceeded the underprotection loss for the YKD breeding population (Table 2). Mean population growth for the YKD population was $\bar{r}$ = 0.003 but highly variable with wide credible intervals (95% CRI -0.145 to 0.153) (Figure 2).

Discussion

Results differed between the two breeding populations; the YKD breeding population met both recovery criteria, however, the ACP breeding population did not meet either. Unsurprisingly, the ACP breeding population was not close to meeting either of the reclassification criteria. Spectacled eiders nest in relatively low numbers across the ACP and the population growth rate combined with low abundance results in a population at greater risk of declining than increasing. Higher underprotection loss than overprotection loss indicates the ACP population is at risk of falling below the quasi-extinction value of 125 breeding pairs in the next 50 years and maintaining threatened status would be the optimal decision (Table 2). However, for the YKD population, overprotection loss exceeds underprotection loss and the 95% LCRI of abundance in 2016 is above abundance threshold criterion indicating the population has met both recovery criteria for delisting (Table 2).

Mean population growth over the time series is near zero for both breeding populations (Table 2). Thus, over and underprotection losses are similar because there is near equivalent overlap of the posterior distribution for negative and positive values of population growth (Table 2, Figure 2). These results highlight a unique feature of symmetrical loss functions which makes overprotection and underprotection errors inversely related. The higher the probability of committing an overprotective error, the lower the probability of committing an underprotective error and vice versa (Taylor et al. 1996). For example, we would expect greater certainty in the classification decision as the overprotection loss nears 1 and underprotection loss nears 0. For this decision problem, the similar loss values indicate there is considerable uncertainty in the probability of reaching quasi-extinction given abundance, process error, and population growth rate estimates. Although this introduces additional uncertainty in the decision space it also provides the decision makers with a probabilistic result of committing a classification error.

A considerable portion of variation in the YKD mean population growth rate can likely be attributed to the low abundance estimate in 2015 (Table 1, Figure 1). The perceived decline in abundance is potentially related to the observation processes that generated the detection adjusted abundance estimates. Lewis et al. (2019) used density-specific visibility correction factors (VCF) averaged from surveys conducted from 1993 to 2014, during which time the same observer conducted the aerial survey each year. Beginning in 2015, a new observer was assigned to conduct the aerial surveys and with significantly lower detection counted very few spectacled eiders (Lewis et al. 2019). The resulting abundance estimate is certainly biased low because estimates from the YKD nest plot survey indicated there were greater than 7,000 nests in 2015 (Fischer et al. 2017, pg. 26 of report). Furthermore, because the VCF applied was constant and applied to all years, the posterior on process variance is likely biased high. In the Bayesian context, a model could be fit with observer and year specific priors on detection estimating these parameters. However, this would lead to greater uncertainty in estimates of population growth rate, process error, and expected loss.

This analysis represents a significant improvement in accounting for observation processes when estimating abundance and growth rate. Prior to the extensive detection studies conducted on the ACP and YKD, population assessment was hindered due to lack of robust data on observation processes. Without such data, assessing the probability of meeting the abundance threshold would require strong assumptions regarding detection. Unadjusted aerial indices for both populations are biased low and would indicate that neither population met the abundance criterion (Table S1). Alternatively, a common practice amongst large scale aerial surveys conducted in remote regions (see Waterfowl Breeding Population and Habitat Survey of North America (BPOP)) is to estimate VCFs based on a single study over limited spatial extent. In such cases, the VCF produced does not account for factors affecting detectability such as habitat, density, survey timing, or inter-annual variability (Lewis et al. 2019). On the YKD, an eider-specific (*Somateria and Polysticta spp.*) VCF was developed in 1968 where VCF = 3.58 (detection rate = 1/VCF) indicating detection probability of eiders on aerial surveys was low (<30%) (Lensink 1968). In 2006 following extensive annual ground surveys of spectacled eider nests beginning in 1985 a new VCF was developed where VCF = 2.35 indicating detection was higher at nearly 43% (Platte and Stehn 2015). In previous work, Dunham and Grand (*in review*) demonstrated that applying either of these VCFs to adjust aerial indices results in overinflated estimates of abundance (see also, Table 5 in Lewis et al. 2019) thereby inaccurately increasing the probability of having met the abundance criterion. Furthermore, without explicitly accounting for nesting density, spatial distribution, or inter-annual variability we risk inappropriately increasing certainty in the abundance estimate. If aerial indices were adjusted using either of the deterministic VCFs the results would provide decision makers with misleading information with potentially significant consequences for the species and the USFWS (Dunham and Grand *in review*).

Conservation and management decisions are commonly based on abundance thresholds (Nichols et al. 2007, North American Waterfowl Management Plan 2014, Boyd et al. 2017, USFWS 2017) and making inference about abundance can be challenging due to multiple pervasive sources of uncertainty stemming from observation and process errors (Williams et al. 2001, Nichols and Williams 2006). Decision-makers are tasked with trying to choose the best action to take for conservation or management despite these uncertainties. The methods employed here provide an example of accounting for these uncertainties in such a way that the decision-makers may understand the probability of committing a classification error. Using Bayesian state-space models we explicitly account for both observation and process error while incorporating prior knowledge of the system (King et al. 2009, Newman et al. 2014). However, such statistical inference alone does not directly provide guidance for decisions. Integrating statistical analyses with decision-theory explicitly links statistical inference to the decision problem creating a rigorous analysis to support decision-making. The combined strengths in these approaches provide a robust framework for formally linking ecological inference to conservation and management decisions under considerable uncertainty (Taylor et al. 1996, Nichols et al. 2007, Regan et al. 2013, Williams and Hooten 2016). Incorporating both the abundance threshold and decision analysis in the reclassification criteria greatly increases the transparency and defensibility of the classification decision for threatened spectacled eiders. Finally, we believe this analysis adds to the growing support for decision-theoretic approaches in applied ecology and conservation (Thompson et al. 2018).

Literature Cited

Berger, J.O. 1985. Statistical decision theory and Bayesian analysis. Springer, New York, New York, USA.

Boyd, C., D.P. DeMaster, R.S. Waples, E.J. Ward, and B.L. Taylor. 2017. Consistent extinction risk assessment under the U.S. Endangered Species Act. Conservation Letters 10(3):328-336.

Dau, C.P., and S.A. Kistchinski. 1977. Seasonal movements and distribution of spectacled eider. Wildfowl 28:65-75.

Ely, C.R., C.P. Dau, and C.A. Babcock. 1994. Decline in a Population of spectacled Eiders Nesting on the Yukon-Kuskokwim Delta, Alaska. Northwestern Naturalist 75:81–87.

Fischer, J.B., R.A. Stehn, T.D. Bowman, R.M. Platte, W.D. Eldridge, J.J. Hodges, and W.I. Butler. 2018. Coordinated aerial and ground surveys document long-term recovery of geese and eiders on the Yukon-Kuskokwim Delta, Alaska, 1985–2014. In Trends and traditions: Avifaunal change in western North America (W. D. Shuford, R. E. Gill Jr., and C. M. Handel, Editors). Studies in Western Birds 2 (*In press*). Western Field Ornithologists, Camarillo, CA.

Fischer, J.B., A.R. Williams, and R.A. Stehn. 2017. Nest population size and potential production of geese and spectacled eiders on the Yukon-Kuskokwim Delta, Alaska, 1985-2016. Unpubl. Rep., U.S. Fish and Wildlife Service, Anchorage, AK.

Flint, P.L., and J.B. Grand. 1999. Incubation behavior of spectacled eiders on the Yukon-Kuskokwim Delta, Alaska. The Condor 101:413-416.

Flint, P.L., J.A. Morse, J.B. Grand, and C.L. Moran. 2006. Correlated growth and survival of juvenile spectacled eiders: evidence of habitat limitation? The Condor 108:901-911.

Flint, P.L., J.B. Grand, M.R. Petersen, and R.F. Rockwell. 2016. Effects of lead exposure, environmental conditions, and metapopulation processes on population dynamics of spectacled eiders. North American Fauna 81:1-41

Gelfand, A.E., and A.F.M. Smith. 1990. Sampling-based approaches to calculating marginal densities. Journal of the American Statistical Association 85(410): 398-409.

Gelman, A., and D.B. Rubin. 1992. Inference from iterative simulation using multiple sequences. Statistical Science 7(4): 457-511.

Gerber, B.D., and W.L. Kendall. 2017. Evaluating and improving count-based population inference: A case study from 31 years of monitoring Sandhill Cranes. The Condor 119(2): 191-206.

Grand, J.B. and P.L. Flint. 1997. Productivity of nesting spectacled eiders on the lower Kashunuk River, Alaska. The Condor 99:926-932.

Kellner, K. 2015. A wrapper around ‘rjags’ to streamline ‘JAGS’ analyses: Package ‘jagsUI’ version 1.4.9. https://github.com/kenkellner/jagsUI

Kellner, K.F., and R.K. Swihart. 2014. Accounting for imperfect detection in ecology: A quantitative review. PLoS ONE 9.

King, R., B.J.T Morgan, O. Giminez, and S.P. Brooks. 2009. Bayesian analysis for population ecology. London: Chapman and Hall/ CRC.

Koons, D.N., D.T. Iles, M. Schaub, and H. Caswell. 2016. A life-history perspective on the demographic drivers of structured population dynamics in changing environments. Ecology Letters 19: 1023-1031.

Kruse, K.L., J.A. Dubovsky, and T.R. Cooper. 2014. Status and harvest of sandhill cranes: mid-continent, Rocky Mountain, lower Colorado River valley and eastern populations. Administrative Report, U.S. Fish and Wildlife Service, Lakewood, CO. 14pp.

Lewis, T.L., M.A. Swaim, J.A. Schmutz, J.B. Fischer. 2019. Improving population estimates of threatened spectacled eiders: correcting aerial counts for visibility bias. Endangered Species Research 39:191-206. doi.org/10.3354/esr00959

Newman, K.B., S.T. Buckland, B.J.T. Morgan, R. King, D.L. Borchers, D.J. Cole, P. Besbeas, O. Giminez, and L. Thomas. 2014. Modelling population dynamics: model formulation, fitting, and assessment using state-space methods. Methods in Statistical Ecology, Springer, New York.

Nichols, J.D., and B.K. Williams. 2006. Monitoring for conservation. Trends in Ecology and Evolution 21:668–673.

Nichols, J.D., M.C. Runge, F.A. Johnson, and B.K. Williams. 2007. Adaptive harvest management of North American waterfowl populations: a brief history and future prospects.

North American Waterfowl Management Plan Committee. 2014. Revised Objectives: An addendum to the 2012 North American Waterfowl Management Plan.

Platte, R.M., and R.A. Stehn. 2015. Abundance and trend of waterbirds on Alaska's Yukon-Kuskokwim Delta Coast based on 1988 to 2015 aerial surveys. Unpublished report, U.S. Fish and Wildlife Service, Anchorage, AK.

Plummer, M. 2012. JAGS version 3.3.0. http://sourceforge.net/projects/ mcmc-jags/files/Manuals/

Regan, T.J., B.L. Taylor, G.G. Thompson, J.F. Cochrane, K. Ralls, M.C. Runge, and R. Merrick. 2013. Testing decision rules for categorizing species' extinction risk to help develop quantitative listing criteria for the U.S. Endangered Species Act. Conservation Biology 27(4): 821-831.

Rotella, J.J., W.A. Link, J.D. Nichols, G.L. Hadley, R.A. Garrott, and K.M. Proffitt. 2009. An evaluation of density-dependent and density-independent influences on population growth rates in Weddell Seals. Ecology 90(4): 975-984.

Stehn, R.A., C.P. Dau, B. Conant, and W.I. Butler. 1993. Decline of spectacled eiders nesting in western Alaska. Arctic 46:264-277.

Taylor, B.L., P.R. Wade, R.A. Stehn, and J.F. Cochrane. 1996. A Bayesian approach to classification criteria for spectacled eiders. Ecological Applications 6(4):1077-1089.

Thompson, G.G., L.A. Maguire, and T.J. Regan. 2018. Evaluation of two approaches to defining extinction risk under the U.S. Endangered Species Act. Risk Analysis 38(5):1009-1035.

Williams, B.K., J.D. Nichols, and M.J. Conroy. 2001. Analysis and management of wildlife populations. San Diego: Academic.

Williams, P.J. and M.B. Hooten. 2016. Combining statistical inference and decisions in ecology. Ecological Applications 26(6): 1930-1942.

Wilson, H.M., R.A. Stehn, and J.B. Fischer. *in prep.* Aerial survey detection rates for spectacled eiders on the Arctic Coastal Plain, Alaska.

USFWS. U.S. Fish and Wildlife Service. 1993. Final rule to list the spectacled eider as threatened. Federal Register 58: 27474–27480.

USFWS. U.S. Fish and Wildlife Service. 1996. Spectacled eider recovery plan. Anchorage, Alaska: U.S. Fish and Wildlife Service.

USFWS. U.S. Fish and Wildlife Service. 2017. Waterfowl population status, 2017. U.S. Department of the Interior, Washington, D.C. USA

Tables

Table 3-1. Detection adjusted abundance estimates for both Alaskan breeding populations of spectacled eiders (*Somateria fischeri*) from 2007 to 2016. Estimates were provided as observed data (y) in the observation process model.

	YKD[a] *Number of breeding birds*			ACP[b] *Number of breeding pairs*		
Year	$\widehat{y_t}$	$\sigma_{\widehat{y_t}}$	95% Confidence intervals	$\widehat{y_t}$	$\sigma_{\widehat{y_t}}$	95% Confidence intervals
2007	12,457	1,408	9,698 – 15,216	3,698	574	2,669 – 4,927
2008	14,599	1,470	11,718 – 17,480	4,424	564	3,399 – 5,621
2009	15,586	1,463	12,718 – 18,454	3,837	583	2,777 – 5,071
2010	13,698	1,273	11,202 – 16,193	4,473	630	3,329 – 5,808
2011	NA	1,409[c]	NA	5,787	692	4,551 – 7,273
2012	14,894	1,375	12,198 – 17,590	3,383	414	2,636 – 4,267
2013	16,171	1,460	13,309 – 19,033	5,565	674	4,349 – 7,000
2014	13,386	1,360	10,719 – 16,052	4,905	745	3,563 – 6,492
2015	5,618	627	4,388 – 6,847	3,828	536	2,869 – 4,976
2016	15,118[d]	1,472[d]	12,233 – 18,003	3,411	546	2,412 – 4,550

[a] Analysis and data reported for 2007 to 2015 in Lewis et al. 2019 (see Tables 5 and 6 for data).

[b] Analysis and data reported in Wilson et al. *in press* (refer to Table 4).

[c] Mean estimated observation error ($\bar{\sigma}_{z_{2011}}$) from linear regression model (see Methods eqns. 4 & 5)

[d] Data reported for 2016 in Swaim 2017 *unpublished report* following methods in Lewis et al. 2019.

Table 3-2. Posterior estimates of population metrics and loss for both Alaskan breeding populations of spectacled eiders (*Somateria fischeri*). Consideration for reclassification from threatened to recovered requires that both populations must reach or exceed the abundance threshold, and overprotection loss must be greater than underprotection loss.

		ACP[a]	YKD[b]
Abundance			
	Mean	3,557	14,541
	SE	471	808
	95% CRI	2,630-4,476	12,840-16,114
Population growth ‘r’			
	Mean	-0.005	0.003
	SE	0.059	0.075
	95% CRI	-0.125, 0.115	-0.145, 0.153
Underprotection		0.190	0.253
Overprotection		0.169	0.283
P(N_{2016} ≥ threshold)		0.000007%[a]	99.80%
Process error		0.218	0.351

[a] ACP metrics refer to the Arctic Coastal Plain breeding population.

[b] YKD metrics refer to the Yukon-Kuskokwim Delta breeding population.

Result of 1 value in posterior of N_{2016} being ≥ 6,000 breeding pairs

Figures

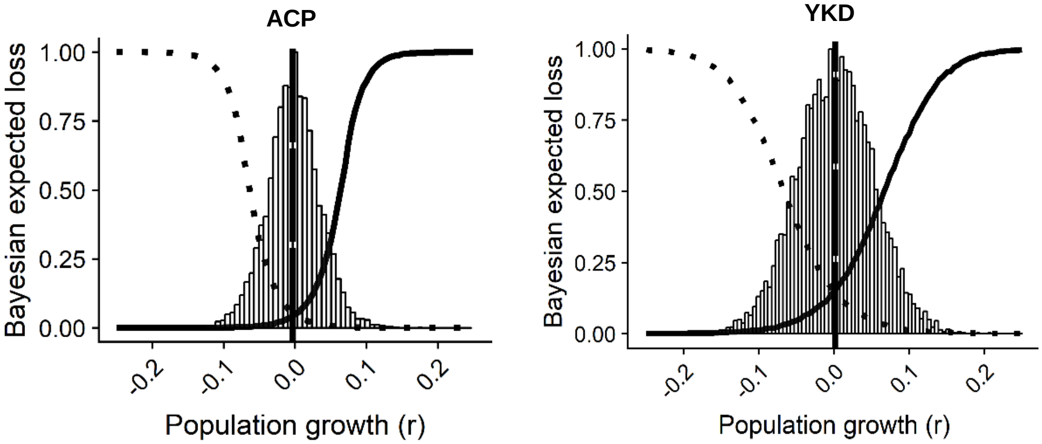

Figure 3-1. Loss functions generated using the probability of quasi-extinction (N <250 adults within 50 years) given population size, growth rate, and process error for the Arctic Coastal Plain (ACP) and Yukon-Kuskokwim Delta (YKD) breeding populations of spectacled eiders (*Somateria fischeri*). The dotted line represents the under protection loss function and the solid line is the over protection loss function. Histograms show the distribution of population growth rate (*r*) estimated by a Bayesian state-space model for the time series from 2007 to 2016. The vertical dashed line represents the mean population growth rate over the time series.

Supporting Information – Chapter 3: Assessing recovery of spectacled eiders using a Bayesian decision analysis

The spectacled eider recovery team identified model structure as a concern for the potential influence on the calculation of misclassification error. Therefore, we constructed three additional models to explore the sensitivity of the decision to the effects of model structure. Model YKD_S1 follows the same structure of the YKD model used in this chapter, but was initiated with non-informative or less informative priors. Changes in prior distributions for YKD_S1 included initial abundance where the mean was the detection adjusted estimate for 2007 but with a much larger variance, $\log(N_{2007}) \sim N(\log(12{,}457), 1000)$. Further, we increased the variance around with the prior $\bar{r} \sim N(0, 1)$, and the variance of mean growth $\sigma_r \sim Gamma(a, s)$ was increased, with shape parameter, $a = 3$, and the scale parameter $s = 2$.

Additionally, we tested two alternative model structures for dealing with the missing observation in 2011. First, model YKD_S2 has no linear regression to estimate the missing observation error, and the 2011 observation is skipped, thereby removing a data point from the time series. For model YKD_S3 we retained the linear regression but skipped the 2011 observation in the observation process model. We developed these models to test influence of our decision to impose constraints on the observation error. In the original model (YKD) we estimate observation error for 2011 using the linear relationship between population size and observation error, but treat this estimate as data.

Bayesian hierarchical models can easily be extended to include NA's in the data set and will estimate those values. Therefore, we altered the observation model to skip the missing observation in 2011. Finally, we were interested in the effect the linear regression had on the key population metrics.

Table Supp. Info. Posterior estimates of population metrics and misclassification error for different model formulations of YKD breeding spectacled eiders (*Somateria fischeri*).

		YKD	YKD_S1	YKD_S2	YKD_S3
Abundance					
	Mean	14,541	14,768	13,838	14,552
	SE	808	821	1,527	811
	95% CRI	12,840-16,114	13,111-16,406	10,825-16,804	12,839-16,122
Population growth 'r'					
	Mean	0.003	0.006	0.005	0.004
	SE	0.075	0.167	0.075	0.076
	95% CRI	-0.15, 0.15	-0.33, 0.34	-0.14, 0.15	-0.15, 0.15
Underprotection		0.253	0.339	0.199	0.204
Overprotection		0.283	0.365	0.246	0.243
P(N_{2016} ≥ threshold)		99.80%	99.78%	88.45%	99.65%
Process error		0.351	0.600	0.346	0.352

The introduction of non-informative prior distributions (YKD_S1) did not have any influence on the estimate of abundance, but nearly doubled the standard error of mean population growth and process error. Ultimately, using this model structure, the population still meets the abundance threshold and overprotection error is greater than underprotection error. However, the variation in annual population growth is more than 3 times what species experts deemed biologically plausible. Model YKD_S2 produced the only results that would indicate the population had not met the abundance threshold but still met the misclassification error criterion. Without the linear regression, the unknown observation error was seemingly absorbed into the estimate of abundance and increases the uncertainty in that estimate. The standard error around mean abundance in 2016 is nearly double that produced by the other 3 models. The removal of the linear regression had no effect on the estimate of population growth, process error, or misclassification error. In model YKD_S3 we reintroduced the linear regression but skipped the missing observation for 2011 in the observation process model. The estimates of abundance, growth, and misclassification error are consistent with the other two models that include the linear regression (YKD, YKD_S1). These results demonstrate there is clearly an effect of the constraints imposed by the assumption of a linear relationship between abundance and observation error. Further research and discussion with the recovery team is warranted to identify the optimal model for decision-making.

Chapter 4: Demographic responses to climate change and predation pressure in a threatened Arctic species

Abstract

The consequences of climate change on Arctic species throughout the annual cycle remain largely unknown due to logistical challenges of studying these species. Spectacled eiders, a sea ice obligate Arctic sea duck, face numerous threats related to climate change and altered biotic communities. Multiple studies monitoring demographic parameters (survival, productivity, abundance) on the Yukon-Kuskokwim Delta of Alaska have produced long-term data sets. We leverage these data to estimate vital rates including those that are unobservable, estimate population size and trend, and quantify ecological relationships. Abundance has increased since listing in the 1990’s and population growth is stable. We found that adult survival was highest in years with a moderate number of days with >95% sea ice cover and declined when ice cover was greater or less than the long term average. Additionally, we found evidence of a similar relationship with extreme sea ice days and hatch year survival. Nest success exhibited a strong, negative correlated with fox abundance, potentially creating a threat to future viability and recovery of the species. The global population of spectacled eiders winters together and ice conditions are projected to become anomalous in the core wintering area. It is likely that extreme sea ice conditions would negatively impact population dynamics through

decreased survival. If both reproductive success and adult survival decline simultaneously and are not compensated for we should expect populations to decline.

Introduction

Climate induced temperature increases in the Arctic have caused profound changes in both terrestrial and marine ecosystems. Effects of climate change on Arctic species may be most pronounced in resident species that inhabit both terrestrial and marine ecosystems. Rapid and unprecedented changes in environmental conditions have had strong and complex impacts on Arctic species habitats, food resources, and biotic interactions (Kubleck et al. 2018).

The consequences of climate change, and specifically sea ice loss, on Arctic species remains largely unknown because it is often challenging to study these species due to logistical difficulties associated with monitoring in remote areas. There remains a critical data gap for many Arctic species (Laidre et al. 2015, Macias-Fauria and Post 2018) and their response to climate change. Species often lack long-term data sets and are studied only during short periods, typically during the breeding season. Yet, they are vulnerable to changes occurring throughout the annual cycle. Changes in response to a warming climate may most notably affect species that require sea ice and terrestrial habitats for life history events. Understanding full annual cycle dynamics in relation to environmental conditions is critical for making predictions and conservation planning.

Quantifying population dynamics is difficult due to complex and often unobservable processes acting upon individuals throughout the annual cycle. Recent developments in statistical modeling have made it possible to integrate data sets (e.g., counts, mark-recapture) in a single modeling framework to estimate processes not directly measured (Schaub and Abadi 2011). Further integration with full annual cycle (FAC) models include effects of events in breeding and non-breeding seasons on population dynamics (Hostetler et al. 2015, Rushing et al. 2017). These combined models can be used to identify and quantify vulnerability to specific threats throughout the annual cycle, estimate population viability, and reduce uncertainty in the true population state.

Spectacled eiders (*Somateria fischeri*), are a sea ice-obligate species listed as threatened under the Endangered Species Act (ESA, as amended 1973) following an estimated population decline of >90% in western Alaska between the 1970's and 1990's (USFWS 2002). Spectacled eiders spend the majority of the annual cycle in marine habitats coming to land only during the breeding season to nest and raise young. Spectacled eiders have a geographically restricted range and the global population winters in the Bering Sea south of St. Lawrence Island, an area historically dominated by sea ice interspersed with openings in the form of leads or polynyas.

Given the species exposure to extreme arctic and sub-arctic conditions through the annual cycle, spectacled eiders face numerous threats related to both indirect and direct effects of climate change. Research indicates that sea ice conditions in the Bering Sea are predicted to become highly variable and sea ice extent is expected to decrease in the future (Wang and Overland 2015). Concentrated sea ice can dampen the effects of waves from major storms and offers roosting habitat for spectacled eiders during the wintering period. However, extremely high sea ice concentrations may make it impossible for eiders to dive for their prey or openings may only be available in suboptimal foraging areas. Furthermore, drastic declines in sea ice due to increased temperatures can have negative impacts on primary productivity and have cascading effects through trophic interactions. Intermediate concentrations of sea ice may be optimal for many sea ice associated species because it provides access to food and offers a resting area (Christie et al. 2018).

Spectacled eiders inhabit large geographically remote breeding habitats across two countries and spend the remainder of the annual cycle in high latitude open ocean or coastal marine habitats (Bowman et al 2015, Sexson et al. 2016). Spectacled eiders are relatively long lived species the exhibit delayed reproduction, high adult survival rates, and variable annual reproductive success (Petersen et al. 2000). Spectacled eiders do not breed until their second or third year. Most monitoring for these species occurs on the breeding grounds, making it difficult or impossible to gather data on non-breeding age birds. While prior demographic analyses have indicated that variation in adult survival has the strongest impact on population growth rate, recruitment to the breeding population likely has considerable influence over annual growth and long-term population dynamics. Recent trends indicate predation pressure on Arctic nesting birds has increased substantially over the past few decades (Kubelka et al. 2018). Using a unified analysis of monitoring data we can link population dynamics to environmental conditions faced throughout the annual cycle and identify limiting factors for population growth.

Multiple studies that monitor demographic parameters (survival, productivity, abundance) of spectacled eiders have produced long-term data sets that have been analyzed only in a piece-meal fashion and have been unable to estimate values for a number of demographic parameters due to a lack of data and integrated analyses. In this study, we used a Bayesian integrated population model to simultaneously analyze long-term mark-recapture data, breeding population counts, and productivity data for spectacled eiders. The primary strength of our approach is the efficient combination of data sources in a unified framework that allows the estimation of first year survival and breeding propensity of 2-year-old birds, for which there are no explicit information available. We applied integrated population models to gain information on vital rates of multiple stage classes and precisely estimate population size and trend on the YKD. Further, we aim to demonstrate how survival and breeding propensity were affected by winter sea ice conditions as well as how nest success was affected by breeding site covariates. This modeling framework enables us to utilize long-term monitoring data from the breeding period to infer full annual cycle population dynamics for a threatened Arctic species.

Methods

Study area and species

Spectacled eiders are a large Arctic sea duck listed as threatened under the Endangered Species Act (ESA as amended, 1973) in 1993 (USFWS 1993). There are two subpopulations of Alaskan breeding spectacled eiders, one population on the Yukon-Kuskokwim Delta (YKD) and the other on the Arctic Coastal Plain (ACP) and a large population breeding in Arctic Russia (USFWS 1993, Flint et al. 2016) (see map; Figure 1). Both Alaskan subpopulations have been monitored annually since the 1980's using aerial surveys and/or nest monitoring and capture-mark-recapture methods. We focused on the Yukon-Kuskokwim Delta breeding population, given the existence of long-term data sets and known population growth.

The coastal plain of the YKD is one of the largest and most productive waterfowl breeding areas in Alaska. The Delta is predominately flat wetlands and tundra interspersed with small ponds, lakes, and rivers. The primary study area was on Kigigak Island (60°50’N, 165°50’W) with primarily high graminoid and intermediate sedge meadows characteristic of the tidally influenced habitats of the YKD (Flint et al. 2016). Spectacled eiders typically arrive on the breeding grounds in late May; males depart 1-2 weeks after incubation begins, and females and their young leave for the wintering grounds in late August. Studies have identified strong breeding and molting site fidelity, important geographical locations, and broad spatiotemporal patterns of spectacled eiders throughout the annual cycle (Petersen et al. 1999, Lovvorn et al. 2014, Sexson et al. 2014, 2016). The global population of spectacled eiders winters in one distinct region in the Bering Sea south of St. Lawrence Island (Petersen et al. 1999, Sexson et al. 2014). Females marked on the YKD used Norton Sound as their primary staging area during fall. Following the wintering period, individuals previously marked on the YKD either went to the Western Bering Strait, Norton Sound, or the YKD prior to the breeding period (Sexson et al. 2014).

Demographic and count data collection

Aerial surveys of spectacled eiders have been conducted on 12,832 km of YKD tundra wetland habitat annually since 1988 (Platte and Stehn 2015, Fischer et al. 2017, Lewis et al. 2019). Eider density varies widely across the YKD with low densities throughout a majority of the region. Lewis et al. (2019) identified three density-specific strata; low-density (0-1.60 nest/km), medium-density (1.60-3.50 nests/km), and high-density (>3.50 nests/km). Ground-based surveys have been conducted annually on the

YKD since 1985 to estimate the numbers of nests for geese and eiders. This survey samples randomly selected plots within the core nesting area of spectacled eiders in the central coast zone encompassing 716 km^2 (Fischer et al. 2017). Estimates of nests and aerial observations among low, medium, and high-density stratum on the YKD were used to calculate density-specific aerial visibility correction factors (VCF) to account for incomplete detection on the aerial surveys. The average density-specific visibility correction factors were used to convert indices of eider abundance to annual estimates of breeding spectacled eiders and variance (Lewis et al. 2019). These estimates are utilized as observation data as are errors in the estimates.

On the YKD, survival and productivity studies were carried out on Kigigak Island (1993-2015) following protocols established by Grand and Flint (1997). For a detailed explanation of field methodologies see Grand and Flint (1997) and Flint et al. (2016). Nest searching began in late May through mid-June at Kigigak Island. Adult females were captured on nests and given metal leg bands, numbered plastic leg bands, and nasal disks. In some years, a subset of females were marked at hatch with radio transmitters and monitored to estimate duckling survival. At approximately 30 days post-hatch ducklings were captured and marked with stainless steel and plastic bands. Most marked birds were adults and thus classified as breeding age. Only the birds marked as ducklings were of known age upon recapture.

Integrated population model

We constructed the following matrix projection model ($\mathbf{A}_t$) based on the life cycle diagram shown in Figure 2 to model survival, transition probabilities, and recruitment of female spectacled eiders

$$\mathbf{A}_t \ = \begin{bmatrix} 0 & 0 & f/2 * \phi_0 & f/2 * \phi_0 \\ \phi_1 * 1 - \alpha & 0 & 0 & 0 \\ \phi_1 * \ \alpha & 0 & 0 & 0 \\ 0 & \phi_2 & \phi_2 & \phi_2 \end{bmatrix}_t$$

where ϕ_i represents annual survival probabilities for hatch-year birds (ϕ_0), immature birds (ϕ_1), and adult birds ϕ_2 age 2 years and older. Spectacled eiders may begin breeding at 2 years of age, but evidence suggests they are less likely to breed than birds age 3 and older (Flint et al. 2016). Because spectacled eiders do not breed until at least their second year, we set the model to estimate the breeding propensity of 2-year-old birds (α). Thus, this matrix allows 1-year old individuals to transition to either non-breeding 2-year-old birds with probability ($\phi_1 * 1 - \alpha$) or breeding 2-year-old birds with probability ($\phi_1 * \ \alpha$) and corresponding fecundity estimates. We assumed adults (3+ year-old-birds) and 2-year-old birds have equal survival rates (ϕ_2) regardless of breeding status. We used a multistate annual random effects framework to model survival and breeding probability allowing the values to vary over time. The states include immature birds, non-breeding 2-year olds, breeding 2-year olds, and breeding adults ages 3 and older. Individuals may be marked as 30 day-old ducklings or as breeding adults on the breeding grounds. Immature and non-breeding 2-year olds do not come to the breeding grounds and are thus unobservable. Therefore, two of the states in our model are unobservable and lack explicit data.

Parameter redundancy is often a problem when there are unobservable states and results may be biased or imprecise (Bailey et al. 2010). Estimates of first year survival and breeding probability of 2-year olds are of high interest, therefore we induced certain constraints to make these parameters identifiable. First, we tested the model's ability to estimate these parameters using simulated data with positive results when initiating these parameters with informative priors (see Supporting Information). Using the spectacled eider data, we constrained immature survival to be a constant proportion of adult survival $\phi_1 = (\phi_2 * 0.8)$ based based on similar relationships between age classes in three closely related species, long-tailed ducks (*Clangula hyemalis*), common eiders (*Somateria mollissima*) and king eiders (*Somateria spectabilis*) (Koneff et al. 2018). Further, because we use a Bayesian framework, we included informative priors on all parameters that had previously been estimated using independent data sets and vague priors on the rest (Flint et al. 2016, Christie et al. 2018) (Table 1).

Count model likelihood

We used the state-space model formulation to model the population count data. The state-space formulation includes equations that describe how population size changes over time through the state process model. An observation model links the observed population count (index of breeding population size, includes males and females) with the estimated population size from the state process model.

The state process model describes the true but unknown dynamics of the population over time. We described this change using the matrix $\boldsymbol{A_t}$ (described above) and multiplying it by a population vector $\boldsymbol{n_t}$,

$$\begin{bmatrix} n_1 \\ n_2 \\ n_3 \\ n_4 \end{bmatrix}_{t+1} = \begin{bmatrix} 0 & 0 & f/2 * \phi_0 & f/2 * \phi_0 \\ \phi_1 * 1 - \alpha & 0 & 0 & 0 \\ \phi_1 * \alpha & 0 & 0 & 0 \\ 0 & \phi_2 & \phi_2 & \phi_2 \end{bmatrix}_t \begin{bmatrix} n_1 \\ n_2 \\ n_3 \\ n_4 \end{bmatrix}_t$$

where n_1 is the number of immature (1 year old) females, n_2 is the number of non-breeding 2 year old females, n_3 is the number of breeding 2 year old females, and n_4 is the number of 3+ year old females. Therefore, the total population size including males and females is $Ntot_t = (n_{1,t} + n_{2,t} + n_{3,t} + n_{4,t}) * 2$ and the breeding population size is $Nbpop_t = \left(n_{3,t} + n_{4,t}\right) * 2$.

The state process model describes the dynamics of the total population but our counts only include the breeding males and females and thus the observation model links the observed number of breeding birds (denoted by (y)) to $Nbpop_t$ through the following equation

$$y_t \sim Normal(Nbpop_t, \sigma_{y,t})$$

where σ_y is the estimated annual observation error and is provided as data. In 2011, aerial surveys were not flown on the YKD and therefore there is no observation for that year. We estimated observation error for 2011 using a zero-intercept linear regression model where $\hat{\sigma}_{x_t}$ is the predicted observation error as a function of estimated population size N_t and $\beta \sim Normal(0{,}30)$

$$\hat{\sigma}_{x_t} = \beta * Nbpop_t \tag{4}$$

$$\hat{\sigma}_{z_t} \sim N(\hat{\sigma}_{x_t}, \sigma) \tag{5}$$

and where $\hat{\sigma}_{z_t}$ is the estimated observation error in year t and is normally distributed about $\hat{\sigma}_{x_t}$ with a standard deviation $\sigma \sim Gamma(a, s)$ where the shape parameter, $a = 2$, and the scale parameter $s = 100$. The complete likelihood for the population count data is $L_{SS}\left(\boldsymbol{y}, \boldsymbol{\sigma_y^2} \middle| \phi_0, \phi_1, \phi_2, \alpha, N, f\right)$.

Capture-recapture likelihood

For the mark-recapture data, we used the multistate formulation of the Cormack-Jolly-Seber model (Lebreton 1992). To decrease computation time and increase efficiency, we converted the captures histories into an m-array utilizing the multinomial likelihood. The likelihood of the multi-state model is denoted as $L_{CR}(\boldsymbol{m}|\phi_0, \phi_1, \phi_2, \alpha, p)$ where $\boldsymbol{m}$ represents the capture-recapture data which contains information about state-specific survival (ϕ_0, ϕ_1, ϕ_2), breeding propensity (α) and recapture probabilities (p).

Productivity likelihood

We model fecundity as the product of clutch size at hatch (cs) and probability of nest success (ns). Nests were monitored near the expected hatch date and the number of eggs hatched was recorded to account for egg mortality. Probability of nest success was modeled as proportion of nests with at least one egg hatched out of the total nests recorded. Nest success was modeled using a binomial regression, it could vary over time, and was modeled using a random effects structure. The likelihood for productivity is $L_{PR}(\boldsymbol{ns}, \boldsymbol{cs}|f)$.

Joint likelihood for the integrated model

The joint likelihood of the integrated population model is the product of the three likelihoods described above and is written as

$$L_{IPM}\left(\boldsymbol{m}, \boldsymbol{ns}, \boldsymbol{cs}, \boldsymbol{y}, \boldsymbol{\sigma_y^2}\middle|\phi_0, \phi_1, \phi_2, p, \alpha, N, f\right) =$$

$$L_{SS}\left(\boldsymbol{y}, \boldsymbol{\sigma_y^2}\middle|\phi_0, \phi_1, \phi_2, \alpha, N, f\right) * L_{PR}(\boldsymbol{ns}, \boldsymbol{cs}|f) * L_{CR}(\boldsymbol{m}|\phi_0, \phi_1, \phi_2, \alpha, p).$$

Environmental covariates

We estimated the relationships between winter sea ice conditions and, respectively, survival and breeding propensity using linear models on the link scale. We calculated the number of days with >95% ice cover (extreme ice days) within the core wintering area during the wintering period as an index of sea ice severity. Winter was defined as 1 November through 30 April. The core wintering area was identified based on utilization distributions of 13 satellite-tagged individuals from 1993-1997 and confirmed by aerial surveys of the wintering area (Petersen 1999). Observed sea ice concentrations were extracted from the core area that spans four grid cells (25 km resolution) derived from passive microwave satellite imagery using the Bootstrap Algorithm and provided by the National Snow and Ice Data Center (NSIDC). The number of days with > 95% ice cover were standardized with a mean of 72 days and standard deviation of 23 days. Additionally, we calculated the number of days with <15% ice cover as a metric of extreme low sea ice conditions. However, extreme ice days and extreme low sea ice conditions are strongly negatively correlated ($r = -0.84$, Pearson's correlation coefficient). Given this consistent relationship we chose to only include the standardized number of days with > 95% ice cover and interpret negative deviations from the mean to be representative of low sea ice conditions.

To determine effects of breeding site conditions on nest success we included standardized precipitation and temperature during the breeding period as well as proportion of nest plots with evidence of foxes as an index of fox abundance as covariates in the nest success model (Fischer et al. 2016). Both arctic (*Vulpes lagopus*) and red foxes (*Vulpes vulpes*) can be found on the YKD but there is no effort to identify signs of fox presence by species (J. Fischer *pers. comm.*). Precipitation data were recorded at Bethel Airport in Bethel, Alaska at the National Weather Service Cooperative Network station (Western Regional Climate Center 2019). Bethel, AK is 108 miles east of Kigigak Island, however, it is the closest weather station and we may expect relatively similar environmental conditions. Temperature anomalies were calculated with respect to the 1981-2010 average and reported by NOAA National Centers for Environmental Information (NOAA 2019). Finally, I constructed a simple linear model ad-hoc to test for trends in spectacled eider nest success and fox presence. Model formulation, parameters, and prior distributions are described in Table 2.

Model implementation

The model was fit using Markov Chain Monte Carlo (MCMC) simulations in a Bayesian analytical context using JAGS (Plummer 2003) software (package "jagsUI", Kellner 2016) in program R (R Development Core Team). We initialized the model with 500,000 iterations, discarded 325,000 after burn in, and thinned by 15. Convergence of each model was assessed based on the Gelman and Rubin statistic (R-hat between 1 and 1.05) for all parameters. Additionally, trace plots were used to visually inspect adequate convergence of the 3 chains.

Goodness of fit

Robust methods to evaluate overall fit of integrated models have yet to be developed. We calculated Freeman-Tukey statistic for the nest success model and calculated a Bayesian P-value. Further, we calculated a Bayesian p-value for the count data using the chi square statistic.

Estimating population growth and correlations with demographic rates

We derived annual population growth rate by dividing the breeding population size (males and females) in year t+1 by the breeding population size in the previous year:

$$\lambda_t = (Nbpop_{t+1})/(Nbpop_t).$$

We assessed the relative contribution of each demographic rate to population growth by calculating the correlation coefficient (*r*) with its 95% credible interval. We used the full posterior sample and calculated the probability that the correlations were positive P(*r*>0) (Schaub et al. 2015, Saunders et al. 2018, Saunders et al. 2019).

Results

Environmental covariates and demographic rates

We tested the effects of the number of extreme sea ice days (>95% coverage) at the core wintering area on survival and breeding propensity. We found strong support for a nonlinear relationship between extreme sea ice days in the core area and adult survival (Figure 3, Figure 4, and Table 2). Additionally, we found evidence for a nonlinear relationship between extreme sea ice days and hatch-year survival (Figure 3, Table 2). These relationships describe the change in survival rates across the values of extreme ice days. In years with a very low number of extreme ice days survival was lower than average, survival was highest in years with an average number of extreme ice days and subsequently declined in years with above average number of ice days (Figure 4). No relationship was detected between breeding probability and extreme ice days (Table 2).

Our results identified fox presence as a strong predictor of annual nest success and provided little evidence for a relationship with precipitation or temperature (Figure 3,

Figure 5, and Table 2). Results of the linear regressions indicates that fox abundance appeared to increase over time ($\beta_{year} = 0.033, 95\%\ CRI\ 0.018, 0.048$) and nest success declined ($\beta_{year} = -0.061, 95\%\ CRI - 0.12, -0.048$). Further, annual nest success and fox abundance were negatively correlated ($r = -0.54$).

Mean adult survival (individuals age 2+) was high 0.87 (0.794 – 0.931) however, there was considerable variation in annual estimates particularly over the last 10 years (Figure 4). Adult survival ranged between 0.47 and 0.99, similar to Christie et al. (2018) who reported mean values between 0.5 and 1.0. We modeled survival from 1-year old to 2-years old as a constant proportion of adult survival and thus it was not explicitly estimated in the model. Mean hatch-year survival was 0.31 (0.125 – 0.578) and annual estimates were variable (Figure 6). Mean breeding propensity was 0.39 (0.028 – 0.583) and highly variable among years (Figure 3). However, there was significant overlap between the posterior and prior indicating potential parameter identifiability problems (overlap >35%, Gimenez et al. 2009). Further simulations are required to understand potential identifiability issues (Supporting Information). Average nest success was high (0.88) but also highly variable across years, particularly in 2001 and 2013 (Figure 5). Many of these years corresponded with high nest predation rates (Moore and Sowl 2017).

Population growth and demographic drivers

Our integrated population model estimated that the YKD breeding population had increased between 1992 and 2014 ($\bar{\lambda} = 1.04$) (Figure 7). Population growth between 2014 and 2015 would indicate a large decline ($\lambda_{2015} = 0.35$), however, in 2015 a new observer started on the aerial surveys and the current data is not adjusted for this observer effect. Thus, for the remainder of this work we focus on the estimate of population growth between 1992 and 2014 for a more accurate representation of population change.

Adult survival was positively correlated with population growth *r*= 0.59 (0.45, 0.74) and the 95% credible interval excluded zero (Figure 8). Breeding probability of 2-year olds had the second highest correlation with annual population growth *r* = 0.29 (-0.05, 0.54). Annual survival of hatch-year birds was not correlated with population growth *r* = 0.04 (-0.31, 0.31).

Goodness of fit

The Bayesian P-values for the state-space model of the counts was 0.52 and for the nest success model was 0.35, indicating both models were a relatively good fit (Figures 9 and 10).

Discussion

Efforts to understand the factors that limit population growth of Arctic species during the annual cycle is often hindered due to a lack of demographic and spatially relevant environmental data. Here, we demonstrate an important advancement in the understanding of climate impacts and predation for a threatened Arctic marine species using an integrated modeling framework. Long-term data sets are critical for understanding effects of climate variation on long-lived species and modeling these data in an integrated framework can help to reduce uncertainty in population trends and identify environmental factors that limit population growth. Analysis of the count data alone uncovered no strong relationship between breeding population size and wintering conditions (Petersen and Douglas 2004). Though prior analysis of a subset of the mark-recapture data identified a linear relationship between survival and sea ice conditions

(Flint et al. 2016), only using the 23-year long data set we are able to determine that there is a non-linear relationship between adult survival and extreme winter sea ice conditions (Christie et al. 2018). Additionally, we analyzed the nesting data within the integrated framework and identified a strong negative relationship between fox abundance and nest success, a previously undetected relationship. Finally, we estimate that population growth has been positive for YKD breeding spectacled eiders over the past 23 years. However, the combined stress of negative effects on survival through variable sea ice during the wintering period and increased predation during the breeding period represent a significant threat to population growth.

Our results provide further evidence for a strong nonlinear relationship between adult survival and the number of extreme ice days (Christie et al. 2018). Adult survival is highest at intermediate conditions (number of days with >95% ice cover are between 65 and 85), and lower when the number of sea ice days is greater than 85 or less than 65 during the wintering period. Seasonal aggregation subjects the entire global population to similar environmental conditions throughout the wintering period (Figure 1). During years of heavy ice cover, individual body condition was poor likely in response to the restricted open leads and subsequent low availability of suitable prey (Cooper et al. 2013, Lovvorn 2015). Alternatively, sea ice can dampen the impacts of waves and provide roosting areas for individuals during the non-foraging period thereby reducing thermoregulation costs (Lovvorn et al. 2003). Both high and low sea ice cover can negatively affect spectacled eider survival through thermoregulation costs, food availability, and overall poor body condition (Figure 4). Sea ice persistence on the Bering Sea has declined since 2012 and has become highly variable in recent years with little to no sea ice coverage over vast areas for extended periods (Grebmeier et al. 2018). Changes in sea ice conditions on the Bering Sea are expected to affect the benthic faunal composition and biomass that supports the marine ecosystem and provides food for Arctic marine predators (Grebmeier 2012). Furthermore, projected changes in sea ice will increase the duration and extent of open water periods, likely altering the spatial distribution of suitable refugia and affecting the spatial structure of benthic communities (Zhang et al. 2012).

Additionally, one of the novel insights from our integrated model is the estimate of hatch-year survival and its nonlinear relationship with extreme ice days. Until now, only mean estimates across the time series were possible using the mark-recapture data alone (Flint et al. 2016, Christie et al. 2018). Prior estimates include 0.22 ±0.02 over the 23-year time series (Christie et al. 2018) and 0.19 ± 0.37 between 1992 and 2004 (Flint et al. 2016). Neither analysis was able to relate hatch-year survival to environmental covariates. Here, we modeled hatch-year survival with a nonlinear relationship to sea ice conditions. Our estimates indicate there is a relationship, although, the 95% CRI does overlap zero (Figure 3, Table 2). Given that this demographic rate includes no explicit data it is unsurprising that it would be difficult to detect a strong relationship with a covariate because latent demographic rates are typically imprecise (Kéry and Schaub 2012). However, we believe we have provided evidence of a potential relationship between hatch-year survival and extreme ice conditions using the integrated modeling approach. Mean hatch year survival from our model was 0.31 (0.125 – 0.578) but did not include survival of ducklings from hatch to 30 days. This may have biased our estimates of hatch year survival high or introduced additional uncertainty. Future work should explicitly estimate this parameter by including data, or include a prior or biologically realistic constant value. Efforts to gather data on hatch-year birds would provide an opportunity to estimate survival more precisely and get a clearer picture of the influence of sea ice conditions on this life stage.

Fox presence had a strong negative impact on nesting success of spectacled eiders (Figure 3, Figure 5, and Table 3). Foxes are a primary predator of Arctic nesting birds and can cause significant damage to annual productivity (Quinlan and Lehnhausen 1982, Mallory 2015). Mammalian predation has been demonstrated to negatively influence nest success of ground nesting species (Mallory 2015, DeGregorio et al. 2016) and our study indicates similar impacts on spectacled eiders. Efforts to eradicate or control fox populations have been effective on small islands but are difficult to implement or monitor over larger areas such as the Yukon-Kuskokwim Delta. Predation pressure typically declines latitudinally where pressure is highest in the tropics and lowest in the high Arctic. Studies have indicated a switch in this pattern on a global scale due to changes in biotic interactions in response to climate change (Kublecka et al. 2018). If fox presence and predation pressure continue to increase there may be negative impacts on spectacled eider recruitment, creating a threat to future viability and recovery of the species.

We found no evidence for an effect of temperature or precipitation on nest success of spectacled eiders (Figure 3, Table 2). Unfavorable conditions (either warm/dry or cold/wet) have had negative effects on nest success and recruitment of common eiders (Iles et al. 2013, Jónsson et al. 2013). The lack of a detectable relationship could be the result of a lack of extreme unfavorable conditions or the conditions reported at Bethel are not representative of those at Kigigak Island, which is much closer to the coast.

Alternatively, regional weather conditions may not affect nest success but could affect duckling survival and ultimately recruitment into the breeding population. We did not parameterize our model to specifically estimate duckling survival. Duckling survival may decline due to exposure to low water temperatures, flooding induced by storms, or cold ambient air temperatures particularly when combined with heavy precipitation (Grand and Flint 1996, Iles et al. 2013). Further, in years with high temperatures and low rainfall, freshwater ponds evaporate increasing salinity particularly along the coast, where eiders tend to nest. Without access to freshwater ponds, ducklings fail to grow and die quickly because their salt glands have not fully developed (Devink et al. 2005). In the Arctic, severe storm frequency and temperatures are expected to continue to increase with complex regional impacts on precipitation (Bintanja 2018, Terenzi et al. 2014). Furthermore, predation is the primary cause of duckling mortality and these effects should be included in any future work (Grand and Flint 1996). Efforts to gather data on duckling survival in response to weather conditions and predation during the breeding season may help us understand the relative impacts of changes in recruitment at the population level.

Eiders demonstrate typical characteristics of slow pace of life species with high adult survival and low levels of recruitment, a pattern consistent with our results (Figure 4. Figure 5, Table 2). However, variability in adult survival has been documented in both spectacled and common eiders (Grand et al. 1998, Flint et al. 2016, Guéry et al. 2017), a trait that should have low variability according to life-history theory. Here, mean adult survival was high (0.87) but annual survival is variable over the past 10 years, which is consistent with estimates produced by others (Christie et al. 2018). Given the relationship between adult survival and sea ice conditions we may expect adult survival to decline as sea ice loss continues. Changes in population growth in long-lived species are typically buffered against low reproductive success because of high adult survival (Orzack and Tuljapurkar 2001, Koons et al. 2014). We have demonstrated an overall declining trend in nest success and a negative linear relationship with fox abundance. If both reproductive success and adult survival decline simultaneously and are not compensated for with drastic increases in juvenile survival and breeding propensity, we should expect populations to decline.

Using the integrated population model, we were able to identify limiting factors affecting population growth via different life stages throughout the annual cycle. Further we were able to estimate annual values for first year survival which were previously inestimable. We believe this study provides further evidence of the importance of long-term demographic studies to identify demographic responses to climate change and identify opportunities for conservation action.

Literature Cited

Bailey, L.L., S.J. Converse, and W.L. Kendall. 2010. Bias, precision, and parameter redundancy in complex multistate models with unobservable states. Ecology 91(6): 1598-1604.

Bardsen, B.-J., S.A. Hanssen, and J.O. Bustnes. 2018. Multiple stressors: modeling the effect of pollution, climate, and predation on viability of a sub-Arctic marine bird. Ecosphere 9(7):e02342. 10.1002/ecs2.2342

Christie, K.S., T.E. Hollmen, P. Flint, and D. Douglas. 2018. Non-linear effect of sea ice: Spectacled Eider survival declines at both extremes of the ice spectrum. Ecology and Evolution DOI: 10.1002/ece3.4637

Cooper, L.W., M.G. Sexson, J.M. Grebmeier, R. Gradinger, C.W. Mordy, and J.R. Lovvorn (2013). Linkages between sea-ice coverage, pelagic-benthic coupling, and the distribution of Spectacled Eiders: Observations in March 2008, 2009 and 2010, northern Bering Sea. Deep-Sea Research Part II: Topical Studies in Oceanography 94:31–43.

DeGregorio, B.A., S.J. Chiavacci, T.J. Benson, J.H. Sperry, and P.J. Weatherhead. 2016. Nest predators of North American birds: continental patterns and implications. BioScience 66(8):655 – 665.

Devink, J-M.A., H.G. Gilchrist, and A.W. Diamond. 2005. Effects of water salinity on growth and survival of common eider (*Somateria mollissima*) ducklings. The Auk 122(2): 523-529.

Ely, C.R., C.P. Dau, and C.A. Babcock. 1994. Decline in a population of spectacled eiders nesting on the Yukon-Kuskokwim Delta, Alaska. Northwestern Naturalist 75:81–87.

Flint, P.L., J.B. Grand, M.R. Petersen, and R.F. Rockwell. 2016. Effects of lead exposure, environmental conditions, and metapopulation processes on population dynamics of spectacled eiders. North American Fauna 81:1-41

Gimenez, O., B.J.T. Morgan, and S.P. Brooks. 2009. Weak identifiability in models for mark-recapture-recovery data *in* Modeling demographic processes in marked populations. Doi: 10.1007/978-0-387-78151-8_48.

Grand, J.B., and P.L. Flint. 1997. Productivity of nesting spectacled eiders on the lower Kashunuk River, Alaska. Condor 99:926–932.

Grand, J.B., P.L. Flint, M.R. Petersen, C.L. Moran. 1998. Effect of lead poisoning on spectacled eider survival rates. Journal of Wildlife Management 62:1103–1109.

Grebmeier, J.M., K.E. Frey, L.W. Cooper, and M. Kędra. 2018. Trends in benthic macrofaunal populations, seasonal sea ice persistence, and bottom water temperatures in the Bering Strait region. Oceanography 31(2):136–151, https://doi.org/10.5670/oceanog.2018.224.

Grebmeier, J.M. (2012). Shifting patterns of life in the Pacific Arctic and Sub-Arctic seas. Annual Review of Marine Science 4:63–78.

Guéry, L., S. Descamps, R. Pradel, S.A. Hanssen, K.E. Erikstad, G.W. Gabrielson, H.G. Gilchrist, and J. Bêty. 2017. Hidden survival heterogeneity of three Common eider populations in response to climate fluctuations. Journal of Animal Ecology 86: 683-693.

Hostetler, J.A., T.S. Sillett, and P.P. Marra. 2015. Full-annual-cycle population models for migratory birds. The Auk: Ornithological Advances 132:433–449.

Iles D.T., R.F. Rockwell, P. Matulonis, G.J. Robertson, K.F. Abraham, et al. 2013. Predators, alternative prey, and climate influence annual breeding success of a long-lived sea duck. Journal of Animal Ecology 82: 683–693.

Jenouvrier, S. 2013. Impacts of climate change on avian populations. Global Change Biology 19: 2036-2057. doi: 10.1111/gcb.12195

Kéry, M., and M. Schaub. 2012. Bayesian population analysis using WinBUGS: A hierarchical perspective. Academic Press, Boston, Massachusetts, USA.

Koons, D.N., G. Gunnarsson, J.A. Schmutz, and J.J. Rotella. 2014. Drivers of waterfowl population dynamics: from teals to swans. Wildfowl 4: 169-191.

Koneff, M.D., G.S. Zimmerman, C.P. Dwyer, K.K. Fleming, P.I. Padding, P.K. Devers, F.A. Johnson, M.C. Runge, and A.J. Roberts. 2017. Evaluation of harvest and information needs for North American sea ducks. PLoS ONE 12(4): e0175411

Kubelka, V., M. Salek, P. Tomkovich, Z. Vegvari, R. P. Freckleton, and T. Szekely. 2018. Global pattern of nest predation is disrupted by climate change in shorebirds. Science 683:680–683.

Lewis, T.L, and J.A. Schmutz. 2019 *in prep*. Using density-adjusted visibility correction factors to improve population estimates of Spectacled Eiders.

Lovvorn, J.R., S.E. Richman, J.M. Grebmeier, and L.W. Cooper. 2003. Diet and body condition of Spectacled Eiders wintering in pack ice of the Bering Sea. Polar Biology 26: 259–267.

Lovvorn, J.R., J.M. Grebmeier, L.W. Cooper, J.K. Bump, and S.E. Richman. 2009. Modeling marine protected areas for threatened eiders in a climatically changing Bering Sea. Ecological Applications 19:1596–1613.

Lovvorn, J.R., A.R. Rocha, S.C. Jewett, D. Dasher, S. Oppel, and A.N. Powell. 2015. Limits to benthic feeding by eiders in a vital Arctic migration corridor due to localized prey and changing. Progress in Oceanography 136: 162–174

Mallory, M.L. 2015. Site fidelity, breeding habitats, and the reproductive strategies of sea ducks *in* Ecology and conservation of North American sea ducks. Studies in Avian Biology, Cooper Ornithological Society.

Moore, C.B., and K.M. Sowl. 2017. Monitoring of nesting spectacled eiders on Kigigak island, Yukon Delta NWR: 2015 Summary Report. USFWS.

Moore S.E., and H.P. Huntington. 2008 Arctic marine mammals and climate change: impacts and resilience. Ecological Applications 18:157 – 165. (doi:10.1890/ 06-0571.1)

NOAA. 2019. NOAA National centers for environmental information. Climate at a glance: Global time series. https://www.ncdc.noaa.gov/cag/ Accessed April 25, 2019.

Orzack, S.H., and S.D. Tuljapurkar. 2001. Reproductive effort in variable environments, or environmental variation is for the birds. Ecology 82:2659–2665.

Petersen, M.R., W.W. Larned, and D.C. Douglas. 1999. At-sea distribution of Spectacled Eiders: A 120-year-old mystery resolved. The Auk 116:1009–1020.

Petersen, M.R., and D.C. Douglas. 2004. Winter ecology of Spectacled Eiders: environmental characteristics and population change. Condor 106: 79-94.

Platte, R.M. and R.A. Stehn. 2015. Abundance and trend of waterbirds on Alaska's Yukon-Kuskokwim Delta Coast based on 1988 to 2015 aerial surveys. Unpublished report, U.S. Fish and Wildlife Service, Anchorage, AK.

Quinlan, S.E., and W.A. Lehnhausen. 1982. Arctic fox *Alopex lagopus* predation on nesting common eiders *Somateria mollissima* at Icy Cape, Alaska. Canadian Field Naturalist 96:462-466.

Rushing, C.S., J.A. Hostetler, T.S. Sillett, P.P. Marra, J.A. Rotenberg, and T.B. Ryder. 2017. Spatial and temporal drivers of avian population dynamics across the annual cycle. Ecology 98(11): 2837-2850. doi: 10.1002/ecy.1967.

Sexson, M.G., J.M. Pearce, and M.R. Petersen. 2014. Spatiotemporal distribution and migratory patterns of Spectacled Eiders. BOEM 2014-665. U.S. Department of the Interior, Bureau of Ocean Energy Management, Alaska Outer Continental Shelf Region, Anchorage, AK.

Sexson, M.G., M.R. Petersen, G.A. Breed, and A.N. Powell. 2016. Shifts in the distribution of molting Spectacled Eiders (*Somateria fischeri*) indicate ecosystem change in the Arctic. Condor 118: 463-476. doi: 10.1650/CONDOR-15-139.1

Schaub, M., J. von Hirschheydt, and M. Grübler. 2015. Differential contribution of demographic rate synchrony to population synchrony in barn swallows. Journal of Animal Ecology 84:1530–1541.

Schaub, M., and F. Abadi. 2011. Integrated population models: a novel analysis framework for deeper insights into population dynamics. Journal of Ornithology 152: S227– S237.

Taylor, B.L., P.R. Wade, R.A. Stehn, and J.F. Cochrane. 1996. A Bayesian approach to classification criteria for spectacled eiders. Ecological Applications 6(4):1077-1089.

Terenzi, J., M. Torre Jorgenson, C.R. Ely, and N. Giguère. 2014. Storm-surge flooding on the Yukon-Kuskokwim Delta, Alaska. Arctic 67(3): 360-374.

Torre Jorgenson, M. G.V. Frost, and D. Dissing. 2018. Drivers of landscape changes in coastal ecosystems on the Yukon-Kuskokwim Delta, Alaska. Remote Sensing 10(8). https://doi.org/10.3390/rs10081280

U.S. Fish and Wildlife Service. 1993. Final rule to list the Spectacled Eider as threatened. Federal Register 58:27374– 27480.

Wang, M., and J.E. Overland. 2015. Projected future duration of the sea-ice-free season in the Alaskan Arctic. Progress in Oceanography 136: 50-59.

Western Regional Climate Center. 2019. Cooperative Climatological Data Summaries. Retrieved from http://wrcc.dri.edu/climatedata/climsum/

Zhang, J., R. Lindsay, A. Schweiger, and I. Rigor. 2012. Recent changes in the dynamic properties of declining Arctic sea ice: a model study. Geophysical Research Letters 39(20): 1-6. doi:10.1029/2012GL053545

Tables

Table 4-1. Parameters, their definitions, and prior distributions used in the spectacled eider integrated population model.

Parameter	Definition	Prior
ϕ_2	Survival of adults 2+ years	Uniform (0,1)
ϕ_1	Survival of 1 year old birds (1-2 years) *Modeled as a constant proportion of adult survival	$\phi_1 = \phi_2 * 0.8$
ϕ_0	Survival of first year birds (30 daysto 1 year)	Uniform (0,1)
α	Breeding probability of 2 year old birds	Uniform (0,1)
ns	Nest success (probability of 1 egg hatching)	Uniform (0,1)
cs	Average clutch size at hatch	Gamma (0.1, 0.1)
fec	Fecundity - number of ducklings per female $fec_t = ns_t * cs_t$	--
n_1	Number of immature (1 year old) birds $n_{1,t+1} = \left(\frac{fec_t}{2} * \phi_{0,t}\right) * (n_{3,t} + n_{4,t})$	Discrete Uniform (1600, 1900)
n_2	Number of 2 year old non-breeding birds $n_{2,t+1} = \phi_{1,t} * (1 - \alpha_t) * n_{1,t}$	Discrete Uniform (500, 900)
n_3	Number of 2 year old breeding birds $n_{3,t+1} = \phi_{1,t} * \alpha_t * n_{1,t}$	Discrete Uniform (200, 400)
n_4	Number of 3+ year old birds $n_{4,t+1} = \phi_{2,t} * (n_{2,t} + n_{3,t} + n_{4,t})$	Discrete Uniform (4000, 5000)
$Ntot$	Total population size (males and females) $Ntot_t = (n_{1,t} + n_{2,t} + n_{3,t} + n_{4,t}) * 2$	--
$Nbpop$	Breeding population size (males and females) $Nbpop_t = (n_{3,t} + n_{4,t}) * 2$	--
y	Annual index of breeding population size	--
σ_y	Annual estimated observation error of y	--
β	Regression coefficients	Uniform (-5,5)
$\sigma_{\phi,\alpha,ns}$	Standard deviation of temporal variability *Used for ϕ, α, ns	Uniform (0,10)
ε	$\varepsilon_t \sim Normal\ (0, \sigma_\theta)$	--

Table 4-2. Posterior estimates of intercepts, regression coefficients, and deviance for model id4frt (nonlinear ice days over core area for survival and breeding propensity and fox presence for nest success).

Parameter	Posterior mean and 95% CRI
mean.phi2	0.87 (0.794 – 0.931)
beta1 (id)	-0.082 (-0.588 – 0.423)
beta2 (id^2)	**-0.496 (-0.983 – -0.012)**
mean.phi0	0.31 (0.125 – 0.578)
beta3 (id)	-0.325 (-1.88 – 1.13)
beta4 (id^2)	**-0.872 (-2.60 – 0.524)**
mean.alpha	0.39 (0.028 – 0.583)
beta5 (id)	-0.953 (-4.58 – 3.381)
beta6 (id^2)	0.695 (-3.643 – 4.637)
mean.ns	0.88 (0.728 – 0.957)
beta7 (fox)	**-2.796 (-4.643 – -0.597)**
beta8 (precipitation)	-0.166 (-0.635 – 0.280)
beta9 (temperature)	0.132 (-0.321 – 0.599)

* **Bolded** values indicated those with >90% of the posterior that is the same sign (positive or negative) as the regression coefficient mean**.**

Figures

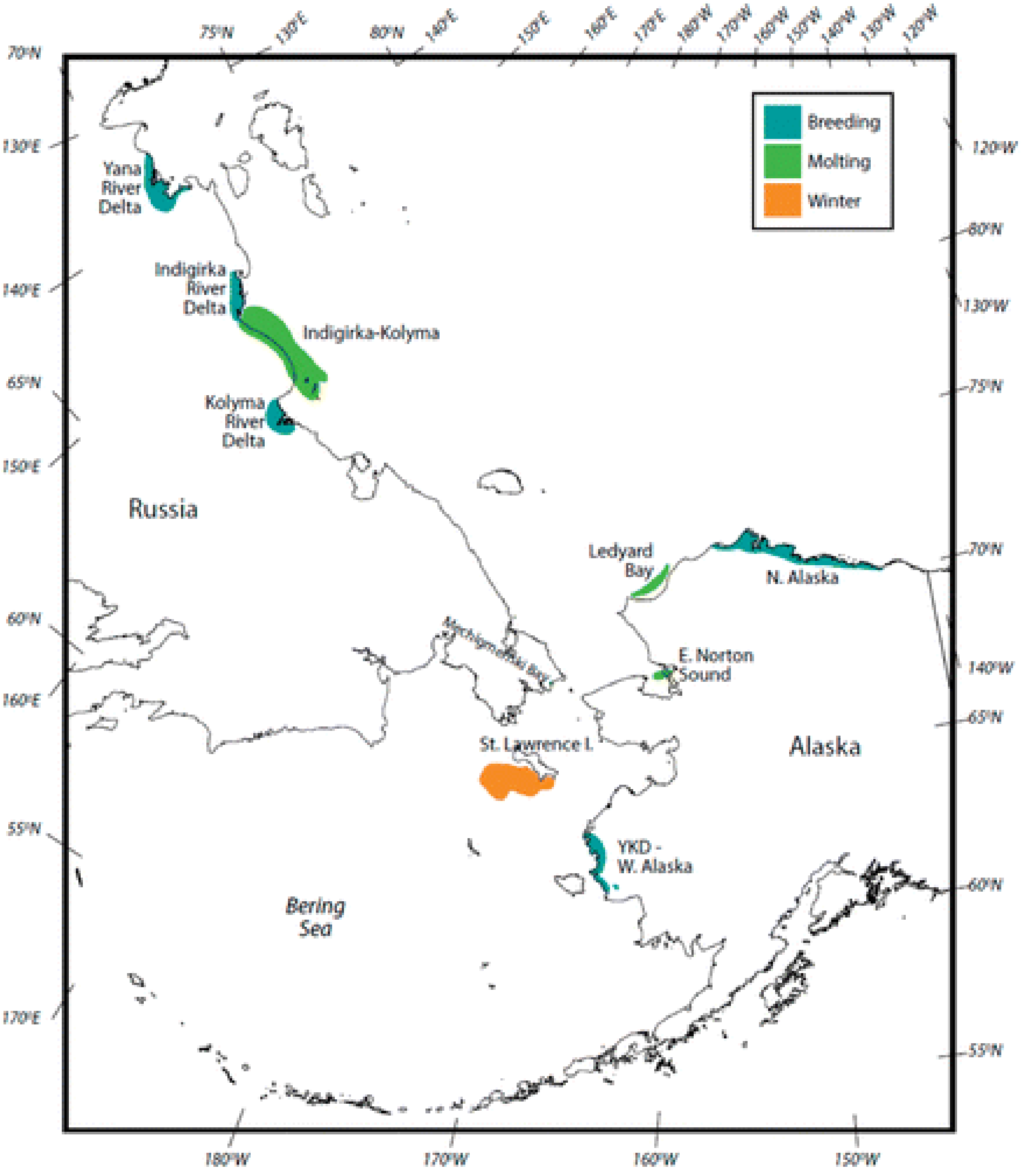

Figure 4-1. Range map of spectacled eiders *Somateria fischeri* illustrating the three primary breeding areas (Yukon-Kuskokwim Delta, Arctic Coastal Plain, and Arctic Russia), molting, and wintering areas. (Figure 1 in Flint et al. 2016).

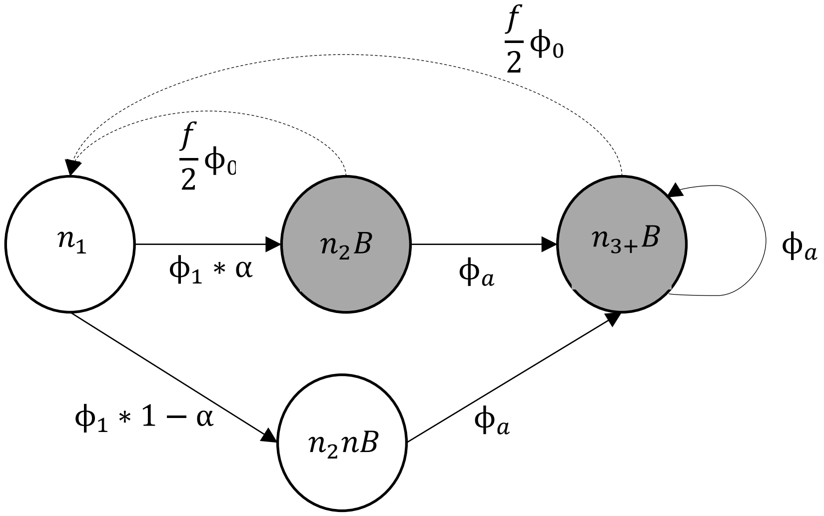

Figure 4-2. Life cycle diagram of spectacled eiders. Circles represent states, n_1 refers to 1-year old individuals, n_2nB refers to non-breeding 2-year olds, n_2B refers to breeding 2-year olds, and $n_{3+}B$ refers to breeding adult birds 3-years and older. Shaded circles represent the observable portion of the population. Dashed lines represent survival and transition probabilities and dashed lines refer to the recruitment process.

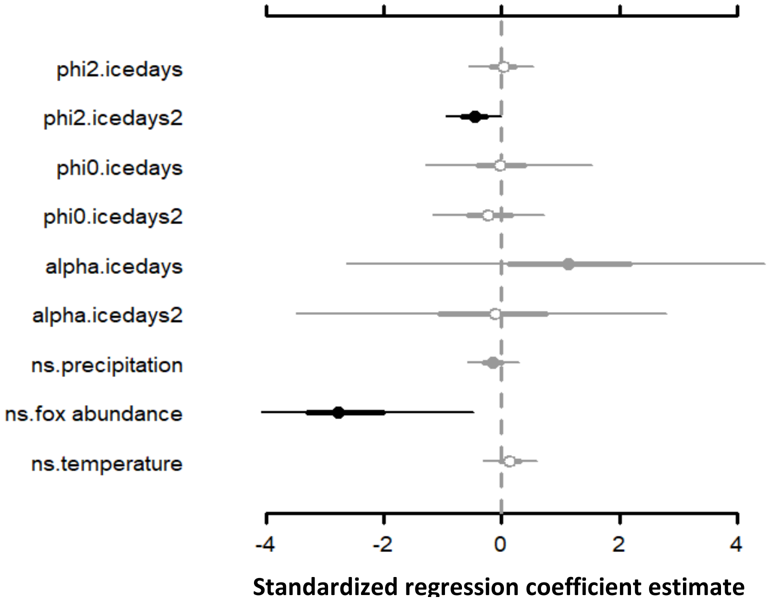

Figure 4-3. Posterior distributions of regression coefficient estimates for relationships between spectacled eider demographic rates and environmental factors. The demographic rates include phi2 which is adult survival, phi0 is hatch year survival, alpha is breeding probability of 2-year old females, and ns which is nest success. Environmental covariates include ice days, which are defined as the number of days with extreme ice cover (>95%) over the core wintering area of spectacled eiders in the Bering Sea. Precipitation, temperature, and fox abundance are covariates tested on nest success with data collected on or near the breeding grounds. The quadratic term for the effect of ice days on adult survival (phi2.icedays2) and the linear term for the effect of fox abundance (ns.fox abundance) on nest success are the only two parameters that the 95% credible intervals do not overlap zero, indicating strong support for the effects of these two covariates. Points represent the posterior median, thick lines include the 50% credible interval, and thin lines represent the 95% credible interval. Open circles occur when the 50% credible interval of a parameter overlaps zero. Parameters where 50 % credible intervals do not overlap 0 and 95 percent credible intervals do overlap 0 are indicated by closed grey circles. Parameters where 95% credible intervals do overlap 0 are indicated by closed black circles.

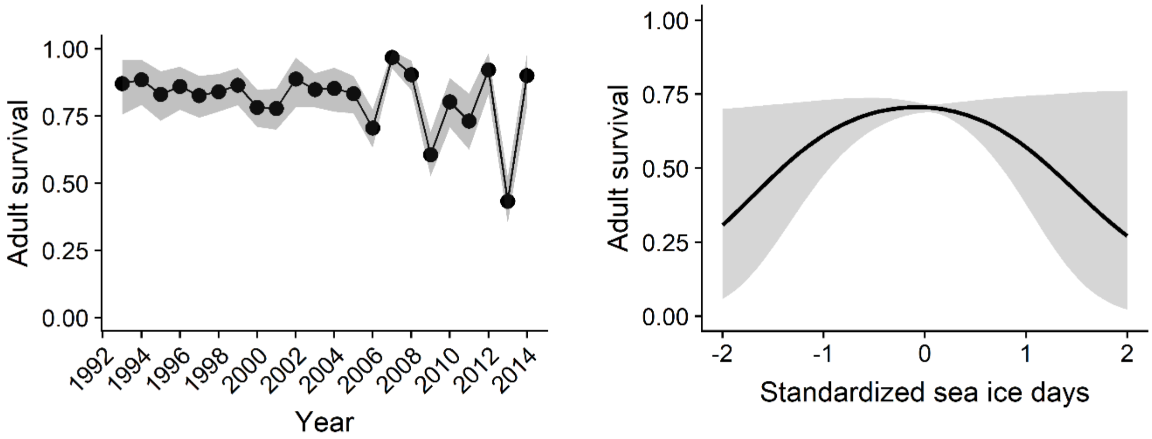

Figure 4-4. Estimates of annual adult survival of spectacled eiders (on the left) and relationship with extreme sea ice days over the core wintering area (on the right). Point estimates are the mean and the gray-banded area is the 95% credible interval. Adult survival is lowest when sea ice is extreme at either end of the spectrum, and highest at its average number of extreme ice days (i.e. 0 on x-axis).

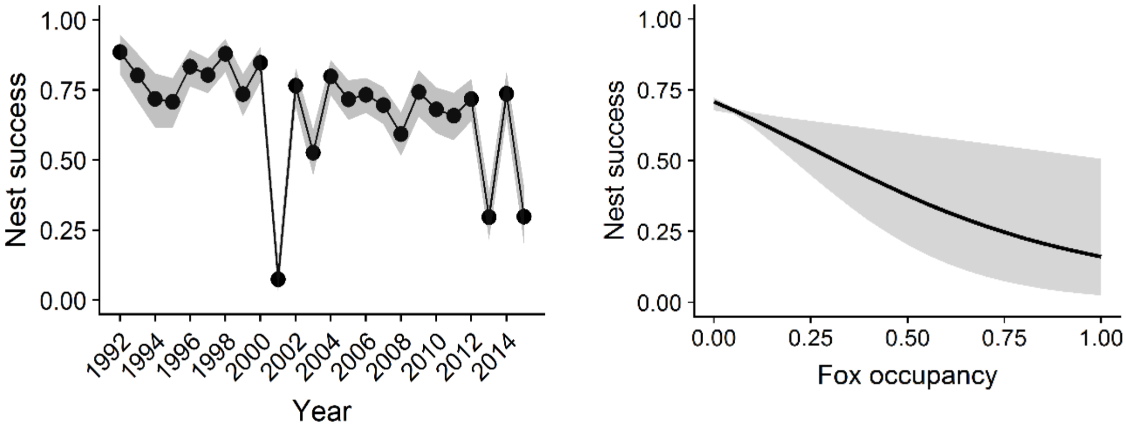

Figure 4-5. Estimates of annual nest success of spectacled eiders (on the left) and relationship between annual nest success and fox presence (on the right). Point estimates are the mean and the gray-banded area is the 95% credible interval of annual nest success estimates. Nest success is defined as the probability of a nest hatching at least one egg. Nest success declined linearly with an increase of fox presence on the breeding grounds.

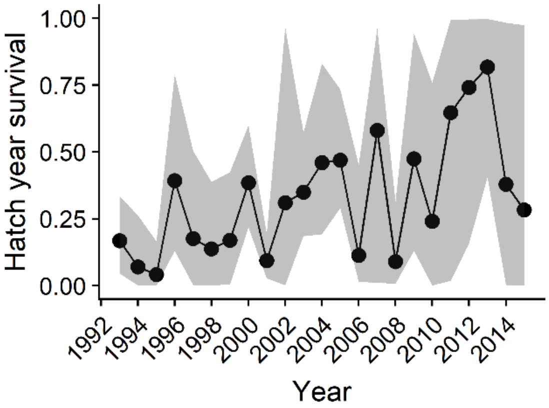

Figure 4-6. Estimates of annual hatch year survival of spectacled eiders. Point estimates are the mean and the gray-banded area is the 95% credible interval. Hatch year survival is highly variable within and across years.

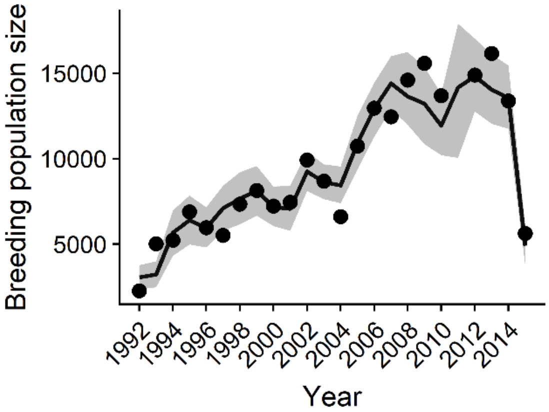

Figure 4-7. Population size estimates for YKD breeding population of spectacled eiders. Black points are the data, the black line is the mean estimate from the IPM, and the gray band is the 95% credible interval around the mean. The apparent low estimate for 2015 is the product of observer error, other surveys indicate the breeding population did not experience this decline.

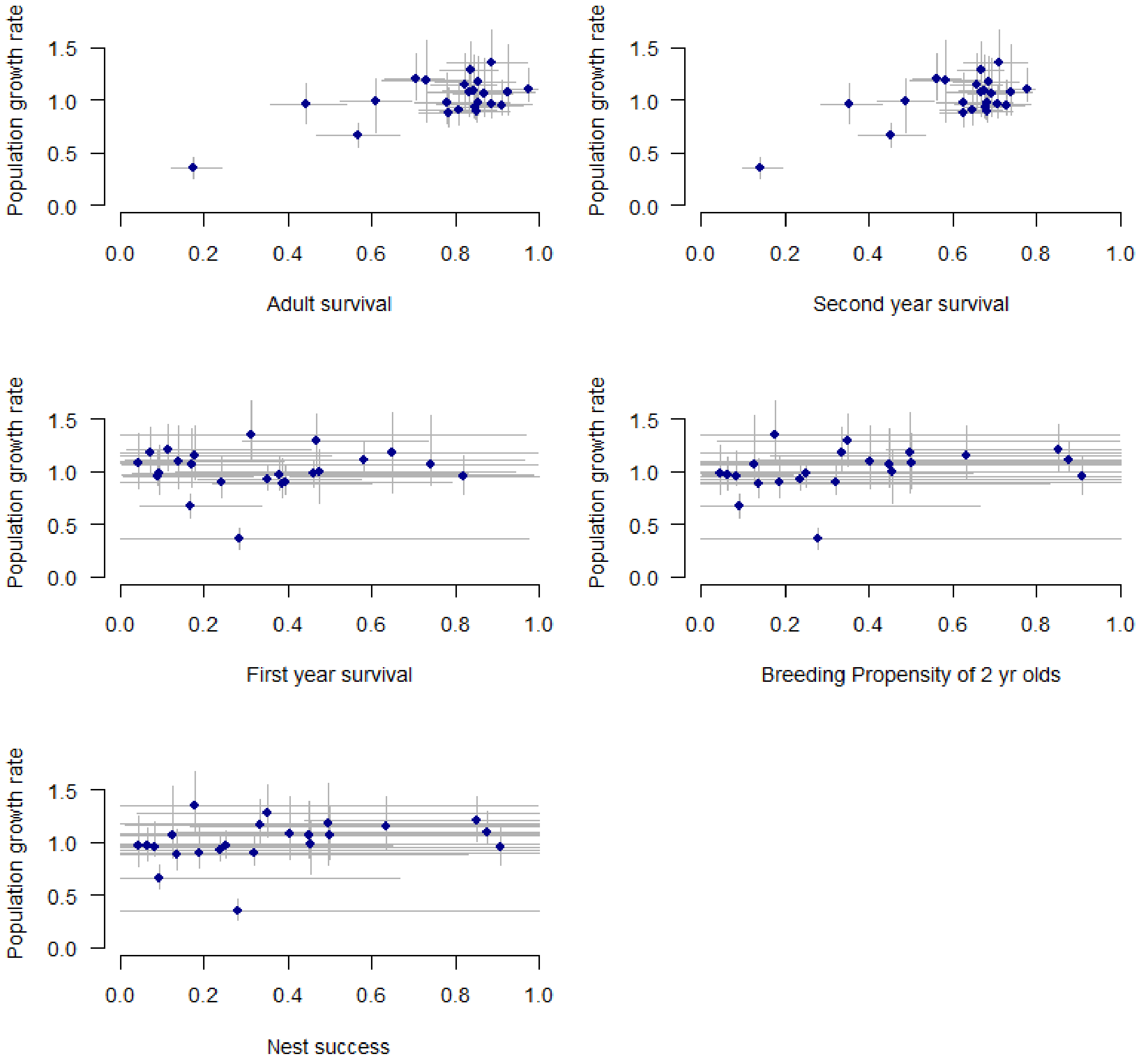

Figure 4-8. Annual posterior means of the YKD breeding population growth rate plotted against annual posterior mean estimates of adult survival, second year survival, first year survival, breeding propensity of 2-year-old birds, and annual nest success.

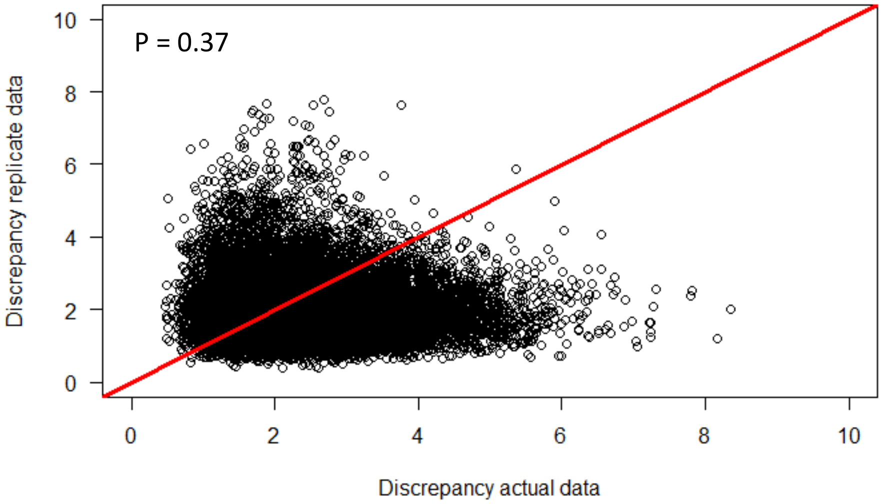

Figure 4-9. Posterior predictive check for fit of nest success using the Freeman-Tukey discrepancy statistic. Bayesian goodness of fit P-value = 0.37 indicating overall good fit of the model to the data.

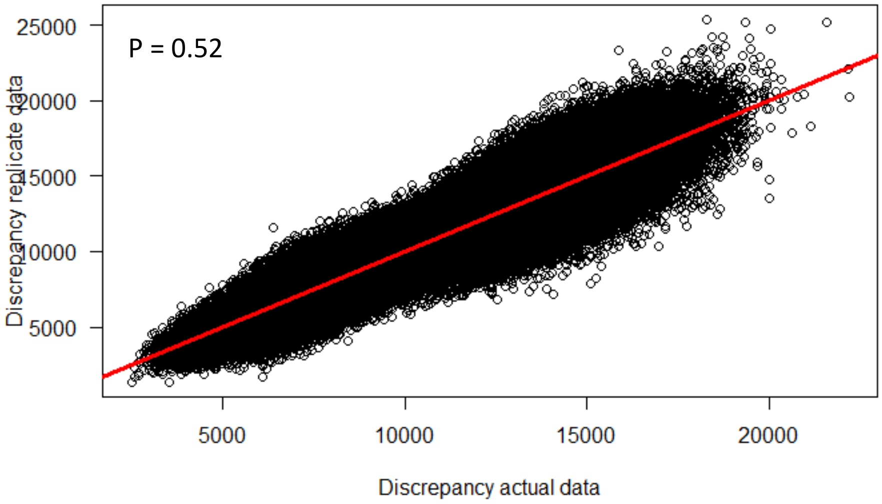

Figure 4-10. Posterior predictive check for fit of state-space count model using the chi-square statistic. Red lines indicated a perfect correlation between model estimates and true values. Bayesian goodness of fit P-value = 0.52indicating overall good fit of the model to the data.

Supporting Information: Methods and results of multi-state capture recapture model with multiple unobservable states and integrated model using simulated data

Data simulation

Given the relative complexities of this model, we chose to move forward by first developing a simulated data set to test each sub-model and the integrated model. We generated multistate capture histories and converted these into the multistate m-array format. We generated nest success data using an informative beta distribution for the probability of success and then estimated the number of successful nests out of total nests. We simulated clutch size using a truncated Poisson distribution (λ = 5, min = 1, max = 6) to emulate underdispered count data similar to that of the Spectacled eider clutch sizes.

To simulate count data, we started by creating the following 4-stage matrix model:

$$A_t = \begin{bmatrix} 0 & 0 & f/2 * \phi_0 & f/2 * \phi_0 \\ \phi_1 * 1 - \propto & 0 & 0 & 0 \\ \phi_1 * \propto & 0 & 0 & 0 \\ 0 & \phi_2 & \phi_2 & \phi_2 \end{bmatrix}_t .$$

Because spectacled eiders do not breed until at least their second year, we set up the simulation model to estimate the breeding propensity of 2-year-old birds ($\propto$). Thus, this matrix allows 1 year old individuals to transition to either non-breeding 2-year-old birds

($\phi_1 * 1{-}\propto$) or breeding 2-year-old birds ($\phi_1 * \propto$) with corresponding fecundity estimates the following year. Both adults (3+ year-old-birds) and 2-year-old birds are assumed to have equal survival rates (ϕ_2) regardless of breeding status. To estimate population size we multiply the matrix **A***ₜ* by a population vector ***n***,

$$\begin{bmatrix} n_1 \\ n_2 \\ n_3 \\ n_4 \end{bmatrix}_{t+1} = \begin{bmatrix} 0 & 0 & f * \phi_0 & f * \phi_0 \\ \phi_1 * 1{-}\propto & 0 & 0 & 0 \\ \phi_1 * \propto & 0 & 0 & 0 \\ 0 & \phi_2 & \phi_2 & \phi_2 \end{bmatrix}_t \begin{bmatrix} n_1 \\ n_2 \\ n_3 \\ n_4 \end{bmatrix}_t$$

where n_1 is the number of 1-year-old birds, n_2 is the number of non-breeding 2-year-old birds, n_3 is the number of breeding 2-year-old birds, and n_4 is the number of adults (3+ year-old-birds). We calculated the stable stage distribution (*ssd*) of matrix **A** to determine the expected number of individuals in each stage in order to avoid any transient dynamics in the data set. Further, the count data available for spectacled eiders only includes breeding birds and thus the first two stages are unobservable. To mimic this process, we created an initial total population size (N_{tot}) and multiplied it by the *ssd* to determine the number of individuals in each state at the initial time step. We projected this population forward for 24 years and kept track of $N_{tot,1:T}$ and calculated the breeding population size

$$N_{bpop,t} = (n_{3,t} + n_{4,t}) * 2.$$

Because the population matrix **A** represents a female only model, and the counts are of the number of breeding individuals (number of breeding males and females) We multiplied the breeding population size by two. Counts were generated from the breeding population size as

$$y_t \sim Normal(N_{bpop,t}, \sigma_t)$$

where $\sigma_t = N_{bpop,t} * 0.25$ to include a sufficient amount of uncertainty in the observed counts.

Fitting the models

Prior to fitting the full-integrated population model, we first needed to assess the fit of each sub-model. We formulated a sub-model for the fecundity data, survival data, and count data. We modeled fecundity data using a simple Poisson regression for clutch size

$$C_t \sim Poisson(\lambda_t)$$

where C_t is annual clutch size and λ in mean clutch size. Nest success was modeled using a binomial where $num.s_t$ is the number of successful nests, $total.nests_t$ is the total number of sampled nests

$$num.s_t \sim Binomial(total.nests_t, nest.success_t)$$

and annual fecundity is the product of clutch size and nest success at each time step

$$F_t = C_t * nest.success_t.$$

To estimate stage specific survival and breeding propensity of 2-year-old birds we analyzed the simulated capture-recapture data using a multistate model with two unobservable states. Spectacled eiders may start breeding at 2-years of age and we assume they breed every year once they are 3 year old. Individuals may be marked and released on the breeding grounds as ducklings or as adult birds (assumed 3+). Those individuals marked as ducklings can then be recaptured as 2-year-old breeders or adult breeders as known-age birds but are unobservable until they return as either 2 or 3 year old’s. Because both unobservable states occur consecutively, the corresponding parameters are likely to suffer from non-identifiability. Therefore, we specifically aimed to determine if these parameters are estimable using information and non-informative priors for both the multistate CMR model alone and the integrated model. Integrated analyses are often used to gain information on unobservable states or parameters for which there are no data. Preliminary results indicate the multistate CMR model and the integrated model converge when initialized with informative priors, however, further evaluation is required to determine the effects of the parameter non-identifiability on estimation. Informative priors for first year and second year survival were generated using survival rates reported for common eiders and long-tailed ducks, two species with similar life history traits and population distributions.

All models were fit using Markov Chain Monte Carlo (MCMC) simulations in a Bayesian analytical context using JAGS software in program R. Convergence of each model was assessed based on the Gelman and Rubin statistic (R-hat between 1 and 1.05). Additionally, trace plots were used to visually inspect adequate convergence of the 3 chains.

Results

When initiated with informative priors the model was able to provide estimates that included the true value within the 95% credible interval. Due to time constraints, each model was only run once and thus we cannot estimate potential biases. Further iterations will need to be conducted to determine the bias associated with estimates of latent parameters. Investigation of alternative parameterizations for latent parameters should be considered to determine the effect of model assumptions on inference.

Additionally, for simplicity the data was simulated assuming constant parameter values. Results may be affected by this assumption and additional complexities such as temporal variation and trends may need to be included to determine if this model is robust.

Tables

Table S4-1. Vital rates used to generate simulated data for testing each demographic sub-model and the integrated model.

			Prior specification	
Model	Parameter	Truth	Informative	Non-informative
Multistate CMR only	$\boldsymbol{\phi_0}$	0.3	0.345 (0.229 – 0.542)	0.460 (0.180 – 0.948)
	$\boldsymbol{\phi_1}$	0.6	0.619 (0.376 – 0.865)	0.487 (0.183 – 0.957)
	ϕ_2	0.8	0.794 (0.782 – 0.805)	0.807 (0.795 – 0.818)
	$\propto$	0.3	0.292 (0.219 – 0.374)	0.235 (0.152 – 0.337)
	p	0.7	0.711 (0.695 – 0.727)	0.698 (0.581 – 0.717)
State-Space Model	r	0.038		0.034
	$N_{breeding,T}$	28,970		25,648 (18,616 – 34,096)
Fecundity	$clutch\ size$	4.5		4.57 (3.75 – 5.45)
	$nest\ success$	0.71		0.647 (0.51 – 0.73)
	$fecundity$	3.24		3.23 ± 1.34
IPM	$\boldsymbol{\phi_0}$	0.3	0.282 (0.202 – 0.442)	0.432 (0.196 – 0.937)
	$\boldsymbol{\phi_1}$	0.6	0.615 (0.442 – 0.937)	0.657 (0.209 – 0.972)
	ϕ_2	0.8	0.792 (0.781 – 0.803)	0.792 (0.781 – 0.803)
	$\propto$	0.3	0.299 (0.224 – 0.381)	0.299 (0.225 – 0.382)
	p	0.7	0.711 (0.695 – 0.727)	0.711 (0.695 – 0.727)
	r	0.038	0.038	0.036
	$N_{breeding,T}$	28,970	27,041 (22,047 – 32,370)	27,177 (22,061 – 32,519)
	$clutch\ size$	4.5	4.56 (3.75 – 5.46)	4.56 (3.75 – 5.36)
	$nest\ success$	0.71	0.647 (0.514 – 0.728)	0.647 (0.514 – 0.728)

Figures

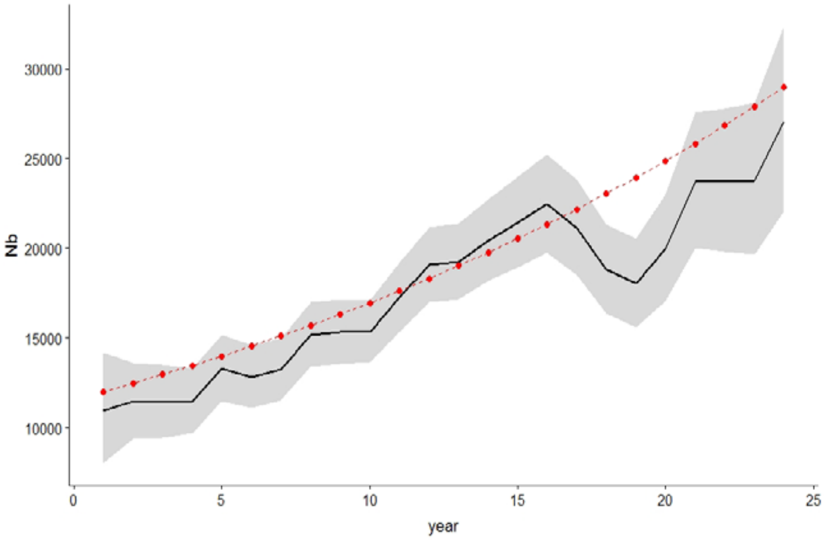

Figure S4-1. Posterior distribution for breeding population size produced by the informative IPM (Nb, black line is mean and grey band is 95% BCI) compared to simulated data (red dots).

Chapter 5: Advantages of integrated population modeling for endangered species classification decisions

Abstract

Integrated analyses have become increasingly popular over the last decade due to increased precision of parameter estimates, estimation of processes that are not directly measured, and explicit accounting of many sources of uncertainty. As our understanding of a system increases through data collection and modeling efforts, it logically follows that uncertainty would decrease, providing stronger ecological and predictive inference. However, inferences gained from integrated models have not been explicitly compared to their non-integrated sub-models in a decision context. We employed integrated population models (IPM) to identify ecological relationships, estimate demographic parameters, and estimate population size and trend for threatened spectacled eiders (*Somateria fischeri*) breeding on the Yukon-Kuskokwim Delta, Alaska. We compared estimates of parameters and ecological relationships from integrated models to analyses on subsets of data. We also compared abundance and trend estimates from IPM to those calculated using a state-space model based on count data. We then examined the effect on a Bayesian decision analysis for listing status. State-space model estimates of abundance were less precise than those from the integrated model, population size had wider confidence intervals and process error was 34% larger. IPM results indicate we are nearly three times more likely to commit an overprotection error than an underprotection

error if the decision were to delist. Alternatively, state-space model results indicate we are less than twice as likely to commit an overprotection error as an underprotection error if the decision were to delist. Finally, using the integrated model we were able to identify important ecological relationships that may pose a threat to future viability. Our study indicates that the integrated analysis reduced uncertainty in the decision space through more precise population estimates and through the identification of potential threats.

Introduction

Decisions regarding the classification of a species under the U.S. Endangered Species Act (ESA) are based on both scientific assessments (Smith et al. 2018) and value-based judgements about the level of extinction risk that warrants protection (Doremus 1997, Cummings et al. 2018). Regulatory protection under the ESA is assigned based on extinction risk and includes three risk categories “endangered”, “threatened”, and “not warranted.” A species may be classified as endangered if it is in imminent danger of extinction throughout all or a significant portion of its range, threatened if it is likely to become endangered in the foreseeable future, or not warranted (16 U.S.C. 1532 et seq.). Alternatively, listed species may be considered for reclassification through downlisting (moving from endangered to threatened status) or delisting (being removed from ESA protections) based on recovery criteria. Optimally, these decisions should be supported by a risk assessment based on species ecology, analyses of current and future responses to stressors and conservation efforts, and the level of risk that warrants a species protection and assignment to each category.

Species status assessments (SSA) were developed as a framework to use the best available information on species ecology, describe current conditions and the likely mechanisms that have influenced abundance, and use this information to predict a species response to future conditions related to environmental conditions and conservation actions (Smith et al. 2018). Collecting data on small or declining populations to identify ecological reasons for species declines can be challenging. Often, species are difficult to study due to their rarity or elusiveness, hesitation to use invasive sampling techniques, or lack of decent samples sizes due to short study periods over small spatial scales (Zipkin and Saunders 2018). In many cases, there may be limited data covering different spatial and/or temporal scales often resulting in separate analyses of sparse, disparate data (Saunders et al. 2019). Deficiencies and biases may be introduced through collection processes due to imperfect detection, non-random sampling in space or among age classes (e.g. sampling only breeding populations), and spatial scale mismatches. Analyzing independent data sets may fail to account for uncertainties leading to unsound inference and misinformed decisions.

Recent developments in statistical modeling have provided a framework to integrate multiple data sources to provide more robust estimates of population size, trend, and vital rates, as well as formally describe important ecological relationships. Integrated population models (IPMs) are useful for obtaining crucial demographic information from limited data (Schaub et al. 2007), improving estimation of population size and trends (Lee et al. 2015), and explicitly link changes in abundance to underlying demographic processes, environmental covariates, and conservation actions (Altwegg et al. 2014, Koons et al. 2016, Mosnier et al. 2015, Zipkin and Saunders 2018). IPM’s can be used to identify critical aspects of species ecology, quantify current conditions of a species habitat, demography, abundance, and population structure, estimate trends, and identify stressors that led the species to its current condition (Coates et al. 2018, Wilson et al. 2016, Zipkin and Saunders 2018). Furthermore, IPM's are easily extended to predict species extinction risk in response to conservation actions and future environmental conditions (Oppel et al. 2014, Saunders et al. 2018). Thus, IPM's may offer a particularly useful framework for use in species status assessments.

A species SSA can be used to help inform its listing or reclassification status as endangered, threatened, or not warranted under the ESA. However, there are no guidelines that explicitly define how to interpret the categorizations of species endangerment complicating the listing process by lacking transparency and consistency. Quantitative criteria have been proposed by many as an alternative to assign species to categories based on extinction probability thresholds over time through population viability analysis (PVA; Taylor 1995, McGowan et al. 2014), but such methods have not been widely adopted (Cummings et al. 2018). PVA, among other quantitative criteria, have not been integrated into law in response to resistance to the widespread use of these methods for assessment, reluctance for setting universal policy standards for risk tolerance, and differences in the way decision makers frame the decision (Doremus 1997, Robbins 2009, Cummings et al. 2018). Inference from analyses of ecological data can be combined with statistical decision theory to directly inform decisions while accounting for uncertainties and incorporating value-based judgements for classification (Berger 1985, Williams and Hooten 2016). However, despite the potential of combining integrated models and decision theoretic methods to improve decision-making under uncertainty, they have yet to be implemented in a conservation decision framework.

Statistical decision theory is a natural extension of statistical inference that incorporates value judgements set by the decision maker (Berger 1985, Williams and Hooten 2016). Demographic and survey data are often collected with the explicit goal to inform management decisions. Statistical decision theory uses the results of a statistical analysis to reduce uncertainty in a decision problem and help the decision maker choose the optimal decision based on the objectives defined (Williams and Hooten 2016). In this framework, we can integrate the results of a population model with a loss function. A loss function describes the loss or cost incurred with the decision and the true state of nature (Berger 1985, Williams and Hooten 2016). In the Bayesian context, loss functions include statistical inference from the data, prior information, and related uncertainties. In this case, we express loss associated with the decision to delist or maintain threatened status for a listed species. Specifically, we seek to estimate the under and overprotection errors associated with the species classification decision based on estimates of population size, trend, and process variation. There are two types of error associated with species classifications, to protect the species when protection is not warranted (overprotection) and to not protect the species when protection is warranted (underprotection) (Taylor et al. 1996). The shape of the loss function is determined by the decision maker and could include symmetric functions that equally penalize the over and under protection loss of a decision. The loss function can take many shapes and is defined by the decision maker's objectives and risk attitude.

We employ a state-space model for count data, an integrated population model for demographic data, and a Bayesian decision analysis to demonstrate the relative benefits of using the combined approaches of statistical analysis and decision theory in the context of species classification decisions. We employ an integrated population model to address species ecology, estimate demographic parameters, and estimate population size and trend for threatened spectacled eiders (*Somateria fischeri*) breeding on the Yukon-Kuskokwim Delta (YKD), Alaska. We compare estimates of parameters and ecological relationships from our integrated model to analyses on independent subsets of data, including abundance and trend estimates from the IPM to those produced from a state-space model based on count data. Results from each model are used in a Bayesian decision analysis to calculate the loss associated with making a reclassification decision. Specifically, we compare the estimates of population size and trend from the IPM and the separate state-space model fit to the count data to: 1) evaluate the probability that the population has met the criteria for reclassification based on population metrics including stable or increasing population growth and minimizing underprotection loss, and 2) determine if there was a measurable benefit to using the outputs of the IPM for informing species classification decisions using the loss functions.

Methods

Study species and monitoring data

Spectacled eiders were listed as threatened under the Endangered Species Act (ESA, as amended) in 1993 following extreme population declines throughout their breeding and nesting range in Alaska (Ely et al. 1994, Flint et al. 2016, Taylor et al. 1996). There are three geographically distinct breeding populations; one in Arctic Russia, one in the Arctic Coastal Plain of Alaska, and the population on the YKD. The global population of spectacled eiders winters in one distinct region south of St. Lawrence

Island in the Bering Sea and thus are subject to similar environmental conditions during the wintering period (Petersen et al. 1999, Sexson et al. 2014, 2016).

Aerial surveys of spectacled eiders have been conducted over 12,832 km^2 of YKD tundra wetland habitat annually since 1988 (Platte and Stehn 2015, Fischer et al. 2017, Lewis et al. 2019). Eider density varies widely across the YKD with low densities throughout most of the region. Lewis et al. (2019)) identified three density-specific strata; low-density (0-1.60 nest/km), medium-density (1.60-3.50 nests/km), and high-density (>3.50 nests/km). Ground-based surveys have been conducted annually on the YKD since 1985 to estimate the numbers of nests for geese and eiders. This survey samples randomly selected plots within the core nesting area of spectacled eiders in the central coast zone encompassing 716 km^2 (Fischer et al. 2017). Estimates of nests and aerial observations among low, medium, and high-density stratum on the YKD were used to calculate density-specific aerial visibility correction factors (VCF) to account for incomplete detection on the aerial surveys. The average density-specific visibility correct factors were used to convert indices of eider abundance to annual estimates of breeding spectacled eiders and variance (Lewis et al. 2019). These estimates are utilized as observation data and error in the models.

On the YKD, survival and productivity studies were carried out on Kigigak Island (1992-2015) following protocols established by Grand and Flint (1997). For a detailed explanation of field methodologies see Grand and Flint (1997) and Flint et al. (2016). Adult females were captured on nests and given metal leg bands, numbered plastic leg bands, and nasal disks. At approximately 30 days’ post-hatch ducklings were captured and marked with stainless steel and plastic bands.

Environmental covariates

During years of heavy ice cover in the core wintering area, spectacled eider body condition suffered, likely in response to the restricted open leads and subsequent low availability of suitable prey (Cooper et al. 2013, Lovvorn 2015). Further studies demonstrated that spectacled eiders save considerable energy during non-foraging periods by resting on ice (Lovvorn et al. 2003, 2009). We estimated the relationships between survival, breeding propensity, and winter sea ice conditions using two different indices of sea ice severity. Previous work has identified a relationship between the number of extreme ice days, defined as the number of days with >95% ice cover, and adult survival (Christie et al. 2018, Flint et al. 2016). Observed sea ice concentrations were extracted from the core area (as defined by Petersen et al. 1999) that spans four grid cells (25 km resolution) derived from passive microwave satellite imagery using the Bootstrap Algorithm and provided by the National Snow and Ice Data Center (NSIDC).

To determine effects of breeding site conditions on nest success we included as covariates the total precipitation and temperature anomalies during the breeding period and proportion of nest plots with evidence of foxes as an index of fox abundance (Fischer et al. 2016). Precipitation data were recorded at Bethel Airport in Bethel, Alaska at the National Weather Service Cooperative Network station (Western Regional Climate Center 2019). Temperature anomalies were calculated with respect to the 1981-2010 average and reported by NOAA National Centers for Environmental Information (NOAA 2019).

Integrated population model

We constructed the following matrix to model survival, transition probabilities, and recruitment of female spectacled eiders

$$A_t = \begin{bmatrix} 0 & 0 & f/2 * \phi_0 & f/2 * \phi_0 \\ \phi_1 * 1{-}\propto & 0 & 0 & 0 \\ \phi_1 * \propto & 0 & 0 & 0 \\ 0 & \phi_2 & \phi_2 & \phi_2 \end{bmatrix}_t .$$

There are three age classes, where ϕ_i represents annual survival probabilities for hatch year birds (ϕ_0), immature birds (ϕ_1), and adult birds ϕ_2 age 2 years and older. Spectacled eiders may begin breeding at 2 years of age, but evidence suggests they are less likely to breed than birds age 3 and older. Because spectacled eiders do not breed until at least their second year, we set the model to estimate the breeding propensity of 2-year-old birds ($\propto$). Females age 3 and older are assumed to breed every year (Flint et al. 2016). Thus, this matrix allows 1-year old individuals to transition to either non-breeding 2-year-old birds ($\phi_1 * 1{-}\propto$) or breeding 2-year-old birds ($\phi_1 * \propto$) with corresponding fecundity estimates. We assumed adults (3+ year-old-birds) and 2-year-old birds have equal survival rates (ϕ_2) regardless of breeding status. We used a multistate framework to model survival and breeding probability. There are five states including hatch year birds, immature birds, non-breeding 2-year olds, breeding 2-year olds, and breeding adults ages 3 and older. Individuals may be marked as ducklings or as breeding adults on the breeding grounds. Immature and non-breeding 2-year olds do not come to the breeding grounds and are thus unobservable. Therefore, two out of the five states in our model are unobservable and lack explicit data. Parameter redundancy is often a problem when there are unobservable states and results may be biases or highly imprecise (Bailey et al. 2010). Estimates of first year survival and breeding probability of 2-year olds is of high interest, therefore we induced certain constraints to make these parameters identifiable. First, we tested the model's ability to estimate these parameters using simulated data. When initiated with informative priors the model was able to provide estimates that included the true value within the 95% credible interval (see Supporting Information). Using the spectacled eider data, we constrained immature survival to be a constant proportion of adult survival $\phi_1 = (\phi_2 * 0.8)$ based on similar relationships between age classes in three closely related species, long-tailed ducks (*Clangula hyemalis*), common eiders (*Somateria mollissima*) and king eiders (*Somateria spectabilis*) (Koneff et al. 2018). Investigation of alternative parameterizations, such as including a strong prior on first year survival, should be considered to determine the effect of model assumptions on inference in the decision context. We used the state-space model formulation to model the population count data. All parameters in the integrated population model are defined in Table 1 along with their prior distributions.

The state process model describes the unknown dynamics of the population over time. We described this change using the matrix $\boldsymbol{A_t}$ (described above) and multiplying it by a population vector $\boldsymbol{n_t}$,

$$\begin{bmatrix} n_1 \\ n_2 \\ n_3 \\ n_4 \end{bmatrix}_{t+1} = \begin{bmatrix} 0 & 0 & f/2 * \phi_0 & f/2 * \phi_0 \\ \phi_1 * 1 {-} \propto & 0 & 0 & 0 \\ \phi_1 * \propto & 0 & 0 & 0 \\ 0 & \phi_2 & \phi_2 & \phi_2 \end{bmatrix}_t \begin{bmatrix} n_1 \\ n_2 \\ n_3 \\ n_4 \end{bmatrix}_t$$

where n_1 is the number of immature (1 year old) females, n_2 is the number of non-breeding 2 year old females, n_3 is the number of breeding 2 year old females, and n_4 is the number of 3+ year old females. Therefore, the total population size including males and females is $Ntot_t = (n_{1,t} + n_{2,t} + n_{3,t} + n_{4,t}) * 2$ and the breeding population size is $Nbpop_t = \left(n_{3,t} + n_{4,t}\right) * 2$.

The state process model describes the dynamics of the total population but our counts only include the breeding males and females and thus the observation model links the observed number of breeding birds (denoted by (y)) to $Nbpop_t$ through the following equation

$$y_t \sim Normal(Nbpop_t, \sigma_{y,t})$$

where σ_y is the estimated annual observation error and is provided as data. For the mark-recapture data, we used the multistate formulation of the Cormack-Jolly-Seber model (Lebreton 1992). To decrease computation time and increase efficiency, we converted the captures histories into an m-array utilizing the multinomial likelihood. We modeled fecundity as the product of clutch size at hatch (cs) and probability of nest success (ns). Nests were monitored near the expected hatch date and the number of eggs hatched was recorded to account for egg mortality. Probability of nest success was modeled as proportion of nests with at least one egg hatched out of the total nests recorded in a binomial regression.

State-space model

In addition to our integrated model, we constructed a state-space model to analyze only the count data to compare posterior results of population estimates and the probability of meeting the species recovery criteria. Our state-space model describes population growth mathematically as

$$\log(N_{t+1}) = \log(N_t) + r_t$$

where N_t is the number of breeding birds (YKD) or breeding pairs (ACP) in year t, r_t is population growth rate and

$$r_t \sim Normal(\bar{r}, \sigma_r).$$

We set the prior distributions for initial abundance equal to the mean detection adjusted estimates for 2005 for the YKD: $\log(N_{2005}) \sim N(\log(y_{2005}), 0.1)$ (Lewis et al. 2019), population growth, $\bar{r} \sim N(0, 0.1)$, and for process error we used a gamma distribution $\sigma_r \sim Gamma(a, s)$ with shape parameters $a = 3$ and $s = 0.2$.

The observation model relates the true population size N_t to the observations corresponding to the detection adjusted abundance indices for each breeding ground. Thus, our observation process was

$$\widehat{y_t} \sim Normal\left(N_t, \hat{\sigma}_{\widehat{y_t}}\right)$$

where the observations, $\widehat{y_t}$, were the detection adjusted abundance indices of spectacled eiders from the aerial surveys on the respective breeding grounds (Lewis et al. 2019). Annual observation errors from aerial survey sampling ($\hat{\sigma}_{\widehat{y_t}}$) were provided as data (see similar approach in Rotella et al. 2009 and Koons et al. 2017).

In 2011, aerial surveys were not flown on the YKD and therefore there is no observation for that year. We estimated observation error for 2011 using a zero-intercept linear regression model where $\hat{\sigma}_{x_t}$ is the predicted observation error as a function of estimated population size N_t and $\beta \sim Normal(0{,}30)$

$$\hat{\sigma}_{x_t} = \beta * N_t \tag{4}$$

$$\hat{\sigma}_{z_t} \sim N(\hat{\sigma}_{x_t}, \sigma) \tag{5}$$

and where $\hat{\sigma}_{z_t}$ is the estimated observation error in year t and is normally distributed about $\hat{\sigma}_{x_t}$ with a standard deviation $\sigma \sim Gamma(a, s)$ where the shape parameter, $a = 2$, and the scale parameter $s = 100$.

Model implementation

We fit the integrated population model in a Bayesian framework using R 3.5.1, JAGS 4.3, and the jagsUI package (Plummer 2003, Kellner 2015, R Core Tea, 2016). We initialized the IPM with 500,000 iterations, discarded 325,000 after burn in, and thinned by 15. The state-space model was also fit using JAGS software in program R. We ran three MCMC chains for 100,000 iterations, set thin to 2, discarded 70,000 as burn-in, and ran 5,000 iterations in the JAGs adaptive phase. Convergence for each model was assessed based on the Gelman and Rubin statistic (R-hat between 1 and 1.05). Additionally, trace plots were used to visually inspect adequate convergence of the 3 chains.

Delisting criteria and Bayesian decision analysis

Criteria for delisting spectacled eiders from threatened status includes when the following quantitative criteria are met, when (1) the minimum estimated breeding population size is ≥ 6,000 breeding pairs (or 12,000 breeding birds) designated by the 95% lower credible interval, and the population is increasing as judged by statistical measures, which includes: the over-protection loss exceeding the under-protection loss, calculated using trend data based on at least 10 years (but no greater than 15 years) and where loss functions symmetrical around r = 0 with a zero loss for both functions when r = 0, and, the minimum estimated population size is > 6,000 breeding pairs; or (2) the minimum estimated population size is >10,000 breeding pairs over > 3 survey years, or the minimum estimate of abundance exceeds 25,000 breeding pairs in any survey (USFWS 2002). Here, we are specifically interested in testing the first criteria.

The decision or loss functions were calculated given the posterior estimates of population growth $r \sim N(\bar{r}, \hat{\sigma}_r)$, including process error, and abundance in the final year N_{2014} converting these metrics into a measure of risk according to probability of extinction. The cost of making decision errors is measured in terms of the probability of decreasing to under 250 adults (125 breeding pairs) in 50 years (USFWS 1993). See Chapter 2 for further detail on calculating loss functions (in this dissertation).

Results

Demographic rates and environmental effects

Adult (2 to 3+ years old) survival probability was consistently high with an average estimate of 0.87 (95% CRI 0.794-0.931). Annual variability in year-specific estimates of adult survival has increased in the past 5 years (Figure 1). Survival of individuals from 1 to 2 years old was modeled as a constant proportion of adult survival and was not explicitly estimated in our model. Hatch year survival was variable over time with a mean of 0.31 (95% CRI 0.125-0.578) and may be biased high because the model does not account for survival between hatch and 30-days. Mean breeding propensity was 0.39 (95% CRI 0.028-0.583) and highly variable among years. However, there was significant overlap between the posterior and prior indicating potential parameter identifiability problems (>35% overlap, Gimenez et al. 2009). Further simulations are required to determine if the bias in hatch year survival and non-identifiability of breeding propensity affect population estimates and the conservation decision.

We tested the effects of the number of extreme sea ice days (>95% coverage) at the core wintering area on survival and breeding propensity. We found strong support for a nonlinear relationship between extreme sea ice days in the core area and adult survival (Figures 4-4, 4-3). Additionally, we found evidence for a nonlinear relationship with extreme sea ice days and hatch year survival (Figure 4-3). These relationships describe the change in survival rates across the values of extreme ice days. In years with a very low number of extreme ice days survival is lower than average, survival is highest in years with an average number of extreme ice days and subsequently declines in years with above average number of ice days. No relationship was detected between breeding probability and extreme ice days (Figure 4-3).

Average nest success was high but also highly variable across years, particularly in 2001, and 2013, years that corresponded with high nest predation events (Moore and Sowl 2017). Overall, nest success has declined over our study period and the index of fox abundance indicates an increase over the same period on the YKD (Chapter 4 this dissertation). The models identified fox presence to be a strong predictor of annual nest success and provided little evidence for a relationship with precipitation or temperature (Figures 4-5, 4-3). The Bayesian p-value for the posterior predictive check of how well the nest success model fit the data was 0.35, indicating relatively good model fit.

Decision analysis

Posterior estimates of population size and growth rate from both the integrated model and the state-space model indicate that the YKD breeding population has met the species reclassification criteria. Based on estimated abundance in 2014, the IPM results indicate the population has 100% probability (P = 1.0) of having met the abundance threshold (95% LCRI $= \widehat{\mathrm{N}} \geq$ 12,000 breeding birds). The 10-year mean growth rate between 2005 and 2014 from the integrated population was positive $\bar{r}$ = 0.025 but variable, evident by the standard error (SE 0.071) and overlapped zero (Figure 5-1). Furthermore, overprotection loss from the integrated population model was greater than underprotection loss (Table 5-2). Estimated mean abundance from the state-space model in 2014 was 14,205 breeding birds (95% CRI 11,832 to 16,538). The 95% LCRI of abundance in 2014 was below 12,000 breeding and output from the SSM does not support the YKD population having met the abundance threshold criterion (Table 5-2). The mean population growth estimate from the state-space model was equal to the IPM estimate ($\bar{r}$ = 0.025) but more variable (SE 0.091) and overprotection loss exceeded underprotection loss (Table 5-2).

Discussion

We developed an integrated population model to estimate demographic rates, population size, population growth rate, and demographic responses to environmental conditions. We provide estimates of latent demographic rates (e.g., hatch year survival) that were previously inestimable through analysis of singular data sets. Hatch year survival was variable but generally consistent with other eider life-history studies (Flint 2015, Koneff et al. 2018), however, the estimate does not include survival between hatch and 30-days which may bias this estimate high. Adult survival was consistently high but exhibited greater annual variation over the past 5 years (Figure 4-4), likely in response to changing sea ice conditions during the wintering period. Nest success was highly variable and was strongly negatively influenced by fox abundance. Variation in adult survival had the greatest influence on population growth, which is consistent with life-history theory. Population growth estimates from both the integrated model and the state-space model indicate the population was most likely stable or increasing between 2005 and 2014, but estimates do overlap zero on the log scale (Figure 5-1). Our results indicate that extreme sea ice conditions (high or low number of days with >95% ice cover) negatively influence adult survival probability. Additionally, we identified fox abundance to be a strong predictor of annual nest success. Using the integrated population model, we identified two potential ecological factors that may limit population growth and threaten population viability.

Species status assessments (SSA's) use the 3 R's of conservation biology to evaluate the current and future condition of the species (Smith et al. 2018). The first, resiliency, is the ability to withstand stochastic disturbance and is positively related to population size and growth rate. Redundancy, ability of a species to withstand catastrophic events by spreading risk among multiple populations or across a large area. Finally, representation, is the ability of a population to withstand changing environmental conditions over time as characterized by the breadth of genetic and environmental diversity within and among populations. The YKD breeding population has exhibited growth and the population size in 2014 was 14,511 (12,496-16,589; IPM estimate) which is substantially greater than the population size at listing in 1992 of 3,046 (2,342-3,772; IPM estimate) breeding birds. However, we have detected an increasing trend in fox abundance and a strong negative relationship with nest success. Further, the relative influence of adult survival on population growth with predicted changes in sea ice conditions may threaten population viability. We did not assess future conditions because this requires the species recovery team to identify scenarios for which to test population viability. Data is limited for both the ACP and Arctic Russia breeding populations and thus we do not know if the same threats (extreme sea ice and fox abundance) apply to those populations. However, given that the global population winters together we may expect similar demographic responses to extreme wintering conditions. Further research is warranted to determine if sea ice conditions and predation pressure are limiting factors for global population growth, or, if there are additional stressors that may affect the other breeding populations and influence global population viability. The decision analysis for species classification could easily be extended to link demographic or population level responses to future environmental conditions.

Population estimates from the integrated model indicate that the YKD breeding population of spectacled eiders has met the designated reclassification criteria in the species recovery plan, however, estimates produced from the state-space model of the counts do not meet the abundance threshold. Although mean intrinsic population growth is positive and overprotection loss exceeds under protection loss in both models (Table 5-2), the lower 95% credible interval of breeding population size produced by the state-space model did not meet the threshold of 12,000 breeding birds (Table 5-2). Estimates produced by the state-space model are less precise, population size has wider credible intervals and process error is roughly two times larger than the estimate produced by the integrated model. Results indicate population growth is positive, although, the posterior distribution of population growth overlaps zero in both models. The posterior of population growth produced by the integrated population model is considerably more precise than that of the state-space model. Results from the integrated model indicate that we are 3.5 times more likely to commit an overprotection error than an underprotection error if the decision were to delist. Alternatively, the state-space model results indicate we are less than two times as likely to commit an overprotection error as an underprotection error if the decision were to delist. The differences in misclassification error are caused by the greater uncertainty from the state-space model estimates propagating through the population projections.

To our knowledge, we are the first to provide empirical data that indicates the effects of gaining precision using an integrated model for identifying both ecological patterns influencing demographic rates and increasing certainty of a conservation decision. We demonstrated that using an integrated model we can estimate previously inestimable demographic rates and ecological relationships providing a better understanding of species ecology and potential threats. Further, we demonstrate that there is a benefit to using an integrated approach over a non-integrated approach for conservation decisions. Increased precision of population estimates provides decision makers with an opportunity to provide clearer and more robust evidence to support their decisions. The combined benefits of the integrated framework holds great promise for understanding critical components of species ecology while aiding conservation and management decisions (Schaub and Abadi 2011, Wilson et al. 2016, Zipkin and Saunders 2018).

While we argue that the precision gained by using the IPM framework increased the probability of overprotection and thus potentially made the decision easier – we recognize that the decision metrics would likely lead to the same conclusion based on minimizing underprotection loss. Our results therefore provide additional support to the growing body of literature on the utility of loss functions and calculating misclassification error for species classifications and other natural resource decisions (Taylor et al. 1996, Regan et al. 2013, Williams and Hooten 2016, Cummings et al. 2018). We also recognize that data are often limited for many species. Integrated models have been extended to include less information-rich data sources such as citizen science data (Robinson et al. 2018) and detection - non-detection data (Zipkin et al. 2017). Loss functions can be used when there is no explicit information on a species current status (i.e. expert opinion) or for data limited species. Eliciting expert opinion to generate a prior is a valid way of generating a loss function for informing decisions (Berger 1985, Williams and Hooten 2016). Models can be updated when information becomes available and can be built for nearly any source of data depending on the objectives (Berger 1985, Regan et al. 2013, Williams and Hooten 2016). The shape of the loss function should be defined by value judgements about risk tolerance and uncertainty. For spectacled eiders, the recovery team chose a symmetrical loss function to represent equal loss associated with underprotection and overprotection. Recovery teams may choose an asymmetrical loss function to emphasize that underprotecting a species is a greater loss than overprotecting a species. Loss functions can take many shapes but as long as the decision makers are clear about their choices, using this approach offers a transparent framework for making species classification decisions.

In this research, we have; 1) quantified effects of ecological processes acting on demographic rates during both the breeding and wintering seasons, 2) identified potential threats to future viability, 3) provided precise estimates of population size and trend, 4) compared two structural forms of population models, and 5) demonstrated the benefits of classifying species based on decision theoretic methods. Using the traditional integrated population modeling approach, we were able to estimate latent demographic parameters, demographic response to environmental conditions and estimate population size and trend. Each of these aspects are critical components for assessing current and future conditions in an SSA. By further integrating the results of our IPM and SSM we were able to estimate the probability of committing overprotection or underprotective errors for the decision to maintain listing or to delist. The probability of committing these errors is directly related to population resiliency given current conditions and can be easily extended to test the probability of committing errors under different future scenarios. We believe the combined approaches of integrated population modeling with decision theoretic methods offers a useful framework for making species classification decisions and on a broader scale, conservation management.

Literature Cited

Altwegg, R., Jenkins, A., Abadi, F., 2014. Nestboxes and immigration drive the growth of an urban peregrine falcon Falco peregrinus population. Ibis 156, 107–115.

Berger, J. O. 1985. Statistical decision theory and Bayesian analysis. Springer, New York, New York, USA.

Christie, K.S., T.E. Hollmen, P. Flint, and D. Douglas. 2018. Non-linear effect of sea ice: Spectacled Eider survival declines at both extremes of the ice spectrum. Ecology and Evolution DOI: 10.1002/ece3.4637

Coates, P.S., B.G. Prochazka, M.A. Ricca, B.J. Halstead, M.L. Casazza, E.J. Blomberg, B.E. Brussee, L. Wiechman, J. Tebbenkamp, S.C. Gardner, and K.P. Reese. 2018. The relative importance of intrinsic and extrinsic drivers to population growth vary among local populations of Greater Sage-Grouse: An integrated population modeling approach. The Auk: Ornithological Advances 135:240–261.

Cummings, J.W., S.J. Converse, D.R. Smith, S. Morey, and M.C. Runge. 2018. Implicit decision framing as an unrecognized source of confusion in endangered species classification. Conservation Biology 32(6): 10.1111/cobi.13185

Doremus, H. 1997. Listing decision under the Endangered Species Act: why better science isn’t always better policy. Washington University Law Quarterly 75:1029–1153.

Ely, C.R., C.P. Dau, and C.A. Babcock. 1994. Decline in a population of spectacled eiders nesting on the Yukon-Kuskokwim Delta, Alaska. Northwestern Naturalist 75:81–87.

Giminez, O., B.J.T. Morgan, and S.P. Brooks. 2009. Weak identifiability in models for mark-recapture-recovery data *in* Modeling demographic processes in marked populations. Doi: 10.1007/978-0-387-78151-8_48.

Grand, J.B., and P.L. Flint. 1997. Productivity of nesting spectacled eiders on the lower Kashunuk River, Alaska. Condor 99:926–932.

Flint, P.L., J.B. Grand, M.R. Petersen, and R.F. Rockwell. 2016. Effects of lead exposure, environmental conditions, and metapopulation processes on population dynamics of spectacled eiders. North American Fauna 81:1-41.

Kéry, M., and M. Schaub. 2012. Bayesian population analysis using WinBUGS: A hierarchical perspective. Academic Press, Boston, Massachusetts, USA.

Koons, D.N., D.T. Iles, M. Schaub, and H. Caswell. 2016. A life-history perspective on the demographic drivers of structured population dynamics in changing environments. Ecology Letters 19: 1023–1031.

Koneff, M.D., G.S. Zimmerman, C.P. Dwyer, K.K. Fleming, P.I. Padding, P.K. Devers, F.A. Johnson, M.C. Runge, and A.J. Roberts. 2017. Evaluation of harvest and information needs for North American sea ducks. PLoS ONE 12(4): e0175411

Lebreton, J.-D., K.P. Burnham, J. Clobert, and D.R. Anderson. 1992. Modeling survival and testing biological hypotheses using marked animals: a unified approach with case studies. Ecological Monographs 62: 67–118.

Lee, A.M., E.M. Bjørkvoll, B.B. Hansen, S.D. Albon, A. Stien, B.-E. Sæther, S. Engen, S. Veiberg, L.E. Loe, and V. Grøtan. 2015. An integrated population model for a long-lived ungulate with Bayesian methods. Oikos 124: 806–816.

McGowan, C.P., D.H. Catlin, T.L. Shaffer, C.L. Gratto-Trevor, and C. Aron. 2014. Establishing endangered species recovery criteria using predictive simulation modeling. Biological Conservation 177: 220– 229.

Mosnier, A., T. Doniol-Valcroze, J.-F. Gosselin, V. Lesage, L.N. Measures, and M.O. Hammill. 2015. Insights into processes of population decline using an integrated population model: the case of the St. Lawrence Estuary beluga (Delphinapterus leucas). Ecological Modelling 314, 15–31.

Oppel, S., Hilton, G., Ratcliffe, N., Fenton, C., Daley, J., Gray, G., et al., 2014. Assessing population viability while accounting for demographic and environmental uncertainty. Ecology 95, 1809–1818.

Regan, T.J., B.L. Taylor, G.G. Thompson, J.F. Cochrane, K. Ralls, M.C. Runge, and R. Merrick. 2013. Testing decision rules for categorizing species' extinction risk to help develop quantitative listing criteria for the US Endangered Species Act. Conservation Biology 27: 821– 831.

Robbins, K. 2009. Strength in numbers: setting quantitative criteria for listing species under the Endangered Species Act. UCLA Journal of Environmental Law and Policy 27(1).

Robinson, O.J., V. Ruiz-Gutierrez, D. Fink, R.J. Meese, M. Holyoak, and E.G. Cooch. 2018. Using citizen science data in integrated population models to inform conservation. Biological Conservation 227: 361-368.

Taylor, B.L., P.R. Wade, R.A. Stehn, and J.F. Cochrane. 1996. A Bayesian approach to classification criteria for spectacled eiders. Ecological Applications 6(4):1077-1089.

Saunders, S.P., F.J. Cuthbert, and E.F. Zipkin. 2018. Evaluating population viability and efficacy of conservation management using integrated population models. Journal of Applied Ecology 55(3): 1380-1392.

Saunders, S.P., M.T. Farr, A.D. Wright, C.A. Bahlai, J.W. Riberio Jr., S. Rossman, A.L. Sussman, T.W. Arnold, and E.F. Zipkin. 2019. Disentangling data discrepancies with integrated population models. Ecology. Doi: 10.1002/ecy.2714.

Schaub, M., and F. Abadi. 2011. Integrated population models: a novel analysis framework for deeper insights into population dynamics. Journal of Ornithology 152: 227–237.

Schaub, M., O. Gimenez, A. Sierro, and R. Arlettaz. 2007. Use of integrated modeling to enhance estimates of population dynamics obtained from limited data. Conservation Biology 21:945–955.

Smith, D.R., N.L. Allan, C.P. McGowan, J.A. Szymanski, S.R. Oetker, and H.M. Bell. 2018. Development of a Species Status Assessment Process for Decisions under the U.S. Endangered Species Act. Journal of Fish and Wildlife Management 9(1): 302-320.

Stenglein, J.L., J. Zhu, M.K. Clayton, and T.R. Van Deelen. 2015. Are the numbers adding up? Exploiting discrepancies among complementary population models. Ecology and Evolution 5(2): 368-376.

Williams, P.J. and M.B. Hooten. 2016. Combining statistical inference and decisions in ecology. Ecological Applications 26(6): 1930-1942.

Wilson, S., K.C. Gil-Weir, R.G. Clark, G.J. Robertson, and M.T. Bidwell. 2016. Integrated population modeling to assess demographic variation and contributions to population growth for endangered Whooping Cranes. Biological Conservation 197:1–7.

Zipkin, E.F., S. Rossman, C. Yackulic, J.D. Wiens, J.T. Thorson, R.J. Davis, and E.H.C. Grant. 2017. Integrating count and detection/nondetection data to model population dynamics. Ecology 98: 1640-1650.

Zipkin, E.F. and S.P. Saunders. 2018. Synthesizing multiple data types for biological conservation using integrated population models. Biological Conservation 217: 240-250.

Tables

Table 5-1. Parameters, their definitions, and prior distributions used in the spectacled eider integrated population model.

Parameter	Definition	Prior
ϕ_2	Survival of adults 2+ years	Uniform (0,1)
ϕ_1	Survival of 1 year old birds (1-2 years) *Modeled as a constant proportion of adult survival	$\phi_1 = \phi_2 * 0.8$
ϕ_0	Survival of first year birds (hatch to 1 year)	Uniform (0,1)
α	Breeding probability of 2 year old birds	Uniform (0,1)
ns	Nest success (probability of 1 egg hatching)	Uniform (0,1)
cs	Average clutch size at hatch	Gamma (0.1, 0.1)
fec	Fecundity - number of ducklings per female $fec_t = ns_t * cs_t$	--
n_1	Number of immature (1 year old) birds $n_{1,t+1} = \left(\frac{fec_t}{2} * \phi_{0,t}\right) * (n_{3,t} + n_{4,t})$	Discrete Uniform (1600, 1900)
n_2	Number of 2 year old non-breeding birds $n_{2,t+1} = \phi_{1,t} * (1 - \alpha_t) * n_{1,t}$	Discrete Uniform (500, 900)
n_3	Number of 2 year old breeding birds $n_{3,t+1} = \phi_{1,t} * \alpha_t * n_{1,t}$	Discrete Uniform (200, 400)
n_4	Number of 3+ year old birds $n_{4,t+1} = \phi_{2,t} * (n_{2,t} + n_{3,t} + n_{4,t})$	Discrete Uniform (4000, 5000)
$Ntot$	Total population size (males and females) $Ntot_t = (n_{1,t} + n_{2,t} + n_{3,t} + n_{4,t}) * 2$	--
$Nbpop$	Breeding population size (males and females) $Nbpop_t = (n_{3,t} + n_{4,t}) * 2$	--
y	Annual index of breeding population size	--
σ_y	Annual estimated observation error of y	--
β	Regression coefficients	Uniform (-5,5)
$\sigma_{\phi,\alpha,ns}$	Standard deviation of temporal variability *Used for ϕ, α, ns	Uniform (0,10)
ε	$\varepsilon_t \sim Normal\ (0, \sigma_\theta)$	--

Table 5-2. Posterior estimates of population metrics and loss for Alaskan breeding populations of Spectacled eiders (*Somateria fischeri*). Consideration for reclassification from threatened to recovered requires that the population size must reach or exceed the threshold, and overprotection loss must be greater than underprotection loss.

	SSM[a]	IPM[b]
Abundance		
Mean	14,205	14,511
SD	1,200	1,051
95% CRI	11,832 – 16,538	12,496 – 16,589
Population growth ‘r’		
Mean	0.025	0.025
Process error	0.14	0.071
Underprotection	0.22	0.065
Overprotection	0.35	0.23
$P(N_{2014} \geq \text{threshold})$[c]	0.94	1.0

[a] Results generated from a Bayesian state-space model of count data only.

[b] Results generated from an integrated population model using demographic data and counts.

[c] Proportion of the posterior above the threshold of 12,000 birds.

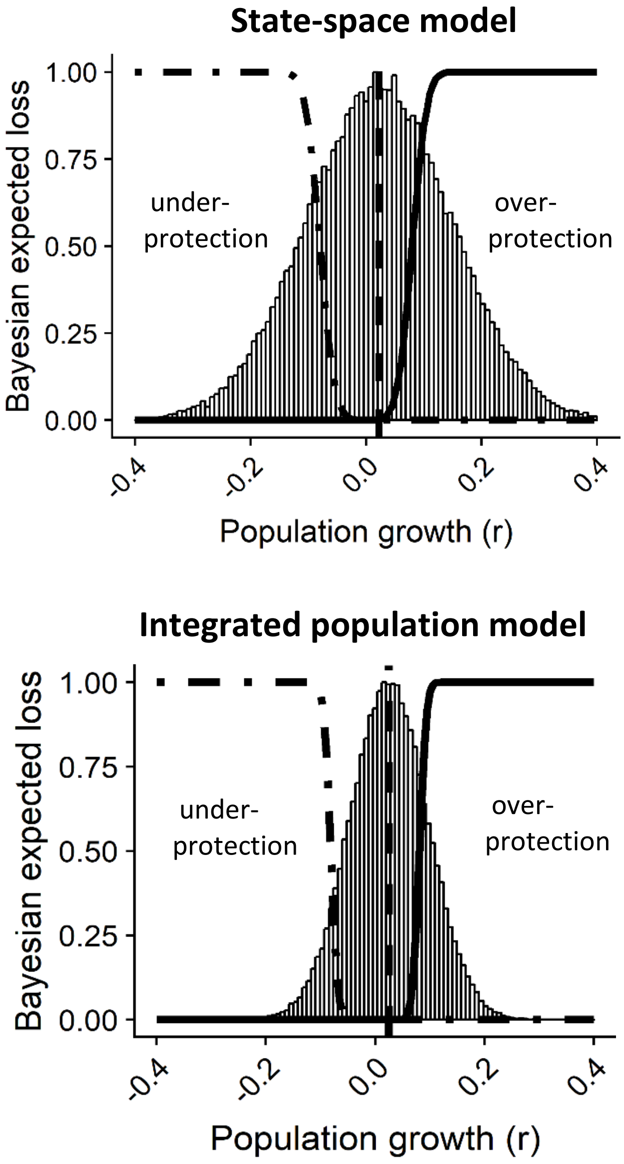

Figure 5-1. Loss functions generated using the probability of quasi extinction (N < 250 adults) given population size, growth rate, and process error estimates for both the state space model (SSM) and integrated population model (IPM) of spectacled eiders on the Yukon-Kuskokwim Delta. The histogram is the posterior distribution of population growth rate from each model. The posterior is wider for estimated growth rate under the state - space model than the integrated model. The vertical dashed line indicates the mean population growth rate and is $\bar{r}$ = 0.025 for both models. The curved lines indicate expected loss or probability of quasi extinction given a value for population growth rate along the x-axis, and model estimated population size and process error. Under- protection (dot-dashed line) refers to the risk of misclassifying the population if the decision were to delist the species for each value of r and is calculated as the product of expected loss and the proportion of values of estimated population growth. Over-protection (solid black line) refers to the risk of misclassifying if the decision were to keep the species listed as threatened when protection is not warranted.

Appendix 1 – Chapter 2 Model Code

Chapter 2: Evaluating the probability of meeting population management thresholds

Matlab Code

```
n = 10000; % number of particles
thold = 12000; % threshold number of BIRDS

%% Detection Parameters
% Uniform detection probability
mind = 0;
maxd = 1;

dUnif = rand(n,1)*(maxd-mind)+ mind;
% High detection probability
detH = 0.7;
% Low detection probability
detL = 0.3;
% High error
seH = 0.2;
% Low error
seL = 0.05;

% Traditional VCF converted to Detection rate
VCF = 3.58;
Tdet = 1/VCF; % No error associated with this detection rate (applied to all eider spp)
% Informed detection distributions
detHH = betaparm(detH,seH,0,1,n,1,0);
detLL = betaparm(detL,seL,0,1,n,1,0);
detHL = betaparm(detH,seL,0,1,n,1,0);
detLH = betaparm(detL,seH,0,1,n,1,0);

%% Count Parameters
% YKD Informed count Fischer report 2016 (personal communication)
YKDcount = 6336; % Indicated breeding birds
YKDse = 511;

cYKD = YKDcount(1)+randn(n,1)*YKDse(1);
% Uniform count
minc = 0;
```

```
maxc = 10000;
cUnif = rand(n,1)*(maxc-minc)+ minc;
%% MODELS %%
%%%%%%%% YKD 1 Uniform detection count from 2016 %%%%%%%
YKD1N = cYKD./dUnif;
x1 = YKD1N >= thold;
t = sum(x1);
pN1 = t/n

YKD1Nx = YKD1N(x1);
YKD1dx = dUnif(x1);
YKD1cx = cYKD(x1);

%% YKD INFORMED DETECTION MODELS %%
%%%%%%%%%%%%%%% YKD 2 Beta detection 0.6 small se count from 2016
YKD2N = cYKD./detHL;
x2 = YKD2N >= thold;
t2 = sum(x2);
pNt2 = t2/n

YKD2Nx = YKD2N(x2);
YKD2dx = detHL(x2);
YKD2cx = cYKD(x2);

%%%%%%%%%%%%% YKD 3 Beta detection 0.6 large se count from 2016
YKD3N = cYKD./detHH;
x3 = YKD3N >= thold;
g = sum(x3);
b = g/n

YKD3Nx = YKD3N(x3);
YKD3dx = detHH(x3);
YKD3cx = cYKD(x3);

%%%%%%%%%%%%%% YKD 4 Beta detection 0.3 small se count from 2016
YKD4N = cYKD./detLL;
x4 = YKD4N >= thold;
xx4 = sum(x4);
Px4 = xx4/n

YKD4Nx = YKD4N(x4);
YKD4dx = detLL(x4);
YKD4cx = cYKD(x4);

%%%%%%%%%%%%%%%%% YKD 5 Beta detection 0.3 large se count from 2016
YKD5N = cYKD./detLH;
```

```
x5 = YKD5N >= thold;
xx5 = sum(x5);
Px5 = xx5/n

YKD5Nx = YKD5N(x5);
YKD5dx = detLH(x5);
KD5cx = cYKD(x5);

%%%%%%%%%%%%%%%%% YKD Traditional VCF applied to all eider spp
%%%%%
YKDvcf = cYKD./Tdet;
x6 = YKDvcf >= thold;
xx6 = sum(x6);
Px6 = xx6/n

YKD6Nx = YKDvcf(x6);
% repmat for Tdet to make it the same dimension as x6
Tdet1 = repmat(Tdet,[5000,1]);
YKD6dx = Tdet1(x6);
YKD6cx = cYKD(x6);

%%%%%%%%%%%%%%%%% YKD Transitional VCF from Stehn and Platte 2015
VCFp = 2.35;
Pdet = 1/VCFp;
YKDvcfP = cYKD./Pdet;
x7 = YKDvcfP >= thold;
xx7 = sum(x7);
Px7 = xx7/n

YKD7Nx = YKDvcfP(x7);
% repmat for Tdet to make it the same dimension as x6
Pdet1 = repmat(Pdet,[10000,1]);
YKD7dx = Pdet1(x7);
YKD7cx = cYKD(x7);

%% Probability of meeting the threshold given ALL detection probabilities
%%%%%%%% Simulated values for multiple detection rates %%%%%%%

YKDsN = zeros(10000,100);
d = [0.01:0.01:1];
for i = 1:numel(d)
   YKDsN(:,i) = cYKD./d(i);
   x1(:,i) = YKDsN(:,i) >= thold;
   t(1,i) = sum(x1(:,i));
   pN1(i) = t(1,i)/n;
end
```

Appendix 2 – Chapter 3 Code

Chapter 3: Assessing recovery of spectacled eiders using a Bayesian decision analysis
R and Jags Code

Yukon-Kuskokwim Delta Model

```
model {

   # ------------------------------------------------------------------------------------------
   # PRIOR DISTRIBUTIONS
   # ------------------------------------------------------------------------------------------

   logN.est[1] ~ dnorm(9.43, 100)      # Prior for initial population size
   mean.r ~ dnorm(0, 1/(0.1)^2)     # Prior for mean growth rate

   sigma.proc ~ dgamma(3, 20)         # Prior for process error
   sigma2.proc <- pow(sigma.proc, 2)
   tau.proc <- pow(sigma.proc, -2)

   # ------------------------------------------------------------------------------------------
   # LIKELIHOODS
   # ------------------------------------------------------------------------------------------

   ## STATE PROCESS ##
   for (t in 1:(T-1)){
     r[t] ~ dnorm(mean.r, tau.proc)
     logN.est[t+1] <- logN.est[t] + r[t]
   }

   ## LINEAR REGRESSION FOR MISSING OBS ERROR ##
    beta ~ dnorm(0, 0.001)
    miss.se ~ dgamma(2,0.01)
    miss.prec <- pow(miss.se, -2)

    for (j in 1:T){
      sigma.pred[j] <- beta*N.est[j]
      sigma.obs[j] ~ dnorm(sigma.pred[j], miss.prec)
    }

   ## OBSERVATION PROCESS ##
   for (i in 1:T) {
     tau.obs[i] <- pow(sigma.obs[i], -2)
```

```
     y[i] ~ dnorm(exp(logN.est[i]), tau.obs[i])
    }

    # --------------------------------------------------------------------------------------
    # POPULATION SIZE ON REAL SCALE
    # --------------------------------------------------------------------------------------

    for (t in 1:T) {
    N.est[t] <- exp(logN.est[t])
    }

# YKD Abundance data
ykd1 <- c(12457, 14599, 15586, 13698, NA, 14894, 16171, 13386, 5618, 15118)
ykd1.se <- c(1408, 1470, 1463, 1273, NA, 1375, 1460, 1360, 627, 1472)
year <- 2007:2016

# Bundle data
jags.data <- list(y = ykd1, T = length(year), sigma.obs = ykd1.se)

# Initial values
inits <- function(){list(sigma.proc = rgamma(1, 3, 20), mean.r = rnorm(1, 0, 1/(0.1)^2),  logN.est
= c(rnorm(1, 9.43, 10), rep(NA, (length(year)-1))), beta = runif(1, 0.01, 0.1) , miss.se = runif(1,
100, 101))}

# Parameters monitored
parameters <- c("r", "mean.r", "N.est", "sigma.proc", "beta", "miss.se", "sigma.obs")


################################################################################
######

# Decision Analysis

rs = seq(-.4,.4,0.005) # sequence of r values to test
#sample location in posterior, maintains posterior correlation and samples across chains
samples = sample(length(ykd_1.ssm$sims.list$sigma.proc),10000)
storage.notclassify = matrix(NA,nrow=10000,ncol=length(rs))
for (i in 1:length(rs)){
  for(j in 1:10000){
    N =  ykd_1.ssm$sims.list$N.est[ samples[j],10]   # SAMPLE POP SIZE
    sr = ykd_1.ssm$sims.list$sigma.proc[ samples[j] ]  # SAMPLE PROCESS SD
    for(k in 1:50){                                  # time loop - 50 years chosen by RT page 30 in
Recovery Plan
      r.new = rnorm(1,rs[i],sr)
      N=N*exp(r.new)
      if(N<250) break
    }
    storage.notclassify[j,i]=ifelse(N<250,1,0)
  }
}

## Over/under protection probabilities generated from MEAN R and SD R (ssm)
```

```
mn.r = ykd_1.ssm$mean$mean.r
sd.r = ykd_1.ssm$sd$mean.r
p=matrix(0,nrow=1:length(rs))
p[1] = pnorm(rs[1],mn.r,sd.r) # Assumes normality
for (i in 2:length(rs)){
  p[i] = pnorm(rs[i],mn.r,sd.r)-pnorm(rs[i-1],mn.r,sd.r)
}
loss1 = sum(p*apply(storage.notclassify,2,mean)[1:length(rs)])
loss2 = sum(p*apply(storage.notclassify,2,mean)[length(rs):1])
loss1 # underprotection loss
loss2 # overprotection loss

## Probability of N >= Nthreshold (12000) in 2016
thold <- 12000
ykdN = ykd_1.ssm$sims.list$N.est[,10]
P.thold <- 100*length(which(ykdN >= thold))/length(ykdN)
P.thold # Probability of N >= 12000 breeding birds (6000 breeding pairs) threshold for delisting
################################################################################
#######
```

Arctic Coastal Plain Population Model

```
model {
   # -----------------------------------------------------------------------------------------
   # PRIOR DISTRIBUTIONS
   # -----------------------------------------------------------------------------------------

   logN.est[1] ~ dnorm(8.21, 10)      # Prior for initial population size
   mean.r ~ dnorm(0, 1/(0.1)^2)      # Prior for mean growth rate

   sigma.proc ~ dgamma(3, 10)         # Gamma dist with mean ~0.3, declining tail towards 1
   sigma2.proc <- pow(sigma.proc, 2)
   tau.proc <- pow(sigma.proc, -2)     # Estimated precision in r

   # -----------------------------------------------------------------------------------------
   # LIKELIHOODS
   # -----------------------------------------------------------------------------------------

   ## STATE PROCESS ##
   for (t in 1:(T-1)){
   r[t] ~ dnorm(mean.r, tau.proc)
   logN.est[t+1] <- logN.est[t] + r[t]
   }

   ## OBSERVATION PROCESS ##
   for (i in 1:T) {
   tau.obs[i] <- pow(sigma.obs[i], -2)
   y[i] ~ dnorm(exp(logN.est[i]), tau.obs[i])
   }

   # -----------------------------------------------------------------------------------------
```

```
    # POPULATION SIZE ON REAL SCALE
    # -------------------------------------------------------------------------------------

    for (t in 1:(T)) {
    N.est[t] <- exp(logN.est[t])
    }
    }

###### Data ######
# NUMBER OF BREEDING PAIRS
nbp <- c(3698, 4424, 3837, 4473, 5787, 3383, 5565, 4905, 3828, 3411)
nbp.se <- c(574, 564, 583, 630, 692, 414, 674, 745, 536, 546)
year <- 2007:(2016 + pyears)


# Bundle data
jags.data <- list(y = nbp, sigma.obs = nbp.se, T = length(year))

# Initial values
inits <- function(){list(sigma.proc = rgamma(1, 3, 10), mean.r = rnorm(1, 0, 1/(0.1)^2), logN.est
= c(rnorm(1, 8.21, 10), rep(NA, (length(year)-1))))}

# Parameters monitored
parameters <- c("r", "mean.r", "sigma2.proc", "N.est", "sigma.proc")

################################################################################
#######
# Decision Model
rs = seq(-.4,.4,0.005) # sequence of r values to test
samples = sample(length(acp_1.ssm$sims.list$sigma2.proc),10000) # sample location in
posterior, maintains posterior correlation and samples across chains
storage.notclassify = matrix(0,nrow=10000,ncol=length(rs))
for (i in 1:length(rs)){
  for (j in 1:10000){
    N = acp_1.ssm$sims.list$N.est[ samples[j],10 ]
    sr = sqrt(acp_1.ssm$sims.list$sigma2.proc[ samples[j] ])
    for (k in 1:50){
      r.new = rnorm(1, rs[i], sr)
      N = N*exp(r.new)
      if(N<125) break
    }
    storage.notclassify[j,i] = ifelse(N<125,1,0)
  }
}

## Over/under protection probabilities generated from MEAN R and SD R (ssm)
p=matrix(0,nrow=1:length(rs))
p[1] = pnorm(rs[1],mn.r,sd.r)
for (i in 2:length(rs)){
  p[i] = pnorm(rs[i],mn.r,sd.r)-pnorm(rs[i-1],mn.r,sd.r)
}
```

```
loss1 = sum(p*apply(storage.notclassify,2,mean)[1:length(rs)])
loss2 = sum(p*apply(storage.notclassify,2,mean)[length(rs):1])
loss1 # Probability of underprotection given r
loss2 # Probability of overprotection given r

## Probability of N >= Nthreshold (6000) in 2016
thold <- 6000
acpN = acp_1.ssm$sims.list$N.est[,10]
P.thold <- 100*length(which(acpN >= thold))/length(acpN)
P.thold # Probability of N >= 12000 breeding birds (6000 breeding pairs) threshold for delisting
```

Appendix 3 – Code for Chapter 4

Chapter 4: Demographic responses to climate change and predation pressure in a threatened Arctic species

R and JAGS code

```
model {

# -------------------------------------------- #
# PARAMETERS #
# phi : age-specific survival probabilities
# alpha : age-specific breeding probabilities
# p : age-specific detection probabilities
# fec : fecundity
# -------------------------------------------- #
# POPULATION STATES #
# N1 : 1-2 yr old birds
# N2 : 2-3 yr old non-breeders
# N3 : 2-3 yr old first yr breeding birds
# N4 : 3 + yr breeding birds
# -------------------------------------------- #
# STATES FOR MULTI-STATE CMR MODEL #
# 1 : first year bird            --> observable as duckling
# 2 : second year bird           --> unobservable
# 3 : non-breeding 2.5 year old  --> unobservable
# 4 : breeding 2.5 year old      --> observable
# 5 : breeding 3+ year old       --> observable
# ------------------------------------------- #

# PRIORS #
# Parameters:
   # phi: age/state-specific survival probabilities
   # alpha: probability to start reproduction at age = 2 years
   # p: recapture probability
   # -----------------------------------------------

# Survival rates
```

```
  for (t in 1:(n.occasions-1)){
    logit(phi2[t]) <- mu.phi2 + beta[1]*ice[t] + beta[2]*(ice[t]*ice[t]) + eps.phi2[t]
    eps.phi2[t] ~ dnorm(0, tau.phi2)

    phi1[t] <- phi2[t]*0.8

    logit(phi0[t]) <- mu.phi0 + beta[3]*ice[t] + beta[4]*(ice[t]*ice[t]) + eps.phi0[t]
    eps.phi0[t] ~ dnorm(0, tau.phi0)

    logit(alpha[t]) <- mu.alpha + beta[5]*ice[t] + beta[6]*(ice[t]*ice[t]) + eps.alpha[t]
    eps.alpha[t] ~ dnorm(0, tau.alpha)

    p[t] <- mean.p
  }

# Mean survival/breeding/detection rates probability scale
  mean.phi2 ~ dunif(0,1)
  mean.phi0 ~ dunif(0,1)

  mean.alpha ~ dunif(0,1)
  mean.p ~ dunif(0,1)

# Mean survival/breeding rates logit scale
  mu.phi2 <- log(mean.phi2/(1-mean.phi2))
  mu.phi0 <- log(mean.phi0/(1-mean.phi0))

  mu.alpha <- log(mean.alpha/(1-mean.alpha))

# Precision of std of temporal variability
  sig.phi2 ~ dunif(0,10)          # standard deviation
  tau.phi2 <- pow(sig.phi2, -2)    # Precision for stand dev
  temp.sig.phi2 <- pow(sig.phi2, 2) # residual temporal variation

  sig.phi0 ~ dunif(0,10)
  tau.phi0 <- pow(sig.phi0, -2)
  temp.sig.phi0 <- pow(sig.phi0, 2)

  sig.alpha ~ dunif(0,10)
  tau.alpha <- pow(sig.alpha, -2)
  temp.sig.alpha <- pow(sig.alpha, 2)

# Regression coefficients
   beta1 ~ dunif(-5,5)
   beta2 ~ dunif(-5,5)
   beta3 ~ dunif(-5,5)
   beta4 ~ dunif(-5,5)
```

```
     beta5 ~ dunif(-5,5)
     beta6 ~ dunif(-5,5)
     beta7 ~ dunif(-5,5)
     beta8 ~ dunif(-5,5)
     beta9 ~ dunif(-5,5)

# Fecundity
    for (t in 1:n.occasions){
      logit(prob.success[t]) <- mu.ns + beta[7]*rain[t] + beta[8]*fox[t] + beta[9]*temp[t] +
eps.ns[t]
      eps.ns[t] ~ dnorm(0, tau.ns)
    }

  # Mean nest success/clutch size probability to logit scale
    mean.ns ~ dunif(0,1)
    mu.ns <- log(mean.ns/(1-mean.ns))

    avg.cs ~ dgamma(0.1, 0.1)

  # Standard deviation, precision, variance
    sigma.ns ~ dunif(0, 10)
    tau.ns <- pow(sigma.ns, -2)
    temp.sig.ns <- pow(sigma.ns, 2)


# INITAL POPULATION SIZE
# Total FEMALE population size
  N[1,1] ~ dcat(pN1)
  N[2,1] ~ dcat(pN2)
  N[3,1] ~ dcat(pN3)
  N[4,1] ~ dcat(pN4)

# ---------------------------------------------------------------------------- #

# STATE SPACE MODEL FOR TOTAL POPULATION #
for (t in 1:(n.occasions-1)){
   N[1,t+1] <- (Fec[t]/2 * phi0[t]) * (N[3,t] + N[4,t])
   N[2,t+1] <- (phi1[t] * (1-alpha[t])) * N[1,t]
   N[3,t+1] <- (phi1[t] * alpha[t]) * N[1,t]
   N[4,t+1] <- phi2[t] * (N[2,t] + N[3,t] + N[4,t])
   }

# TOTAL POPULATION SIZE
for(t in 1:n.occasions){
  Ntot[t] <- (N[1,t] + N[2,t] + N[3,t] + N[4,t])*2
}
```

```
# BREEDING POPULATION SIZE #
for(t in 1:n.occasions){
  Nb[t] <- ((N[3,t] + N[4,t])*2)
}

    ## LINEAR REGRESSION FOR MISSING OBS ERROR ##
     beta.se ~ dnorm(0, 0.001)
     miss.se ~ dgamma(2, 0.01)
     miss.prec <- pow(miss.se, -2)

     for (j in 1:n.occasions){
       sigma.pred[j] <- beta.se*Nb[j]
       sigma.obs[j] ~ dnorm(sigma.pred[j], miss.prec)
     }

# OBSERVATION MODEL FOR BREEDING POPULATION SIZE #
for(t in 1:n.occasions){
  tau.obs[t] <- pow(sigma.obs[t], -2) # Provided as data
  count[t] ~ dnorm(Nb[t], tau.obs[t])
}

### Derived Parameters ###
for(t in 1:(n.occasions-1)){
   lambda.Nb[t] <- Nb[t+1]/Nb[t]
   r.Nb[t] <- log(lambda.Nb[t])
}

# To compare posterior predictions and estimate Pvalue
for (i in 1:n.occasions){
   Nb.pred[i] ~ dnorm(Nb[i], tau.obs[i])
}

## ----------------------------------------------------------------------------------------------------
--

## FECUNDITY MODEL ##

# Likelihood of single data set
    for (t in 1:n.occasions){
       clutch.size[t] ~ dpois(avg.cs)
       num.success[t] ~ dbin(prob.success[t], tot.nests[t])
       Fec[t] <- clutch.size[t] * prob.success[t]
       # logliikns[t] <- logdensity.bin(num.success[t], prob.success[t], tot.nests[t])
      }
```

```
# Freeman Tukey Fit Statistics
    for (t in 1:n.occasions){
      # Compute fit for observed data
      exp.ns[t] <- prob.success[t]*tot.nests[t]
      exp.orig.ns[t] <- pow((pow(num.success[t],0.5)-pow(exp.ns[t],0.5)),2)
      # Generate data and compute fit
      ns.new[t] ~ dbin(prob.success[t],tot.nests[t])
      exp.new.ns[t] <- pow((pow(ns.new[t],0.5)-pow(exp.ns[t],0.5)),2)
    } # End fit loop

fit.ns <- sum(exp.orig.ns[])
fit.ns.new <- sum(exp.new.ns[])

## --------------------------------------------------------------------------------------------------------------------
--

## SURVIVAL MODEL ##

# Multistate capture-recapture model
# Define state-transition and reencounter probabilities
    for (t in 1:(n.occasions-1)){
    psi[1,t,1] <- 0
    psi[1,t,2] <- phi0[t]
    psi[1,t,3] <- 0
    psi[1,t,4] <- 0
    psi[1,t,5] <- 0
    psi[2,t,1] <- 0
    psi[2,t,2] <- 0
    psi[2,t,3] <- phi1[t] * (1-alpha[t])
    psi[2,t,4] <- phi1[t] * alpha[t]
    psi[2,t,5] <- 0
    psi[3,t,1] <- 0
    psi[3,t,2] <- 0
    psi[3,t,3] <- 0
    psi[3,t,4] <- 0
    psi[3,t,5] <- phi2[t]
    psi[4,t,1] <- 0
    psi[4,t,2] <- 0
    psi[4,t,3] <- 0
    psi[4,t,4] <- 0
    psi[4,t,5] <- phi2[t]
    psi[5,t,1] <- 0
    psi[5,t,2] <- 0
    psi[5,t,3] <- 0
    psi[5,t,4] <- 0
    psi[5,t,5] <- phi2[t]
```

```
  po[1,t] <- 0
  po[2,t] <- 0
  po[3,t] <- 0
  po[4,t] <- p[t]
  po[5,t] <- p[t]

# Calculate probability of non-encounter (dq) and reshape the array for the encounter
probabilities
  for (s in 1:ns){
  dp[s,t,s] <- po[s,t]
  dq[s,t,s] <- 1-po[s,t]
  }

  for (s in 1:(ns-1)){
   for (m in (s+1):ns){
    dp[s,t,m] <- 0
    dq[s,t,m] <- 0
   }
  }

  for (s in 2:ns){
   for (m in 1:(s-1)){
    dp[s,t,m] <- 0
    dq[s,t,m] <- 0
     }
   }
  } # end time loop

# Define the multinomial likelihood
  for (t in 1:((n.occasions-1)*ns)){
   marr[t,1:(n.occasions*ns-(ns-1))] ~ dmulti(pr[t,], rel[t])
  }

# Define the cell probabilities of the m-array
# Define matrix U: product of probabilities of state-transition and non-encounter
  for (t in 1:(n.occasions-2)){
   U[(t-1)*ns+(1:ns), (t-1)*ns+(1:ns)] <- ones
   for (j in (t+1):(n.occasions-1)){
    U[(t-1)*ns+(1:ns), (j-1)*ns+(1:ns)] <- U[(t-1)*ns+(1:ns), (j-2)*ns+(1:ns)] %*%
psi[,t,] %*% dq[,t,]
   }
  }
  U[(n.occasions-2)*ns+(1:ns), (n.occasions-2)*ns+(1:ns)] <- ones

# Define the cell probabilities of the multistate m-array
```

```
    for (t in 1:(n.occasions-2)){
      pr[(t-1)*ns+(1:ns),(t-1)*ns+(1:ns)] <- U[(t-1)*ns+(1:ns),(t-1)*ns+(1:ns)] %*% psi[,t,]
%*% dp[,t,]

# Above main diagonal
    for (j in (t+1):(n.occasions-1)){
      pr[(t-1)*ns+(1:ns), (j-1)*ns+(1:ns)] <- U[(t-1)*ns+(1:ns), (j-1)*ns+(1:ns)] %*%
psi[,j,] %*% dp[,j,]
    }
    }
    pr[(n.occasions-2)*ns+(1:ns), (n.occasions-2)*ns+(1:ns)] <- psi[,n.occasions-1,] %*%
dp[,n.occasions-1,]

# Below main diagonal
   for (t in 2:(n.occasions-1)){
      for (j in 1:(t-1)){
        pr[(t-1)*ns+(1:ns),(j-1)*ns+(1:ns)] <- zero
      }
    }

# Last column: probability of non-recapture
    for (t in 1:((n.occasions-1)*ns)){
      pr[t,(n.occasions*ns-(ns-1))] <- 1-sum(pr[t,1:((n.occasions-1)*ns)])
    }
}

# Bundle data
ns <- 5   # Number of states
Ninit <- matrix(NA, nrow = 4, ncol = 1)
Ninit[1,1] <- 1000
Ninit[2,1] <- 500
Ninit[3,1] <- 400
Ninit[4,1] <- 3000

# Function to create a discrete uniform prior
disc.unif <- function(A, B){
  pprob <- c(rep(0, A-1), rep(1/(B-A+1), (B-A+1)))
  return(pprob)
}

# - based on stable stage distribution:
A <- matrix(c(0,           0,     2.5/2*0.3,  2.5/2*0.3,
              (1-0.3)*0.6, 0,     0,          0,
              0.3*0.6,     0,     0,          0,
              0,           0.8,   0.8,        0.8), ncol = 4, byrow = TRUE)
```

```
u <- which.max(Re(eigen(A)$values))
revec <- Re(eigen(A)$vectors[,u])
stable.stage <- revec/sum(revec)

4900*stable.stage[1]/(stable.stage[3]+stable.stage[4])
4900*stable.stage[2]/(stable.stage[3]+stable.stage[4])
4900*stable.stage[3]/(stable.stage[3]+stable.stage[4])
4900*stable.stage[4]/(stable.stage[3]+stable.stage[4])

# - priors then +/- around the mean
pN1 <- disc.unif(1600, 1900)
pN2 <- disc.unif(500, 900)
pN3 <- disc.unif(200, 400)
pN4 <- disc.unif(4000, 5000)

bugs.data <- list(pN1 = pN1, pN2 = pN2, pN3 = pN3, pN4 = pN4, ice =
SIindex$icedays4.stand[2:25], fox = fox$prop_plot_fox, rain = rain$summ_standard,
temp=temp$Value, marr = msarr, n.occasions = ncol(rCH), rel = rowSums(msarr), ns =
ns, zero = matrix(0, ncol = ns, nrow = ns), ones = diag(ns), clutch.size = fecdat$mncs,
num.success = fecdat$num.success, tot.nests = fecdat$total.nests, count = popdata$y,
sigma.obs = popdata$sd)

inits <- function(){list(mean.alpha = runif(1,0.1,0.6),mean.phi0 = runif(1,0,0.75),
mean.phi2 = runif(1,0.2,1), mean.p = runif(1,0,1), mean.ns = runif(1,0.1,1), beta.se =
runif(1, 0.01, 0.1) , miss.se = runif(1, 100, 101), ind = rbinom(6,1,0.5))}

# Parameters monitored
parameters <- c("mean.phi2", "mean.alpha","mean.phi0", "mean.ns", "beta[1]", "beta[2]",
"beta[3]", "beta[4]", "beta[5]", "beta[6]", "beta[7]", "beta[8]", "beta[9]", "fit.ns",
"fit.ns.new", "prob.success", "phi2","r.Nb", "Nb", "Fec", "Nb.pred")
```